Study on permanent magnetic synchronous motor parameter identification based on its current signal

THESIS

Study on Parameter Identification of Permanent Magnet Synchronous Motor Based on Its Current Signals

季　翔

Department of Environment and Energy System

Graduate School of Science and Technology, Educational Division, Shizuoka University

December 2015

Table of contents

1. Introduction

1.1. Introduction

A synchronous motor is an alternating current (AC) motor in which, at the steady state,[1] the rotation of the shaft is synchronized with the frequency of the supply current; the rotation period is perfect just equal to an integral number of AC cycles. Synchronous motors contain multiphase AC electromagnets on the stator of the motor that create a magnetic field which rotates in time with the oscillations of the line current. The rotor with permanent magnets or electromagnets turns in step with the stator field at the same rate and as a result, provides the second synchronized rotating magnet field of any AC motor. A permanent synchronous motor is only considered doubly fed if is supplied with independently excited multiphase AC electromagnets on both the rotor and stator.

The synchronous motor and induction motor are the most widely used types of AC motor. The difference between the two types is that the synchronous motor rotates in exact synchronism with the line frequency. The synchronous motor does not rely on current induction to produce the rotor's magnetic field. By contrast, the induction motor requires slip, and the rotor must rotate slightly slower than the AC current alternations, to induce current in the rotor winding. Small synchronous motors are used in timing applications such as in synchronous clocks, timers in appliances, tape recorders and precision servomechanisms in which the motor must operate at a precise speed; speed accuracy is that of the power line frequency, which is carefully controlled in large interconnected grid systems.

Synchronous motors are available form sub-fractional self-excited sizes[2] to high-horsepower industrial sizes.[1] In the fractional horsepower range, most synchronous motors are applied where precise constant speed is required. These machines are commonly used in analog electric clocks, timers and other devices where correct time is required. In high-horsepower industrial sizes, the synchronous motor provides two important features. First, it is a highly efficient means of converting AC

energy to work; Second, it can operate at leading or unity power factor and thereby provide power-factor correction.

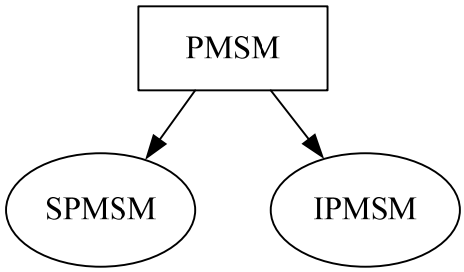

Fig 1.1 Classification of permanent motor.

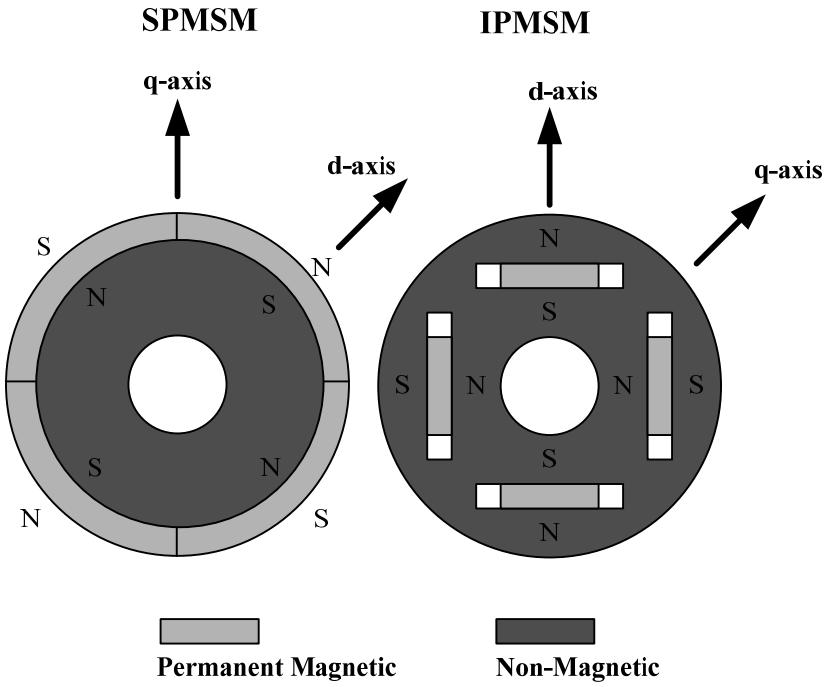

Fig 1.2 Structure of SPMSM and IPMSM.

Synchronous motors fall under the more general category of synchronous machines which also includes the synchronous generator. Generator action will be observed if the field poles are driven ahead of the resultant air-gap flux by the forward motion of

the prime mover. Motor action will be observed if the field poles are dragged behind the resultant air-gap flux by the retarding torque of a shaft load.[1]

There are mainly two different types of synchronous motors depending on how the rotor is magnetized: first is non-excited and second is direct-current excited.[3]

A permanent magnet synchronous motor (PMSM) usually uses permanent magnets embedded in the steel rotor to create a constant magnetic field. The stator carries windings connected to an AC supply to produce a rotating magnetic field. At synchronous speed of the rotor poles lock to the rotating magnetic field. These motors are not self-starting. Because of the constant magnetic field in the rotor these cannot use induction windings for starting.[4][5][6][7][8]

The main difference between a permanent magnet synchronous motor and an asynchronous motor is the rotor. Some studies seem to indicate that NdFeB permanent magnet synchronous motors are more efficient (around 2%) than the highest-efficiency asynchronous motors using the same stator laminations and similar variable-frequency speed controllers.[9]

Based on the rotor structure the PMSM can be divided in to two different types, i.e, and surface permanent magnet synchronous motor (SPMSM) and interior permanent magnet synchronous motor (IPMSM) as shown in Fig 1.1. As shown in Figure 1.2, the SPMSM had a simple structure comparing with the IPMSM. The SPMSM's permanent magnetic is mounted on the rotor's surface. Because of that the d-axis and q-axis inductance are same. And the mathematic model of the SPMSM is shown in Figure1.3. In Fig 1.3 the d-axis and q-axis inductance are same. Therefore, three parameters are required to be identified in the SPMSM.

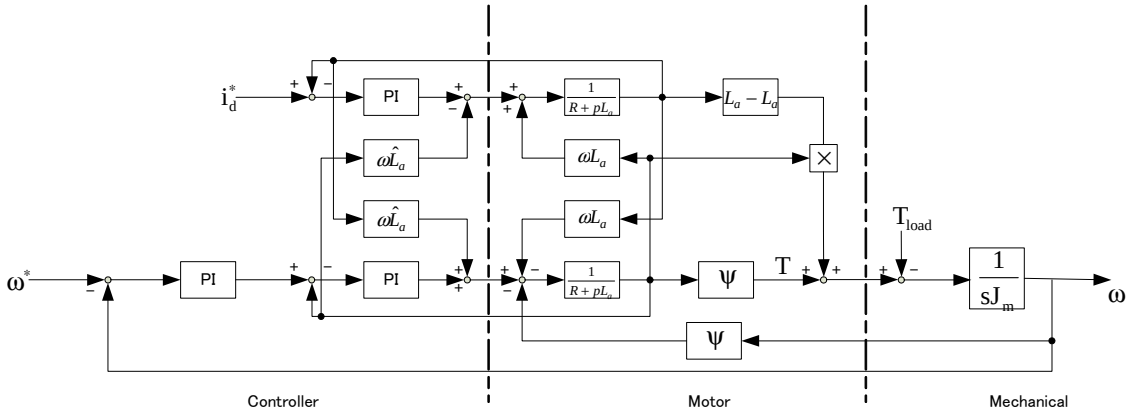

Fig.1.3 Mathematic model of SPMSM.

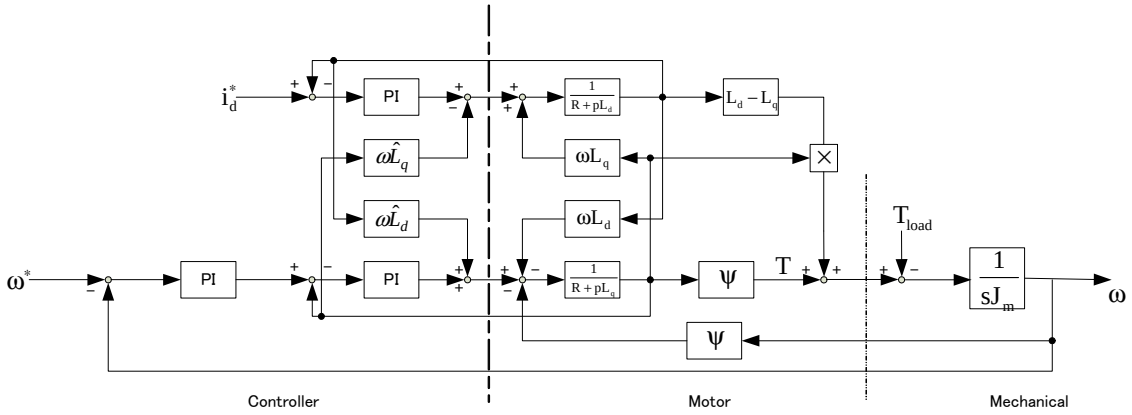

Fig. 1.4 Mathematic model of IPMSM control system

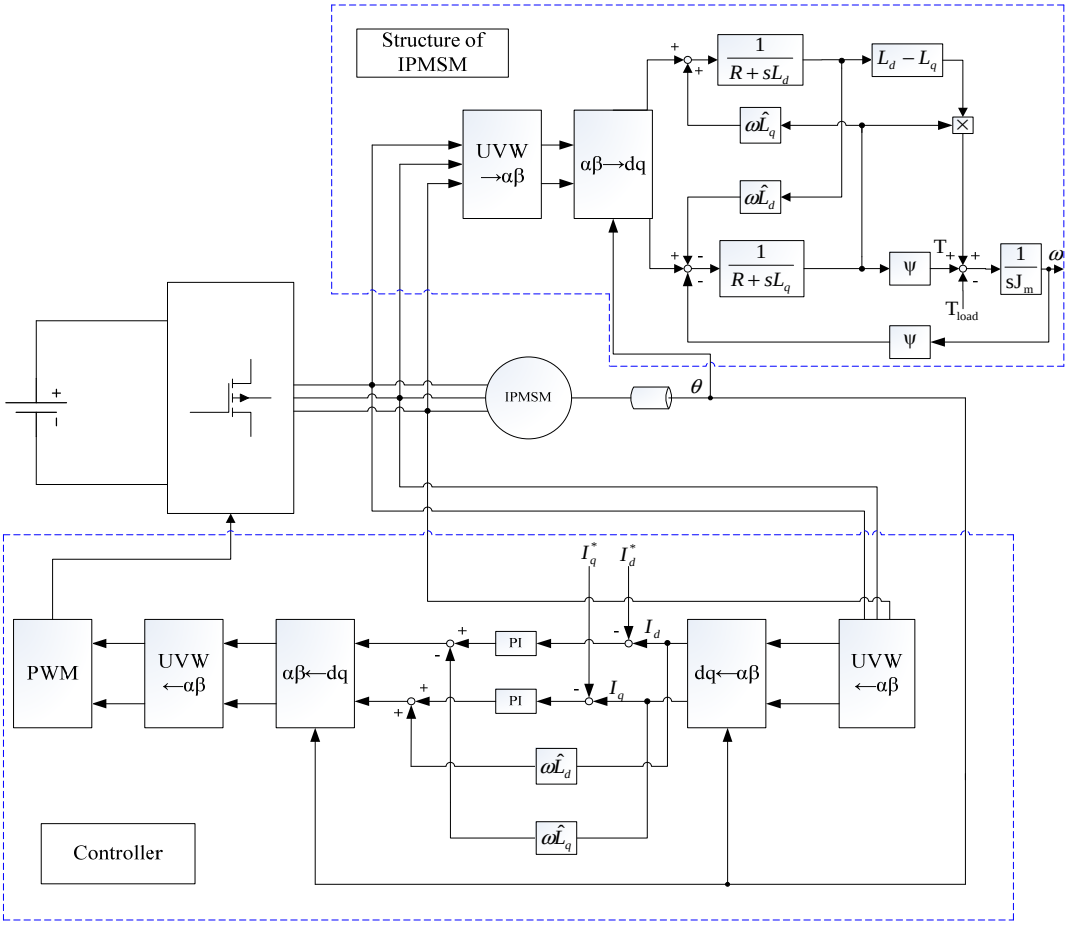

Fig 1.5 IPMSM with the control loop.

In recent years, interior permanent magnet (IPM) synchronous motors are widely used in a variety of industry, home appliance and automotive applications, owing to their high-efficiency and high-power-density features. The IPM motor is usually controlled by means of a field-orientation technique (vector control), and requires a current controller on the synchronous rotating reference frame (dq-reference-frame) for the instantaneous torque and the magnetic flux control. The current control on the dq-reference-frame mainly consists of the coordinate transformation, the PI regulation, and the decoupling compensation, which is based on the mathematical model of the motor. Therefore, it is indispensable not only to detect the magnetic-pole-position and the motor currents, but also to know the motor parameters accurately. Identification of the motor parameters is important to control the motor properly in starting up of the control as well as the running operation, and the off-line parameter identification is particularly required for the initial controller setup and starting up. Unfortunately the

off-line identification method requires a complex test equipment, and the hill-climbing method also needs lots of times. To overcome these problems the on-line identification is proposed, by employing the on-line identification method the experiment can be finished without complex test equipments. And the two points speculate method could also reduce the identification times and be finished identification in a fixed time.

Based on the structure shown in Fig 1.6 the IPMSM's d-axis inductance and q-axis inductance are different. And the IPMSM mainly has four parameters to be identified. They are the q-axis inductance L_q, the d-axis inductance L_d, the magnetic flux linkage ψ, and the winding resistance R. Each of the motor parameters must independently with a manner as simple as possible.

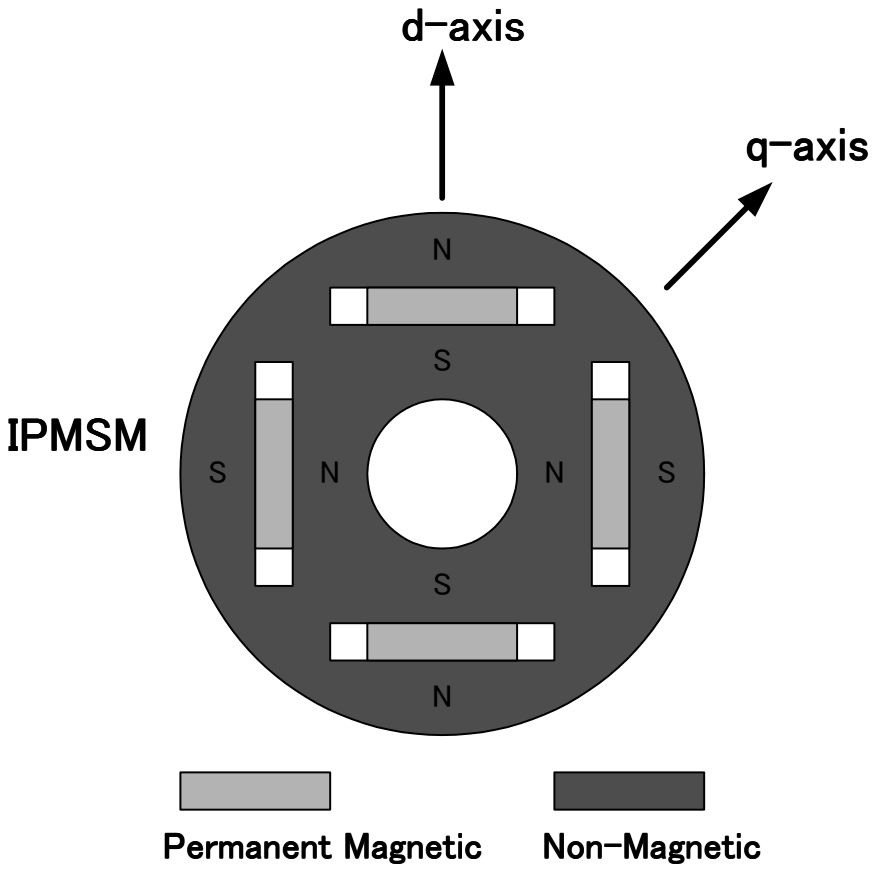

Fig. 1.6 Structure of the rotor of IPMSM.

This paper mainly proposed two kinds of methods to identify the interior permanent

magnet synchronous motor (IPMSM) parameters based on using the current signals. They are off-line and on-line identification methods. The difference between these two identification methods is that the off-line identification method required a drive equipment to control the IPMSM's rotation speed, while the rotation speed can be control by on-line identification method.

In the off-line parameter identification of a permanent magnet synchronous motor, its current norm is used. The current norm changes as a parameter mismatch varies, and the minimum or the maximum value is obtained when the parameter mismatch is completely eliminated. And the proposed identification technique includes mainly two kinds of identification systems. By changing the identification condition, these two identification systems can achieve q-axis inductance (L_q), d-axis inductance (L_d), resistance (R) and magnetic flux linkage (Ψ) identification, and the identification is divided into four steps.

By using this current norm characteristic, a simple hill-climbing method to search the minimum or the maximum point of the current norm, is possible to achieve the off-line parameter identification.

This thesis described a basic operation of the proposed approach, and shows relationship between the parameter mismatch and the current norm on the basis of the motor mathematical model, both computer simulations and experimental results were used to confirm the off-line parameter identification method which required two set of IPMSM control units. But this kind of method need two set of IPMSM control units to finished the experiment.

To overcome this problem and make the identification experiment simple. Another on-line identification method is also proposed.

This proposed new approach is to achieve on-line identification of the interior permanent magnet synchronous motor (IPMSM) based on the relationship between the mismatch of parameters and the feedback current. And the proposed identification technique also includes mainly two kinds of identification systems. By changing the identification condition, these two identification systems can achieve q-axis inductance

(L_q), d-axis inductance (L_d), resistance (R) and magnetic flux linkage (Ψ) identification, and the identification is divided into four steps.

The value of the feedback current depends on the mismatch of the parameters mismatch and the consecutive samplings of the feedback current, making it possible to calculate the true value of the unknown parameters. The proposed identification technique is examined through some computer simulations and experiment test. And the proposed system which has no sensitivity to resistance was also checked. The results of demonstrates the fast convergence of the identified value to the true one with a small error.

The good characteristic of off-line IPMSM parameters identification method and on-line IPMSM parameters identification method is that they are not sensitive to the winding resistance, which would be checked in the experimental part of this thesis.

Fig 1.5 shows the IPMSM control circuit which includes the angle calculation part and the controller part. Figure 1.7 is the control loop of this kind of system.

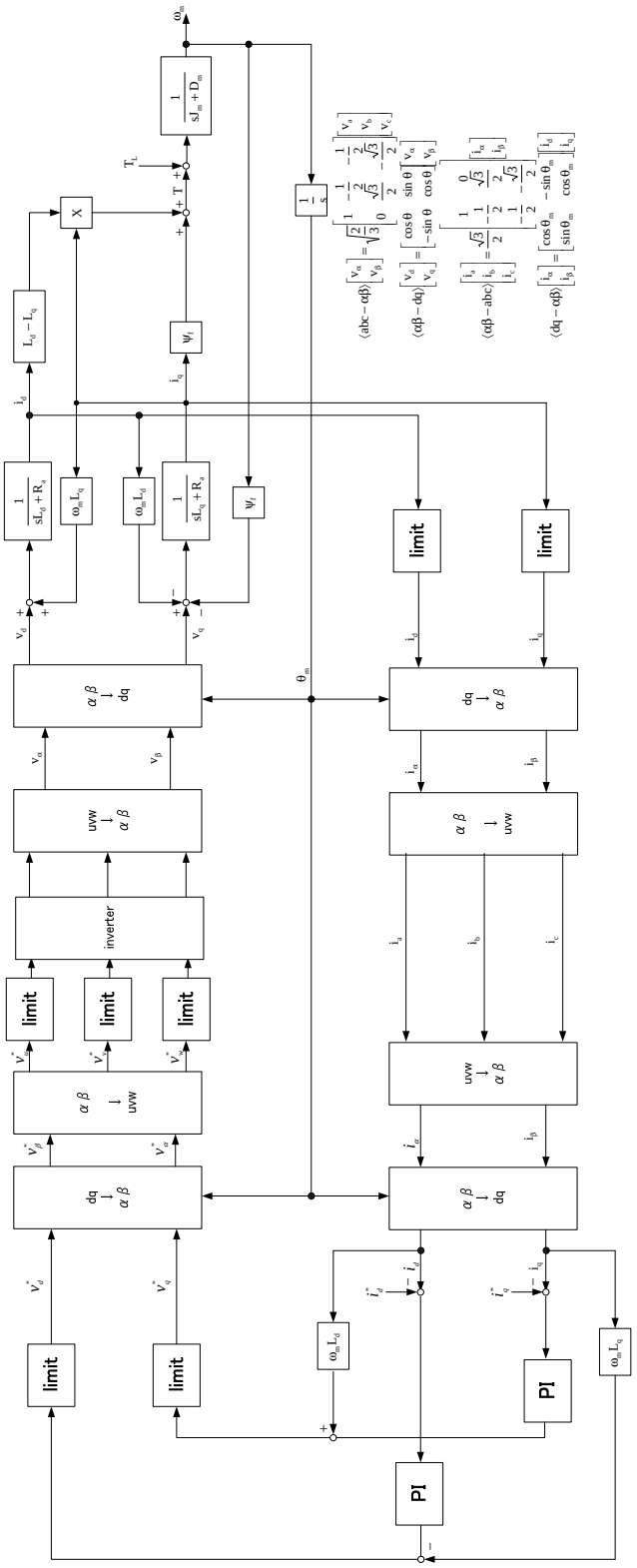

Fig 1.7 Control loop of the IPMSM.

1.2. Previous research case

Until now there are many kinds of methods can be used to identify the interior permanent magnet synchronous motor (IPMSM)'s parameters.

For example some of identification methods applied a mechanical senseless drive system for an interior permanent-magnet synchronous motor, for which parameters including the inverter are identified, is proposed in this paper. The rotor position is estimated by a signal-injection senseless scheme at standstill. The resistance, including the on-resistance of the insulated-gate bipolar transistor, the voltage error caused by the dead time of the inverter, and the d-axis and q-axis inductances are identified at standstill using the estimated position. After the motor starts by the signal-injection senseless control, the senseless scheme changes to a scheme based on the extended electromotive force estimation, which uses the identified parameters. The magnet flux linkage is also identified under the senseless operation.

And some of the methods choose focus on internal parameters of the motors and generators. They can become a cause of the changing internal parameters because they have sensitive characteristics due to external conditions. The changed parameters can generate the outputs which include error values from the speed and current controllers. Also, it can bring the temperature increase and mechanical damage to the system. Therefore, internal parameters of the motors and generators need to obtain their values according to the external conditions because it can prevent the mechanical damage caused by the changed parameters.

Most of these identification methods choose to use the voltage signal to identify the parameters.

In this thesis the current signal is chosen to identify the IPMSM parameters.

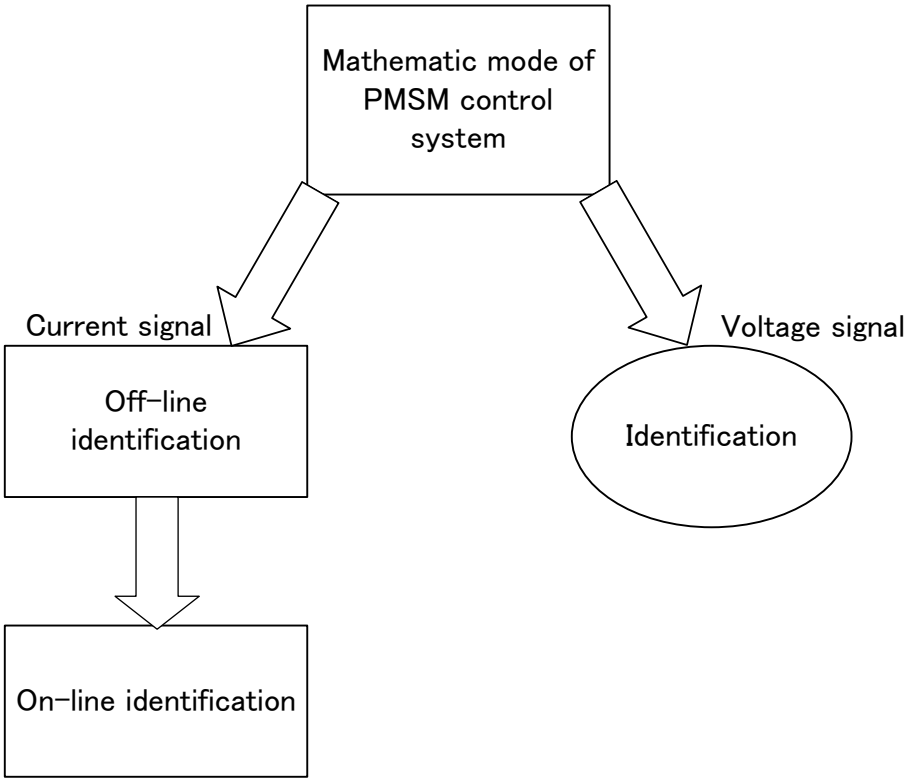

Fig. 1.8 Position of the proposed identification.

1.3. Research purposes

Most of the PMSM parameters identification are based on using the voltage signal. Because of the voltage sensor is indispensable to support these kinds of identification theory. But under some extreme situation, voltage signal is hardly to get. To serve this kind of situation, novel parameter identification method is necessary.

The purpose of this research is to check the possibility of only using the current signals to identify the unknown PMSM parameters. If the current signals can identify the PMSM parameters it means that it is possible to achieve parameters identification only by using the current sensor. And in some special situation if only the current signals is known that by using these current signals the PMSM parameters can be identified.

And the other identification method had some sensitive problem with the winding resistance. So the novel identification method also needs to serve the sensitive problem to winding resistance. Because of the proposed identification method using the current signals, theoretically the proposed identification method had no sensitive problem with the winding resistance when the PMSM is working in the steady state.

1.4. Overview

In this thesis the PMSM identification method had been proposed.

In chapter 2, the off-line identification method of SPMSM is proposed and confirmed by the simulation results further due to the SPMSM and IPMSM share similar mathematic model. Because of the SPMSM and IPMSM share similar mathematic model. And based on the simulation results this proposed identification method is possible to achieve the IPMSM's parameters identification.

Then two different kinds of IPMSM parameters identification methods are proposed. One is off-line IPMSM identification method; another is on-line IPMSM identification method. The off-line identification method confirms the possibility of using the current signal to identify the IPMSM parameters. To make the identification be simple, the on-line identification is proposed.

In chapter 3 the off-line IPMSM parameters identification theory is proposed and confirmed by the simulation results and experiment results. The hill-climbing method is used to identify the IPMSM’s parameters. In the end of this chapter, the sensitive problem is confirmed by experiment.

Chapter 4 introduced the on-line IPMSM parameters identification by employing the similar identification theory proposed. And the simulation and experiment are used to confirm the proposed identification theory. By taking two different points on the current characteristic, the true value of IPMSM's parameters can be speculating.

Chapter 5 informed the proposed identification method to identify the SPMSM and IPMSM parameters. And this proposed method had been confirmed by the simulation and experiment results. And this proposed identification method, can help to setup the controller when starting the motor.

2. Off-line SPMSM parameters identification theory

2.1. Introduction

The SPMSM and IPMSM had a similar mathematic structure. And based on this mathematic model the only difference between them is the inductance.[10][11] To check the proposed identification method can achieve the IPMSM identification, it is necessary to achieve the SPMSM identification first.

In this chapter the identification theory by using current signals is proposed to identify the SPMSM parameters. As the mathematic model of SPMSM control systems shown in Fig 2.1. The SPMSM had a simple structure and only three parameters to identify.

And the mathematic model of SPMSM control systems had shown in Fig 2.1. The decoupling control system is shown in Fig 2.2. The SPMSM had a simple structure and it only had three parameters need to identify.

And in the off-line identification, the rotation speed is controlled by another motor equipment. In the off-line identification only need to focus on the decoupling control system.

If the proposed identification method can achieve the SPMSM identification, then this identification theory also had a possibility to achieve IPMSM identification, because the SPMSM and IPMSM share the similar mathematic model. And the only difference between the SPMSM and IPMSM is the IPMSM had two different inductances. The proposed method had a possibility to achieve the IPMSM identification. [12]

The unknown SPMSM parameters are L_a, Ψ and R. And the identification is divided into three steps. In each identification step the identification conditions are different. Then in this chapter each parameter identification is introduced.

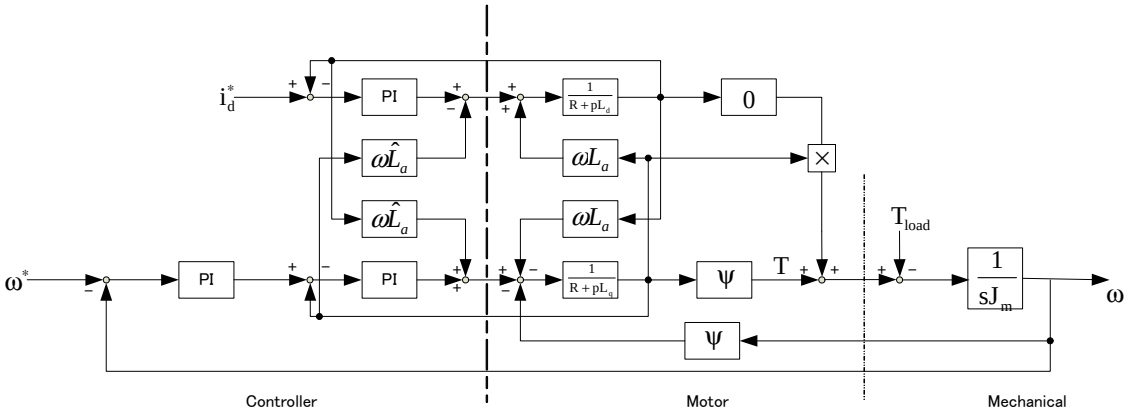

Fig. 2.1 Mathematic model of SPMSM control system

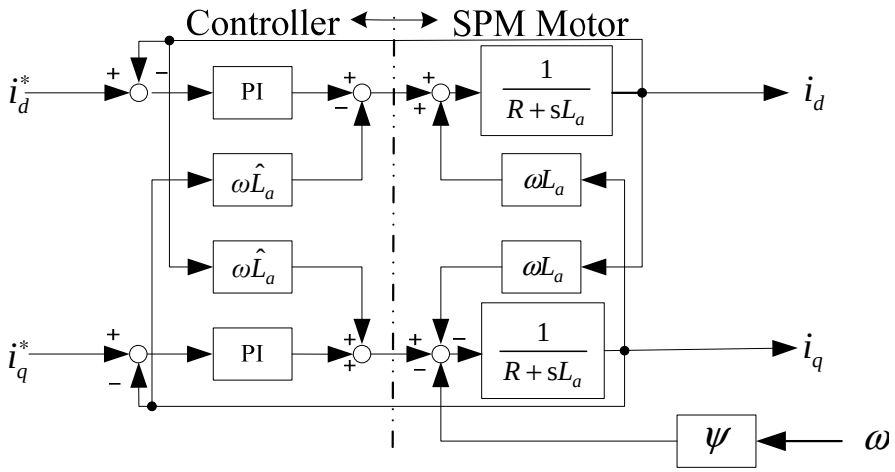

Fig. 2.2 Decoupling current control system of SPMSM

2.2. L_a identification

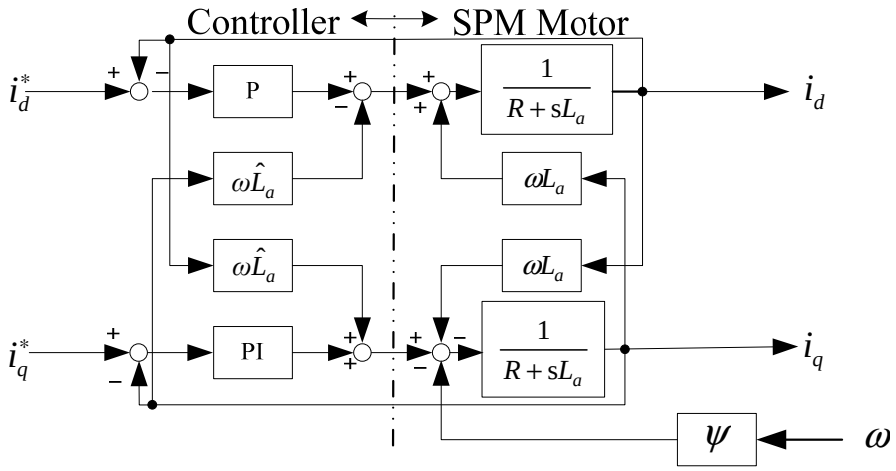

Fig. 2.3 Proposed L_a identification system.

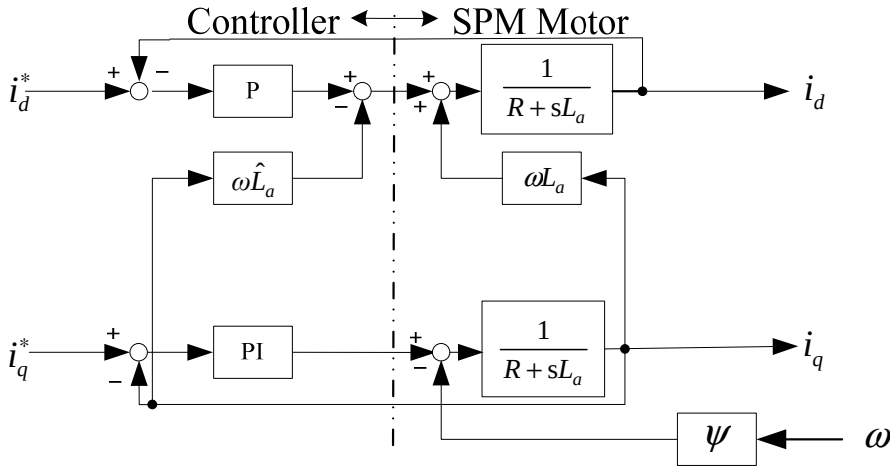

Fig. 2.4 Simplified proposed L_a identification system.

The proposed inductance identification system applied the P regulator to replace the PI regulator in the d-axis. And the proposed identification system is shown as Fig 2.3. Then the proposed system can be simplified to Fig 2.4.

In the proposed identification system, the d-axis current only receive the unknown inductance effect. And in the q-axis the PI regulator could isolation the other

parameters influences. Then based on the proposed identification system, the d-axis and q-axis could expression by the following formula:

$$i_d = \frac{i_d^* G_{pd}(G_{pq}+R) - i_q^* G_{pq}\omega(\hat{L}_a - L_a) + \omega^2(\hat{L}_a - L_a)\psi}{(G_{pd}+R)(G_{pq}+R) + \omega^2(L_a - \hat{L}_a)^2}$$

$$i_q = \frac{i_q^* G_{pq}(G_{pd}+R) + \omega i_d^* G_{pd}(\hat{L}_a - L_a) - \omega\psi(G_{pd}+R)}{(G_{pd}+R)(G_{pq}+R) + \omega^2(L_a - \hat{L}_a)^2}$$

by employing the identification condition: $i_d^* = 0, G_{pd} = G_{pq} = G_p$

the current norm is following as $I_n = \sqrt{i_d^2 + i_q^2} = \frac{\left| i_q^* G_p - \omega\psi \right|}{\sqrt{(G_p+R)^2 + \omega^2(L_a - \hat{L}_a)^2}}$.

Based on the formula the mismatch of inductance appeared in the denominator of the formula. When the inductance mismatch is equal to zero, the current norm value reaches the maximum point of it. As the mismatch increased the current norm value is reduced and it had a parabolic current norm characteristic. Then the simulation results by employed table. I parameters had been confirmed.

TABLE I PARAMETERS USED IN SIMULATION.

Symbol	Description	Value
R	Winding resistance	0.48 Ω
P	Rated output power	1.5 kW
ζ	Damping coefficient	0.0002 Ns/r
p	Number of poles	4
ω	Rotation speed	150 r/s
ψ	Magnetic flux linkage	0.0674 Wb
L_a	Inductance	27 mH
G_p	P regulator gain	1.0 V/A

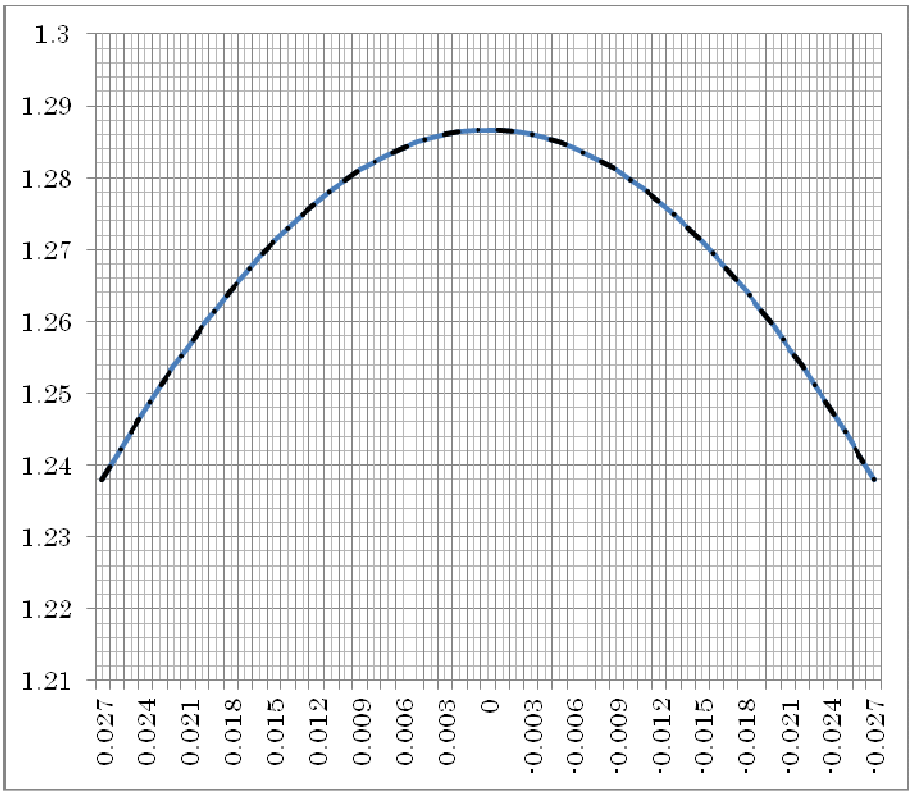

Fig 2.5 Current norm characteristic of changing L_a.

And the current norm characteristic of L_a is shown in Fig 2.5. Compared with the calculate results, the simulation results had a same characteristic and reached the maximum point when the mismatch of inductance is zero.

Because of the current norm had a parabolic characteristic and the maximum point is the true value of inductance. By searching the maximum point it is possible to identify the unknown inductance. And the hill-climbing method can help to search the maximum point.

2.3. ϕ identification

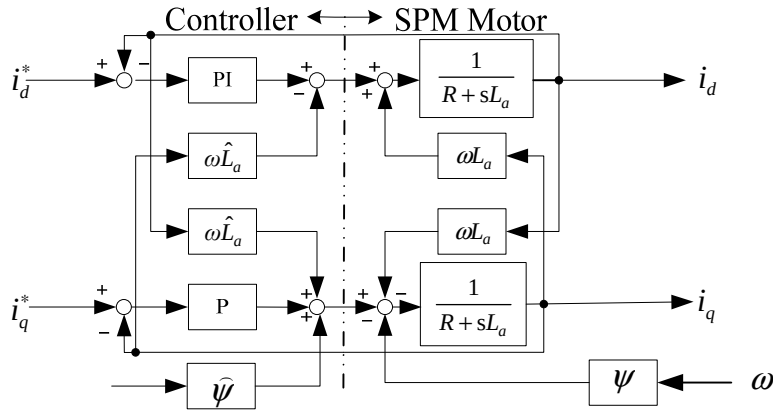

Fig 2.6 Proposed Ψ identification method.

Fig 2.6 shows the proposed Ψ identification system, in which q-axis PI regulator is changed to P regulator, and the d-axis command signal need to setup to zero. Because the command signal is setup to zero after the PI regulator works, the d-axis current also equal to zero. As the L_a had been identified, the proposed identification system can simplified to Fig 2.7.

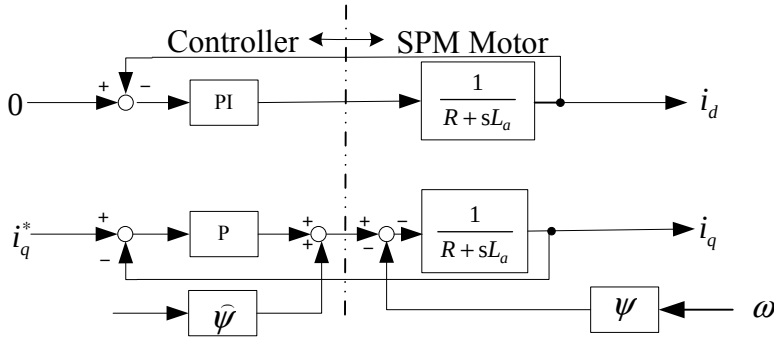

Fig 2.7 Simplified proposed Ψ identification method.

And based on the Fig 2.7 the q-axis current formula is: $i_q = \frac{\omega_c(\hat{\psi}-\psi)}{K_{Pq}+R} + \frac{i_q^* K_{Pq}}{K_{Pq}+R}$

This formula is constitute by two different parts. To get the special current norm characteristic it is necessary to reduced second part of this formula.

The method of reduced the second term of this expression, is just set the q-axis command signal to zero. Then the modified $i'_q = \frac{\omega_c(\hat{\psi} - \psi)}{K_{Pq} + R}$ q-axis current can be get. By using this expression and simulation, it is possible to get the characteristic curves and two curves shows same characteristics in Fig 2.8. As the characteristic shows the curve had a minimum with it.

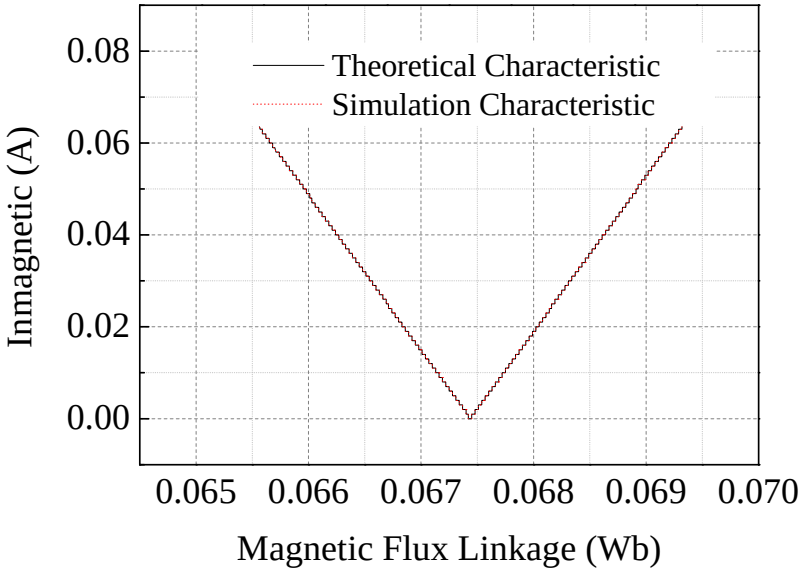

Fig. 2.8. Simulation result of motor current norm characteristic with respect to ψ mismatch.

When the magnetic flux linkage setup in the controller is equal to the true value of it, the current norm also reach the minimum point of it.

2.4. *R* identification

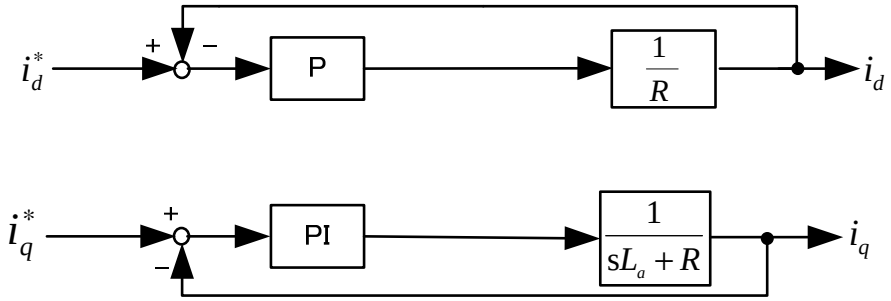

Fig.2.9 Simplified resistance identification system.

After the inductance and magnetic flux linkage had been identified, Only the resistance still unknown. Because the proposed identification method focusing on using the current signal to identify the parameters, so in this chapter, the resistance identification also use current signal to finish identification.

Fig 2.9 shows the proposed resistance identification system. In the proposed system, because of the inductance and magnetic flux linkage had already identified. The simplified resistance identification system can ignore the effect from identified inductance and magnetic flux linkage.

In the proposed identification system, the d-axis PI regulator is replaced by P regulator to get the current value. The identification system structure is as same as the inductance identification system. But the identification conditions are different. And by using this current value the resistance can be identified.

And by forcing on the d-axis, the resistance identification formula is shown as:

$$R = \frac{K_d (i_d^* - i_d)}{i_d} \;;\; (i_d^* \neq 0)$$

In this formula, the resistance is expressed by the P regulator gain, d-axis current

value and d-axis command signal. And the common point between these three participation amounts is these value can be known or setup by myself. It means the value of resistance can be calculated. By using this expression the *R* can be identified.

Theoretically test in low rotation speed rang can reduce the back EMF effect. In other words it could reduce the identification system influence. In this way it could improve the identification error.

3. Off-line IPMSM parameters identification

3.1. Introduction

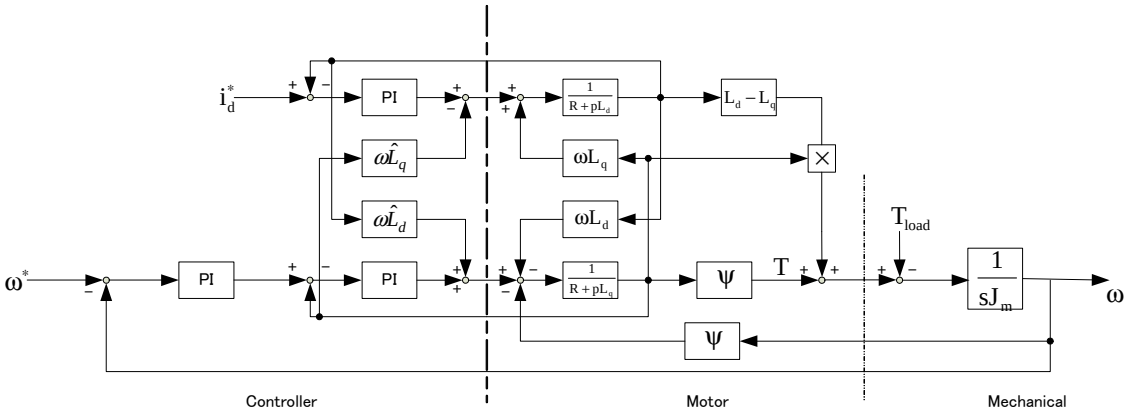

Fig. 3.1 Mathematic model of IPMSM control system

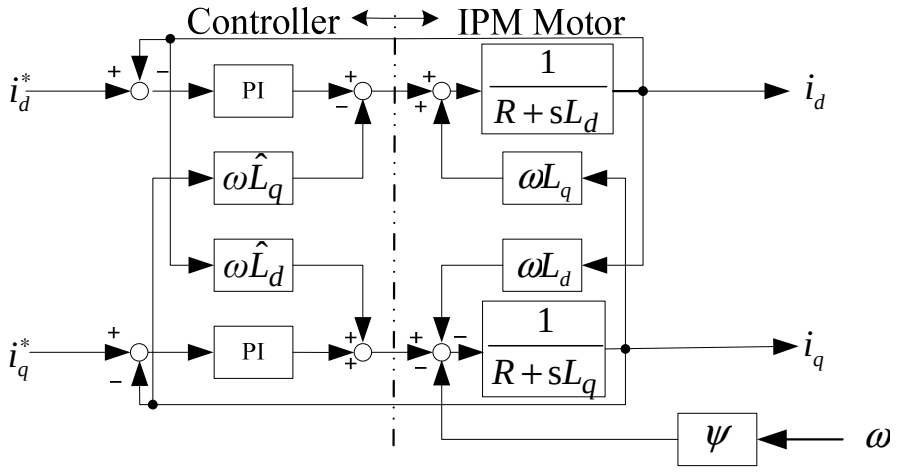

Fig. 3.2 Decoupling current control system of IPM motor

In previous chapter, the proposed system can create a special current norm characteristic and by using this current norm characteristic it is possible to identify the unknown SPMSM parameters. And by employ the hill-climbing method the parameters can be identified by searching the maximum point or the minimum point.

Also in previous chapter, this novel parameters identification theoretical for achieve the surface permanent magnet synchronous motor (SPMSM) had proposed. Because of the SPMSM and IPMSM share the similar mathematic model. Then proposed identification method is possible to achieve the interior permanent magnet synchronous motor (IPMSM) unknown parameters identification.

Throughout the identifications steps, only the current information and angle signals are required. The proposed technique does not use the voltage signal, but uses the current information and use several steps to complete the identification of all the parameters. And the current controller structure and identification condition also changed for each parameter's identification.

In this chapter the off-line IPMSM parameters identification method had introduced. The off-line parameters identification method created specific current norm characteristic and the current characteristic had a minimum point with it. Every time when the parameter setup in the controller is equal to the true value of the parameter the current norm also reach the minimum point of it. And by using this current norm characteristic it is possible to find the true value of the unknown parameters.

Fig 3.1 is the normal IPMSM control system, because the proposed off-line identification system mainly forcing on the current signals then the decoupling control system shown in Fig 3.2 is taken out for analysis.

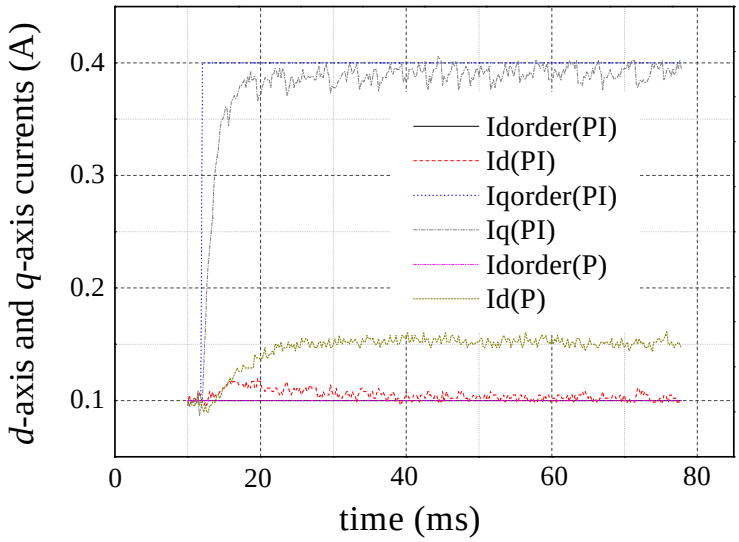

Fig. 3.3. Current step responses of P and PI regulators.

In the standard control system of the IPM motor, the field-oriented control (the vector control) technique is often used to control the instantaneous torque and the magnetic flux. The field-orientation is achieved by controlling the two-axis armature current components, i.e., the d-axis current and the q-axis current on the synchronously rotating dq-reference-frame. Figure 3.1 shows the normal control system block diagram including the decoupling current controller and the IPM motor. In the figure 3.1, the three-to-two-phase coordinate transformation and the rotational coordinate transformation are omitted for convenience because the magnetic-pole-position is accurately acquired by the mechanical position sensor such as a rotary encoder or a resolver. As can be seen in the block diagram, several motor parameters are required to compose the two-axis current control loops and to control the two-axis currents independently.

Figure 3.2 shows the main decoupling control system of the IPMSM.

The motor parameters can be simply calculated by using the voltage and current information on the basis of the inverse motor model. However, detecting the real voltage is not pragmatic because no voltage sensors are installed in the standard controller. Even though the voltage commands generated by the current regulators are

used instead of the real voltages, there must be errors in the voltage commands because of the dead time and the voltage drop of the power transistors in the inverter. On the other hand, the accurate current detection is inherently available in the controller by employing some Hall-effect current transducers. It is the simplest and the most pragmatic way, therefore, to utilize only the current information without any complicated mathematical calculation in the motor parameter identification. In addition, it is necessary to avoid the undesirable mutual interferences among the parameters in each parameter identification process.

In order to achieve this goal, the proposed technique introduces modifications of the current control loop structure, and focuses on the motor current norm characteristics with respect to the parameter mismatches. By change the structure of the control system. Figure 3.3 shows the experiment results after employ P regulator to replace the PI regulator. Based on the experiment results, that when using the PI regulator the current signal is under the control and equal to the command signal. After changing the PI regulator to P regulator the current is out of control, and bigger than the command signal.[14][15] The proposed identification system is based on using this P regulator feature.

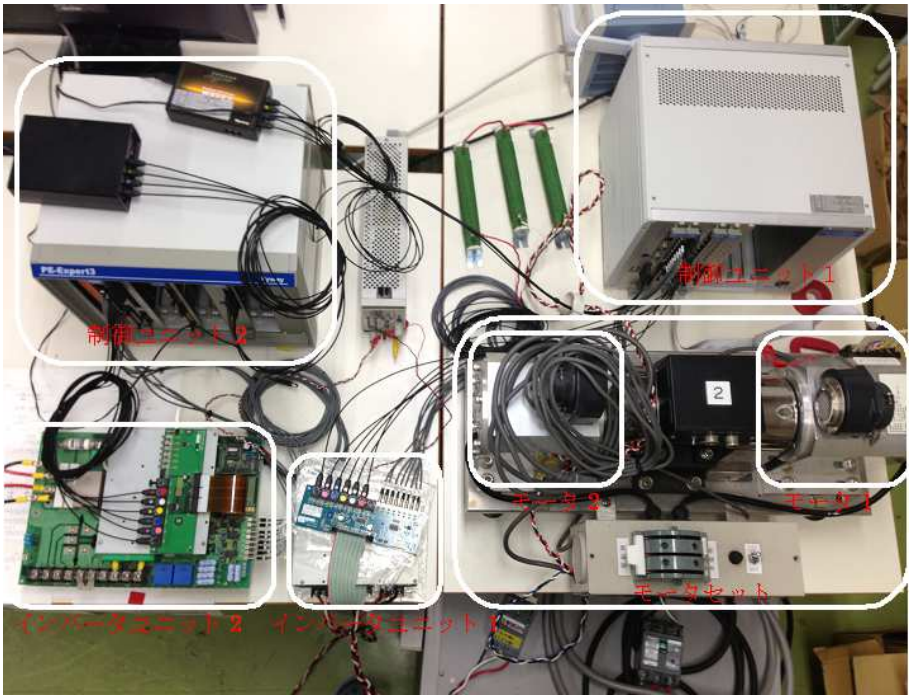

Fig. 3.4. Off-line experiment test equipments.

As shown in Fig 3.4, two IPM motor were used, and connected between each other. Also two inverter units had been used to control these two IPM motors. One IPM motor's mission is to control the rotation speed and another IPM motor is use for testing the proposed identification method.

In the end, the experiment results of identify the d-axis and q-axis inductance values by the proposed method and measured method are compared with each other is shown in Figure 3.5. And the experiment results shows that two identification methods test results have very similar trends. In other way that experiment results shown in Figure 3.5 that effectiveness of the proposed identification methods has been verified.

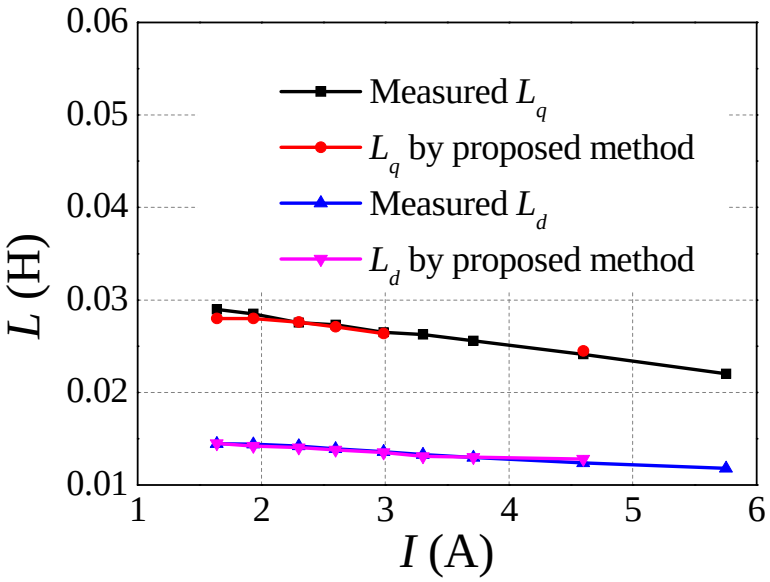

Fig. 3.5. Experiment inductance compare.

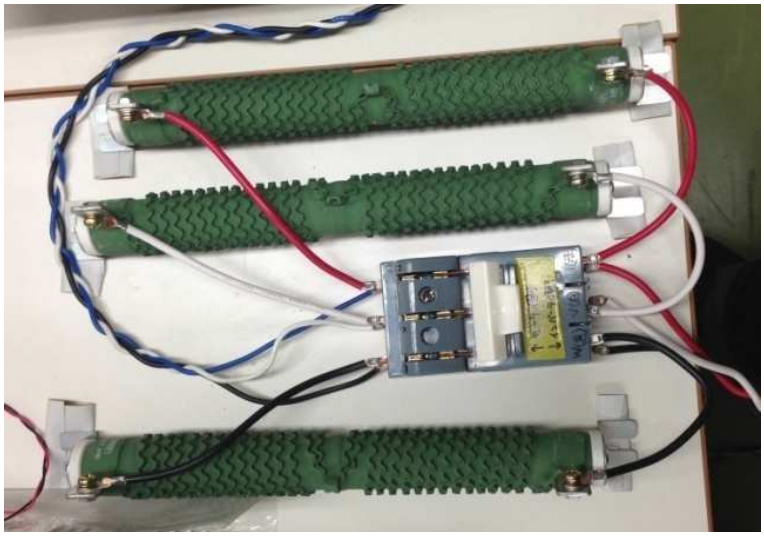

Fig. 3.6. Off-line experiment test equipments of extra resistance.

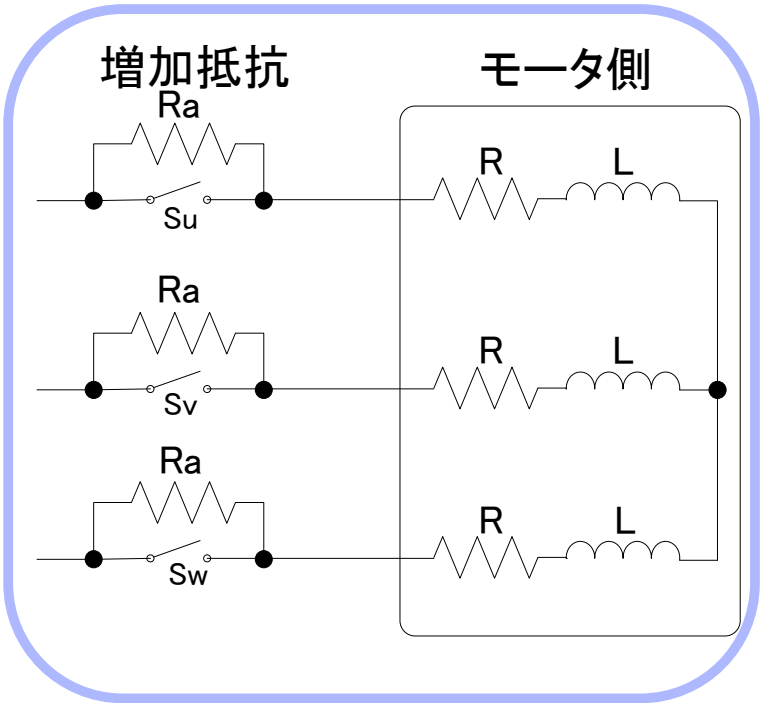

Fig. 3.7. Extra resistance connection circuit.

One feature of the proposed identification system is had no sensitive problem to the winding resistance. It means when the temperature changed, the winding resistance is also changed because the resistance is sensitive to the temperature. But the proposed identification method still could serve this problem. Because the proposed method was forcing on search the current characteristic minimum point or the maximum point. After each parameter is identified same resistance is connected into the system for testing the sensitive problems.

As in the simulation results parts shows. That the proposed method had no sensitive problems to the resistance. To confirm this problem, the sensitivity to the winding resistance is also checked by the experimental test. Fig 3.6 and Fig. 3.7 shows the circuit connecting of the experiment. As shown in Fig 3.7 three same resistances are connected into the circuit parallel with switching device. Following the formula (a), the resistance changing can simulate temperature changing for 133.2 degree.

$$\frac{234.5+T}{234.5+25}=\frac{0.68}{0.48}=1.42, \quad T=133.2 \quad \text{(a)}$$

And based on the experiment results that the identification error is bigger than the simulation results. Considering to reduce these identification errors the following possible reasons are inform:

1) Ripples of the motor current norm, and

2) Undesirable fluctuation of the low-rotation-speed, which has an impact to the current norm.

To overcome these problems, the following countermeasures can be effective solutions:

1) Reduction of ripple effects using averaging scheme of the motor current norm, and

2) Testing in higher speed region to reduce the fluctuated speed effect or adding the speed control loop to the proposed identification system to make the speed control more stable.

3.2. L_q identification

3.2.1. L_q identification theory

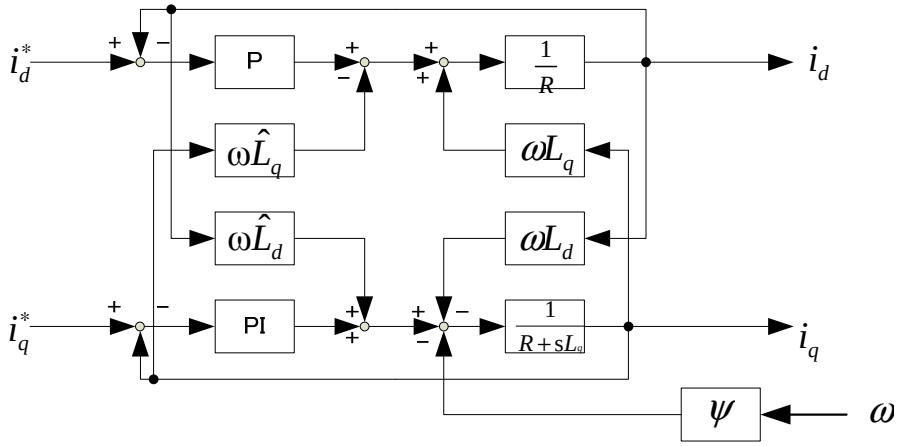

Fig. 3.8 q-axis inductance identification system.

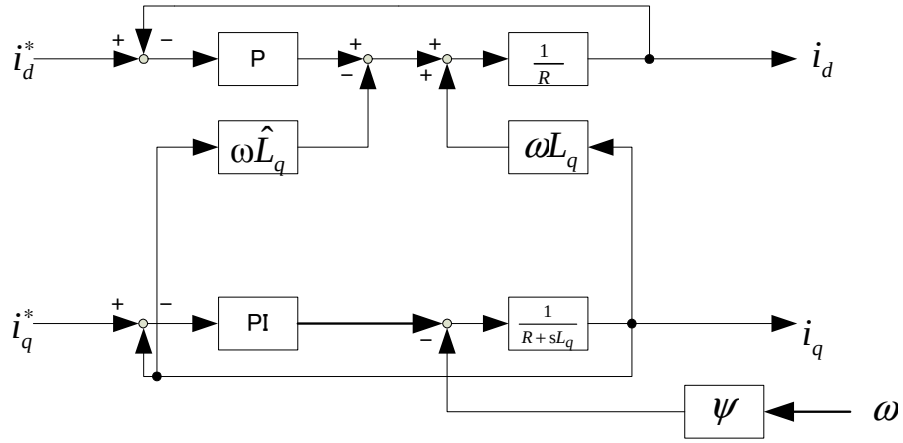

Fig. 3.9 Simplified q-axis inductance identification system.

In the case of the L_q identification, the structure of the current control loops is changed as shown in Fig. 3.8, where the d-axis PI regulator is replaced with a low-gain P regulator to let the current norm have a large variation. On the contrary, the q-axis current regulator remains the PI form to suppress the interferences from the d-axis and the back electromotive force (e.m.f.).[16][17] No matter how much parameter mismatch

exists between the real d-axis inductance L_d and the set value $\hat{L}_d$ in the controller, the steady state error of the q-axis current is perfectly eliminated because the PI regulator is employed in the q-axis current control loop, i.e., $i_q^* = i_q$ is guaranteed in the steady state.

Therefore, the modified current controller in Fig. 3.8 can be simplified as shown in Fig. 3.9 in the steady state. The q-axis PI regulator has the following transfer function:

$$G_{PIq}(\mathrm{s}) = K_q\left(1+\frac{1}{\mathrm{s}\tau_q}\right). \qquad \text{(b)}$$

In the above transfer function, the P gain K_q and the integral time constant τ_q are designed as follows:

$$K_q = \omega_c L_q, \text{ and } \tau_q = \frac{L_q}{R}, \qquad \text{(c)}$$

where ω_c is a designed crossover frequency of the q-axis current control loop.

From the simplified current controller shown in Fig. 3.9, the following relationship is mathematically derived:

$$i_q = i_q^*, \qquad \text{(d)}$$

$$i_d = \frac{i_q^*\omega_c(\hat{L}_q - L_q)}{K_d + R}, \text{ and} \qquad \text{(e)}$$

$$i_n = \sqrt{i_d^2 + i_q^2}\ . \qquad \text{(f)}$$

In the above equations, i_n is the motor current norm. It is found that i_n is a

parabolic function of the L_q mismatch and that it takes the minimum value when the L_q mismatch is completely canceled out. It should be also noted that i_n always becomes minimum when $\hat{L}_q = L_q$ regardless of any other variables and parameter values.

It other words the q-axis inductance identification problem had changed to searching the minimum point of the current characteristic problem. Based on the formula (e), the P regulator gain or the resistance changing only effect the parabola amplitude, but the minimum point always appears when the mismatch is zero.

3.2.2. L_q identification simulation

Table 1. Parameters of IPMSM.

Number of poles	4
Winding resistance	0.48 Ω
Rated output power	1.5 KW
Rated rotation speed	7200 r/min
Field flux linkage	0.06737 Wb
Damping coefficient	0.00019 Ns/rad
Q-axis inductance	12 mH
D-axis inductance	7.3 mH
Simulation speed	3000 r/min

In this section the simulation is using to check the identification theory. Table 1 is the parameters setup in the simulation system. And the simulation test using the Power Simulation (PSIM) software.[33][34]

Then the simulation control circuit had been created as showing in Fig 3.10. The simulation circuit only shows the decoupling control system of IPMSM. The left part instead of the controller and the right hand side is the motor of the IPM.

Then the simulation results had been proved in Fig 3.11. Based on the simulation results as q-axis inductance setup in the controller increased from 0.0mH to 15.0mH. The current norm shows a parabolic characteristic. This parabolic characteristic reaches the minimum point when q-axis inductance setup in the controller equal to its true value. The true value of the simulation motor is 12.0 mH, the minimum point is 12.013 mH. This result had a error about 0.11%.

A further confirmation between the simulation results and calculation results also checked. In this part the rotation speed and command signal of q-axis current had been changed.

In the end, the comparison results shows in Fig 3.12. Two current characteristic

shows similar parabolic characteristic. And the two current norm characteristics curve are same. The horizontal axis is the mismatch of q-axis inductance. When the mismatch equal to zero, the current norm reach the minimum point of it.

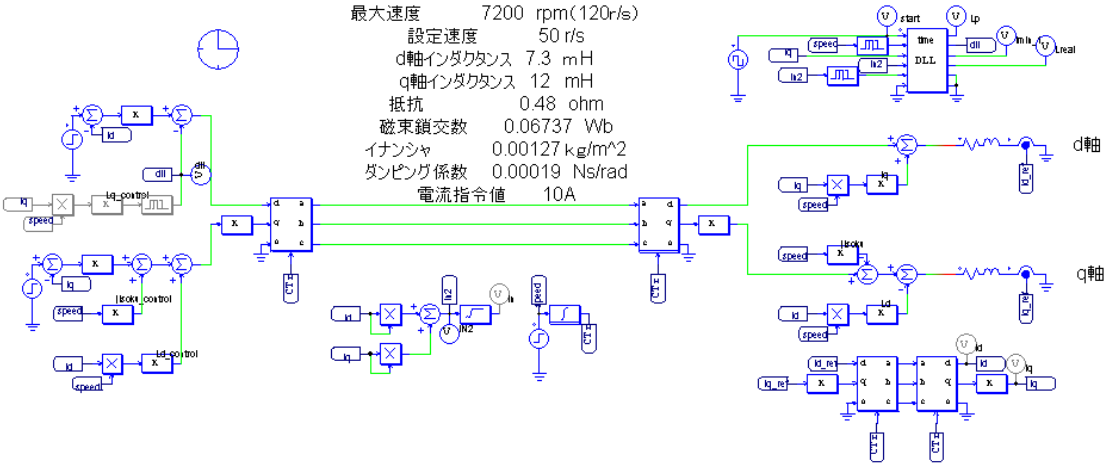

Fig. 3.10 Control circuit of identification system.

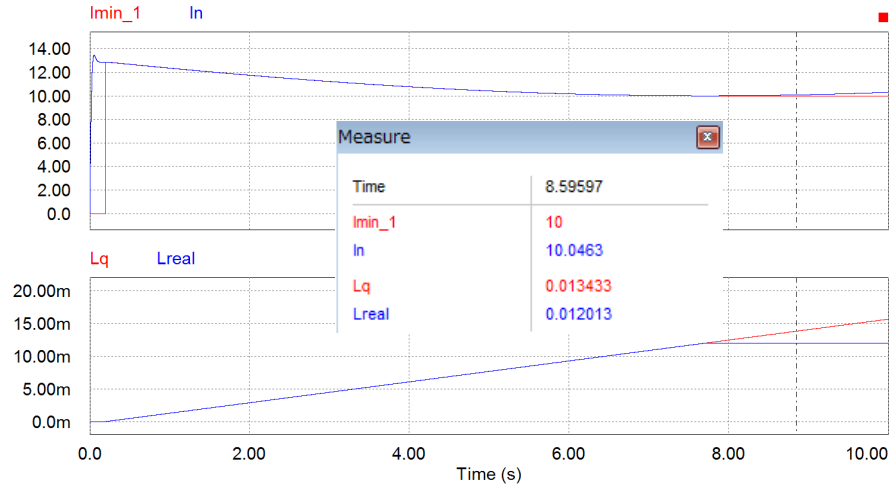

Fig. 3.11 Simulation results of current characteristics.

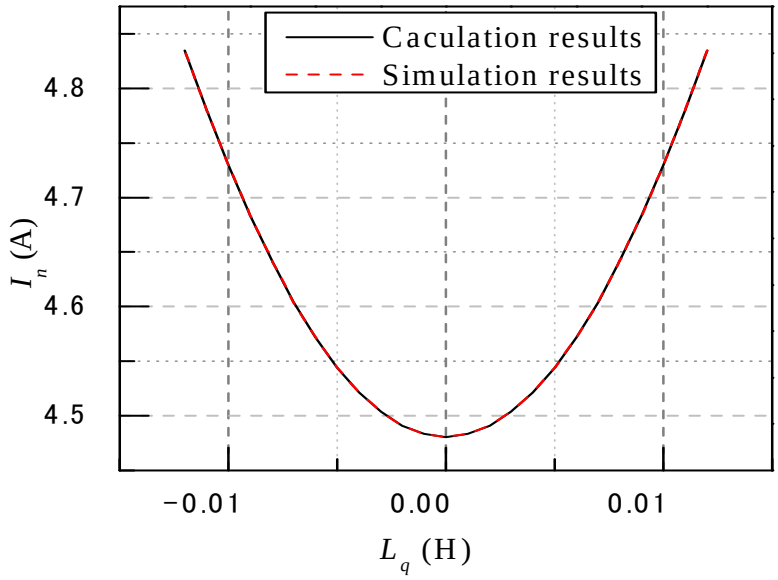

Fig. 3.12 Characteristic comperiation between caculation and simulation results.

As the current norm characteristic had confirmed by simulation results and caculation results. Then the identification problem is changed to searching the minimum point. To searching this minimum point of the current norm characteristic, the hill-climbing method had been proposed for minimum point searching.

Figure 3.13 shows the simulation identification results by employing hill-climbing method. At first the q-axis inductance setup in the controller changing by the same difference. And in this time the current norm value keep reducing anyway. When the current norm value increased, the difference reduce to its half and q-axis inductance changing direction also changed. In the end the identification stops at 12.0341mH. Identification error is 0.108%.

As the parabolic characteristic was confirmed in the above preliminary test, the simulation adopting the hill-climbing-algorithm was conducted to check the dynamic behavior of the L_q identification.[35] Table 1 shows the fundamental physical constants of the simulation. Figure 3.13 shows the simulation result. It is found that the set value in the controller stably converges to the true value within the identification error of 0.3 %.

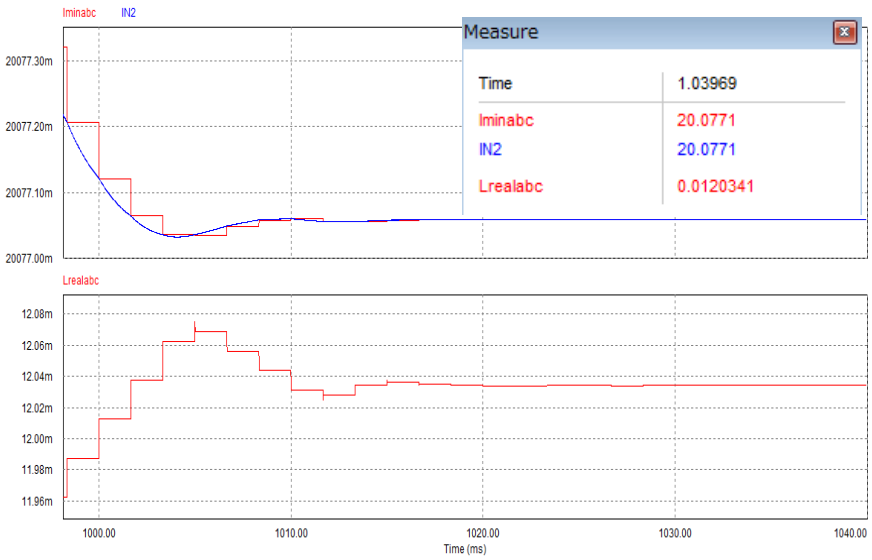

Fig. 3.13. Simulation result of employing hill climbing method.

3.2.3. L_q identification experiment

This section is mainly introduced the q-axis inductance identification experiment results. In this section, first the current norm characteristic will be checked, and then the hill-climbing method is employed to find the minimum point of the current norm characteristic. In the end of this section, the sensitive of resistance problem also checked by experiment. The experimental setup is shown in the Table 2.

Table 2. Physical constants of test setup.

Symbol	Description	Value
R	Winding resistance	0.48 Ω
L_d	d-axis inductance	13.0 mH
L_q	q-axis inductance	24.5 mH
ψ	Magnetic flux linkage	0.0674 Wb
K_d	d-axis P regulator gain	1.0 V/A
K_q	q-axis P regulator gain	1.0 V/A
p	Number of poles	6
P_o	Rated output power	1.5 kW
I^*	Current command	4.5 A

Off-line experiment test equipment had two same IPM motors and was mechanically connected through the torque meter. One motor is controlled by the current controller as shown in Fig. 3.4, and the other is used merely as a generator with load resistors. The operations parameters of the experimental setup are listed in Table 2, whose most parameters, are the same as those used in the simulations.

In the chapter the off-line q-axis inductance identification experiment results are informed. As Fig. 5.5 shows the motor current norm characteristics obtained by the simulation and the experimental test, where the black and the red lines are the simulation and the experimental results, respectively. As can be seen in the graph, the two curves have the minimum points at the same values of L_q. However, the experimental test was broken off in the range of the high L_q region, and the parabolic characteristic was lost due to the unstable rotation of the test motor.

As the parabolic characteristic was confirmed in the above preliminary test, the simulation adopting the hill-climbing algorithm was conducted to check the dynamic behavior of the L_q identification.

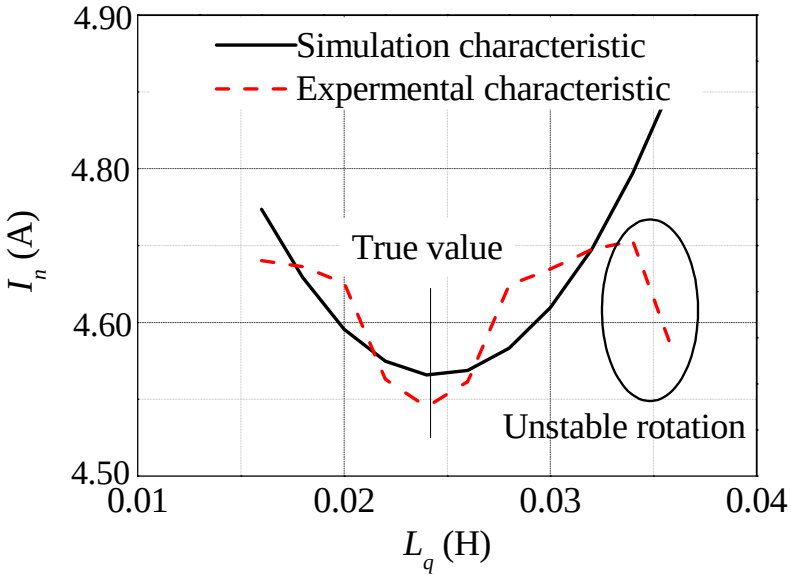

Fig. 3.14. q-axis inductance current characteristic.

Attention must be paid to the initial parameter values set in the controller, i.e., ψ and L_d intentionally have the initial errors. These errors make it possible to verify the robustness of the proposed identification technique. Prior to the experimental tests of the proposed technique, the relationship between the motor current norm and the L_q mismatch was confirmed, where the set value in the controller $\hat{L}_q$ had the tuning range from 16.0 to 36.0 mH as indicated in Table 4.

Figure 3.14 shows the motor current norm characteristics obtained by the simulation and the experimental test, where the black and the red lines are the simulation and the experimental results, respectively. As can be seen in the graph, the two curves have the minimum points at the same values of L_q. However, the experimental test was broken off in the range of the high L_q region, and the parabolic characteristic was lost due to the unstable rotation of the test motor.

As the parabolic characteristic was confirmed in the above preliminary test, the simulation adopting the hill-climbing algorithm was conducted to check the dynamic behavior of the L_q identification.

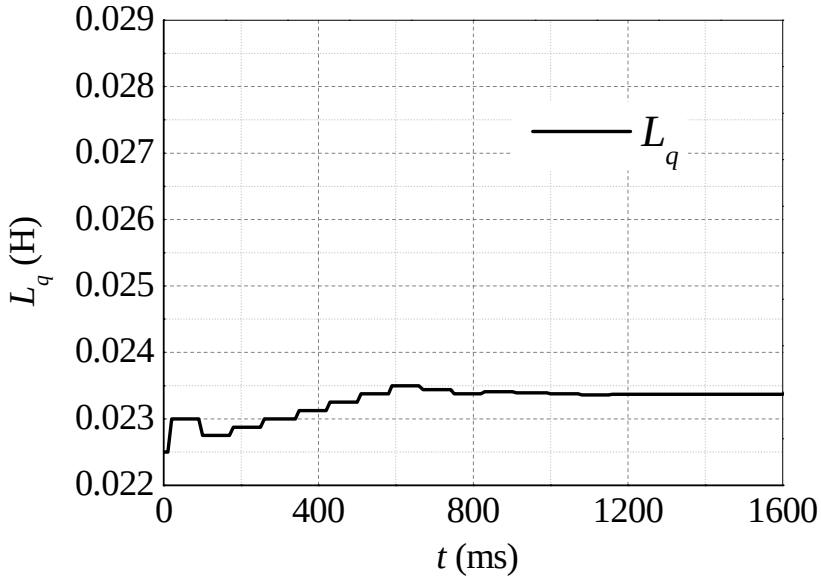

Fig. 3.15. q-axis inductance identification results.

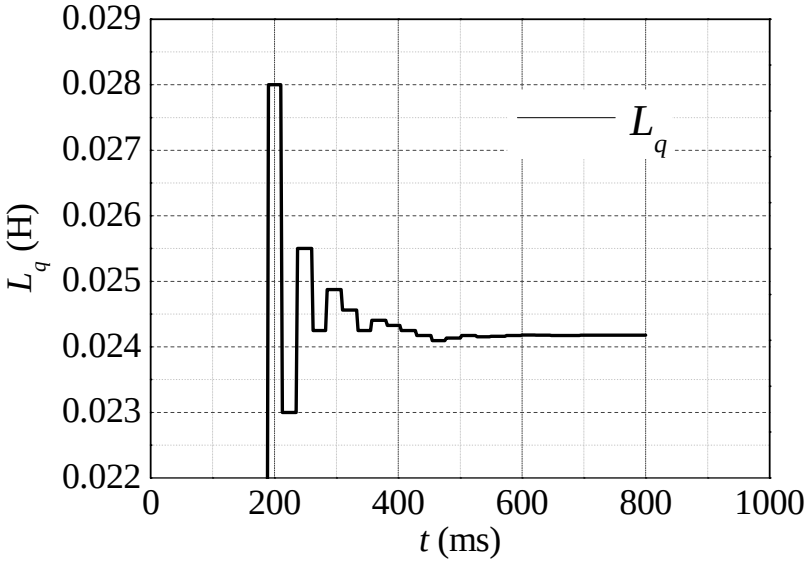

Fig. 3.16 Experiment L_q identification.

Figure 3.15 shows the experimental result of the proposed technique. The dynamic convergence behavior of the set value of L_q has a slight overshoot with a damping, and the final converged value is 23.4 mH. The true value of L_q is 24.5 mH, so the identification error is 4.5 % in the test. From this result, the proposed technique is capable to identify L_q stably within the error of approximately ±5 %. In the first chapter the reason of the identification error also proposed. The identification program stops when the q-axis inductance changing difference is smaller then 0.05mH.

Then the advantage of this proposed identification method had no sensitive problem to resistance was checked by experiment. To simulate the resistance variation due to the temperature change, the external resistance is inserted between the motor and the inverter. The added external resistance is 0.2 Ω. Compared with the motor winding resistance, the total resistance is changed by 41.7 %, and this can simulate the winding temperature rise of over133.2°. Figures 3.16 shows parameter identification result. The resultant identified value of L_q is 0.0242 mH (error 0.5 %). The identification error is within approximately 5 %.

3.3. ψ identification

After q-axis inductance had been identified, the next identification step is the magnetic flux linkage identification. The ψ identification system structure is similar as the d-axis inductance identification system, only the identification conditions are different.

The reason of identify the ψ in the first step is because d-axis inductance influence can be easily eliminate by setting the d-axis command signal to zero. In that kind of situation the ψ is the only ingredient left in the identification system. It is also easy to check the affect of it.

3.3.1. ψ identification theory

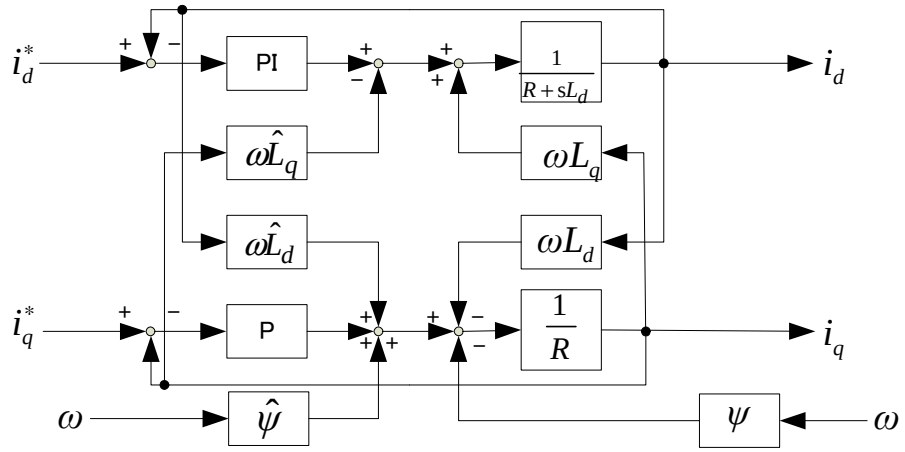

Fig. 3.17. Structure of current control loops on ψ and L_d identification.

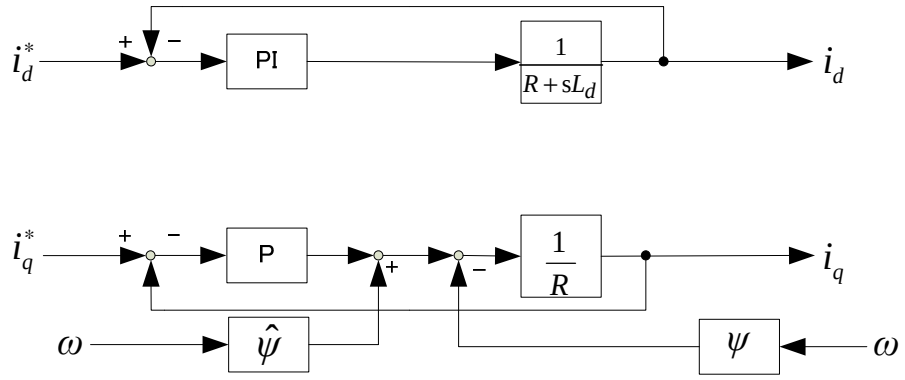

Fig. 3.18. Simplified current control loops on ψ and L_d identification when $i_d^* = 0$.

In a similar manner, ψ and L_d can be identified with the same approach. However, some minor modification is required to identify these parameters separately. After L_q is identified as described in the previous section, the current control loop structure is changed to that shown in Fig. 3.17. Figure 3.17 shows the configuration of the current control loops changed for the ψ and L_d identifications, where the d-axis employs the PI regulator but the q-axis current regulator is replaced with a low-gain P regulator. Therefore, the steady state error in the d-axis current control loop is perfectly eliminated, but the q-axis current involves some amount of the steady state error due to the back

e.m.f. and the L_d mismatch. In order to carry out the separate identification of these two parameters, the identification process is divided into the following two steps.

In the first identification step of ψ, the d-axis current command $i_d^* = 0$ is given to the controller. Since the d-axis current control loop employs the PI regulator, $i_d = 0$ is achieved with no steady state error. In addition, a cross decoupling term through ωL_d and $\omega \hat{L}_d$ from the d-axis to the q-axis can be ignored because $i_d = 0$ is guaranteed.

In this case, only the parameter mismatch of ψ affects the steady state error of the q-axis current. Taking the above discussion into account, the current controller structure can be simplified as shown in Fig. 3.18, where the back e.m.f. compensation block is virtually added to the q-axis current control loop in the controller for the purpose of the ψ identification.

Mathematical expressions of i_d and i_q can be derived from Fig. 3.7 as presented by (g) and (h):

$$i_d = i_d^* = 0, \text{ and} \qquad \text{(g)}$$

$$i_q = \frac{\omega_c(\hat{\psi} - \psi)}{K_q + R} + \frac{i_q^* K_q}{K_q + R}. \qquad \text{(h)}$$

The second term of the right-hand side in (h) affects the identification of ψ, so this part must be eliminated from the calculation without using the winding resistance of the motor. This can be done by two different method.

First kind of method is using the d-axis current control loop as a simulator of the second term in (h). As mentioned previously, d-axis current control loop no longer has any interference from the q-axis because L_q has been already identified, i.e., $\hat{L}_q = L_q$.

Therefore, if the d-axis current regulator is changed to a P regulator whose gain is equal to K_q and the d-axis current command is changed to the value equal to i_q^*, the resultant d-axis current comes to have the same value as the second term of (h). This implies that the second term of (h) can be found with no knowledge of the winding resistance. By memorizing the simulated second term value in the d-axis current control loop from and by subtracting the memorized value (h), the most important part can be extracted from (h) as follows:

$$i_q' = \frac{\omega_c(\hat{\psi} - \psi)}{K_q + R}. \qquad \text{(i)}$$

Besides the identification works in the steady state, and R is assuming constant. By using (g) and (i), the motor current norm is expressed as

$$i_n = \sqrt{i_d^2 + i_q'^2} = \frac{\omega_c(\hat{\psi} - \psi)}{K_q + R}. \qquad \text{(l)}$$

By tuning the set value $\hat{\psi}$ in the controller, the value of i_n varies accordingly and becomes zero (the minimum value) when $\hat{\psi} = \psi$. And this kind of method can used in not only off-line identification but also in on-line identification. But the disadvantage of this method is this method make the identification complex.

But the second kind of method is much more simple then the first kind of method. Because it is off-line identification, so it is possible to just set the q-axis command signal equal to zero. Then the second term of (h) can be eliminated. In the end formula (i) and (l) also can be get from this kind of method.

No matter which kind of method is employed, theoretically the current norm characteristic do not change.

3.3.2. ψ identification simulation

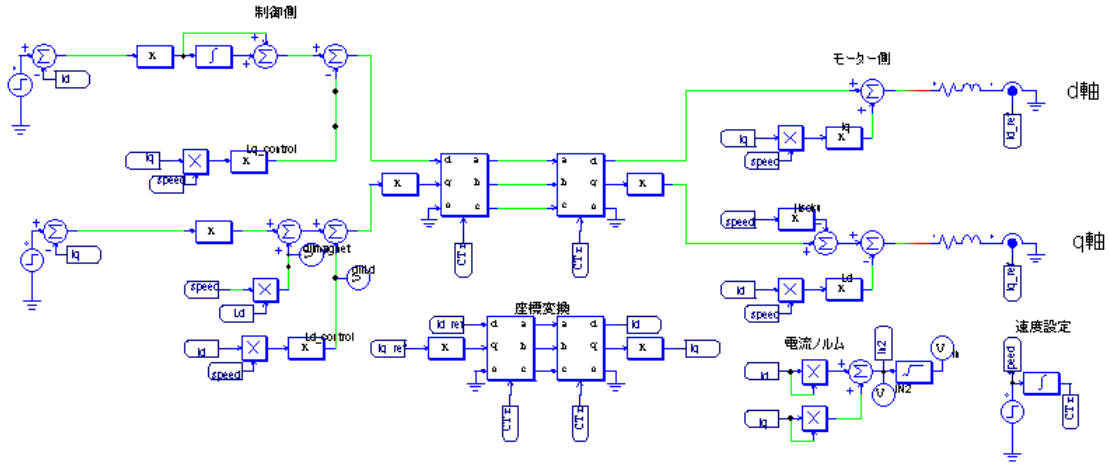

Fig. 3.19 Simulation circuit of Ψ identification.

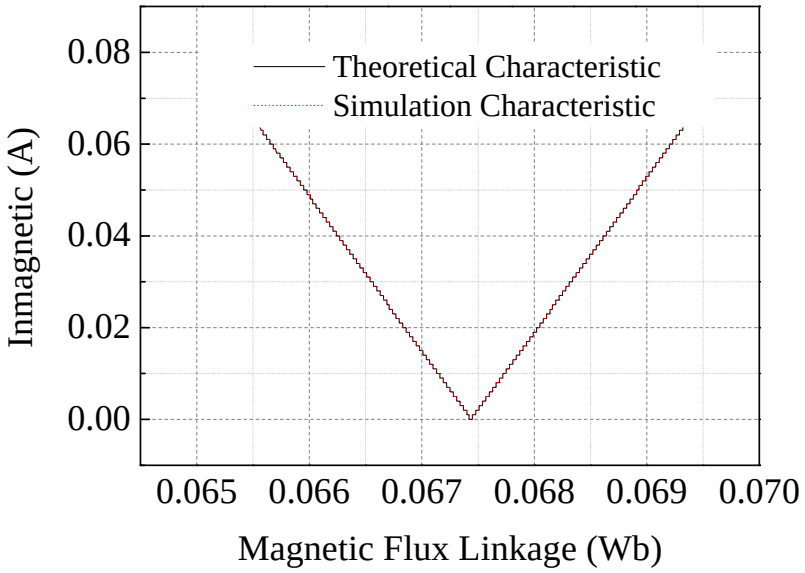

Fig. 3.20 Calculate results of current norm characteristic.

The identification system is proposed in Fig 3.19. This identification system is formed by Fig 3.17 which the P regulator is used in q-axis and the PI regulator used in d-axis. Because of that when setup the d-axis command signal equal to zero, the

d-axis inductance influence can be eliminate. Then only the Ψ set in the controller and in the real motor will affect the q-axis current value. This supply a perfect situation for testing the affect between the mismatch of Ψ and current norm.

First simulation results are the current norm characteristic compare result between the simulation results and calculation result. Figure 3.20 shows two current norm characteristic is same. Based on this the current norm characteristic had a turning point, and this turning point is also the minimum point of it. In the simulation and calculation the Ψ changing rang is from 0.0655 to 0.0695 Wb. The minimum point appears at the true value of Ψ.

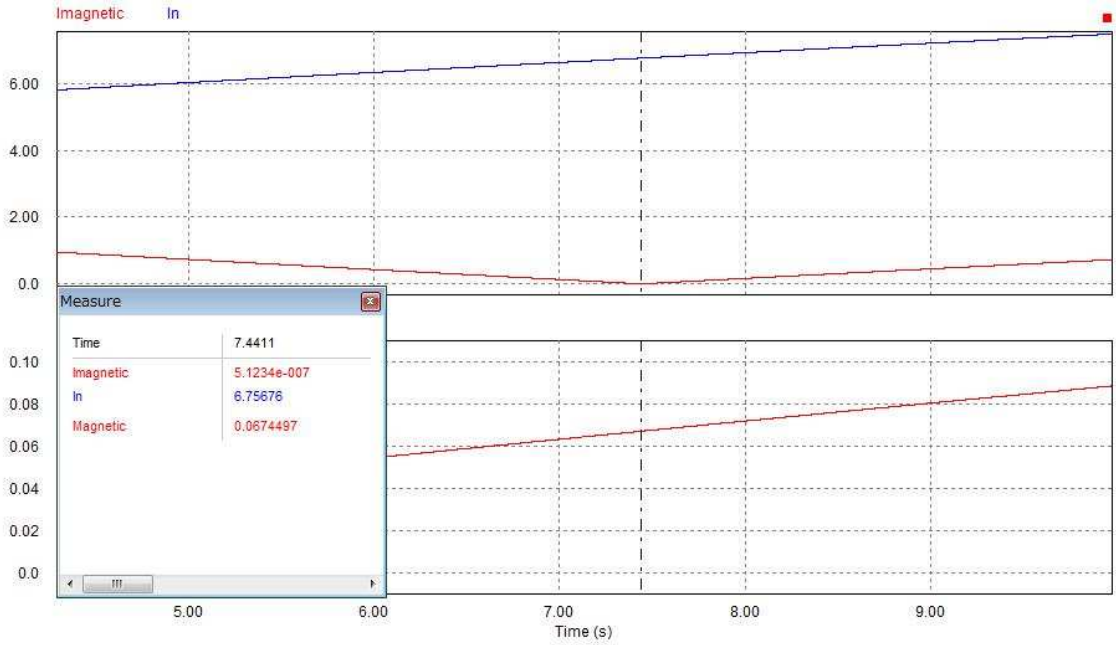

Fig. 3.21 Simulation current characteristic confirm of Ψ.

The current norm characteristic modified by eliminating the second term in (7) is shown in Fig. 3.20. Based on Fig. 3.17 the simulation circuit Fig. 3.19 had been created. In Fig.3.19 the controller had divided in two axes. In d-axis the PI regulator is used to reduce the effect from q-axis inductance and the command signal of d-axis current also setup to zero to kept d-axis current equal to zero. In q-axis the P regulator is used to replace the PI regulator. Because of that, the q-axis could accept the effect from the unidentified magnetic flux linkage. And by changing the magnetic flux

linkage setting in the controller could help to changing the effect to q-axis current. When q-axis current reach the minimum of it, the magnetic flux linkage setting in the controller is just equal to the true value of the magnetic flux linkage. And at the same time because of the d-axis current is just equal to zero, it helps to reduced the unidentified d-axis inductance effect.

By using Fig.3.19 system, the current characteristic can be confirmed and the current characteristic is shown in Fig 3.21. In the simulation results as the magnetic flux linkage changes the current norm had a minimum point with it. When the current norm reaches the minimum point of it, the magnetic flux linkage also reaches the true value of it.

3.3.3. ψ identification experiment

By tuning the set value $\hat{\psi}$ in the controller, the value of in varies accordingly and becomes zero (the minimum value) when $\hat{\psi} = \psi$.

To confirm this, the experiment was conducted. From Fig. 3.21 that the current norm characteristic with respect to ψ is not parabolic but linear, but that the current norm takes the minimum value when the mismatch of ψ is cancelled out. And it is similar with the simulation results.

To achieve the ψ identification the hill-climbing method is also employed here. and by changing the value which setup in the $\hat{\psi}$ current also changed. By using the current signal the hill-climbing method can find out the minimum point of the current value. Figure 3.23 shows the identification result of ψ sought by means of the hill-climbing-algorithm, also. The identification errors of ψ *is* 1.0 % respectively.

In ψ identification, equipment parameters are following as Table 2. The true value of the magnetic flux linkage is 0.0674 Wb.

First experiment test is the current norm characteristic configuration. Based on the simulation results that the modified current norm characteristic had a turning point with it, and the turning point is not only the minimum point but also equal to the true value of magnetic flux linkage. To make the experiment simple the method of eliminated the second part of formula (h) is setup the q-axis current command signal equal to zero.

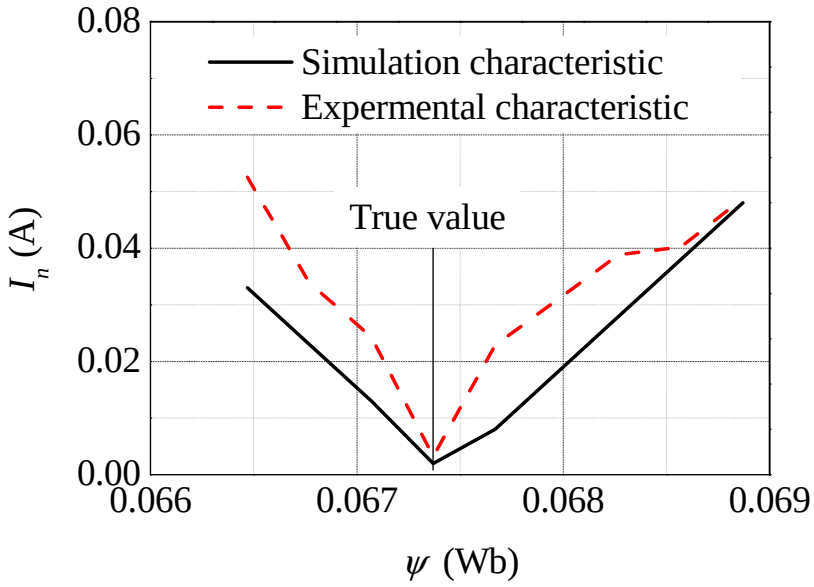

Fig. 3.22 Current characteristic of Ψ.

As the current norm characteristic had been confirmed then the problem is to searching the minimum point of this current norm characteristic. In the previous chapter the hill-climbing method is employ to searching the minimum point. Then in the experiment, the hill-climbing method is employ to help identify the unknown magnetic flux linkage.

Figure 3.23 is the experiment result of identify the magnetic flux linkage employ the hill-climbing method. Identification variation changed into its half when the current value changed. At last the identification stop at 0.068 Wb, identification error is around 1 %.

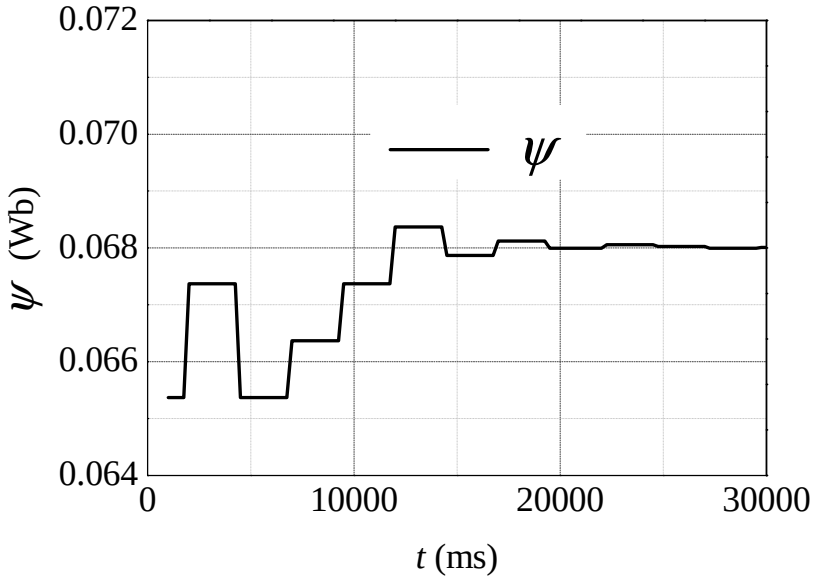

Fig. 3.23. Experiment results of Ψ identification.

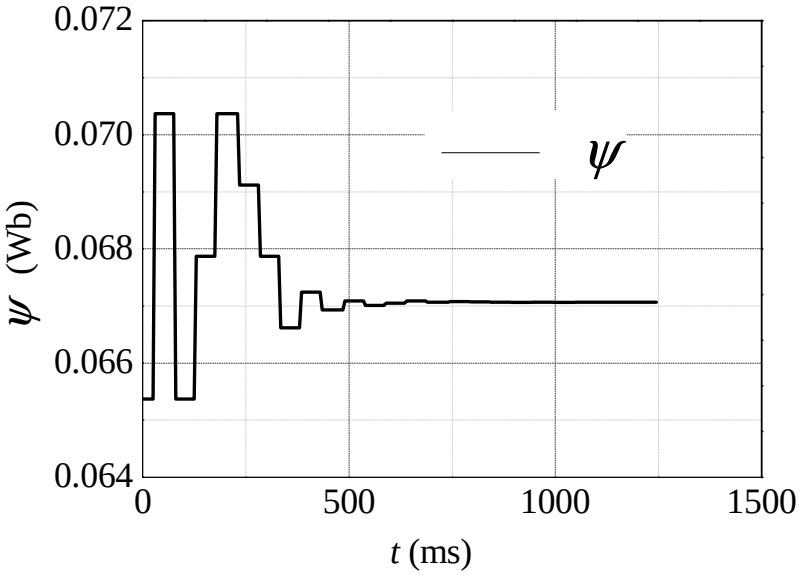

Fig. 3.24. Experiment test of identification Ψ.

The proposed ψ identification method also had no sensitive problem based on the simulation results and theoretical analysis.

To simulate the resistance variation due to the temperature change, the external resistance is inserted between the motor and the inverter. The added external resistance is 0.2Ω. Compared with the motor winding resistance, the total resistance is changed by 41.7 %, and this can simulate the winding resistance temperature rise of over 133.2° . Figure 3.24 show parameter identification result. The resultant identified value of ψ is 0.0671Wb (error 0.5 %).

According to the experiment results, the identification error is within approximately 5 %. And these identification errors are acceptable for magnetic flux linkage identification.

3.4. L_d identification

The off-line d-axis inductance identification system shares the same identification structure using in magnetic flux linkage identification. But the identification condition is different, in d-axis inductance identification the d-axis current must not equal to zero. Because when the d-axis current equal to zero the influence effect will be eliminate.

After current norm characteristic is confirmed by simulation, the hill-climbing method also employs to identify the d-axis inductance. In the end of this chapter, the experiment are use to confirm the identification theory and sensitive problem.

3.4.1. L_d identification theory

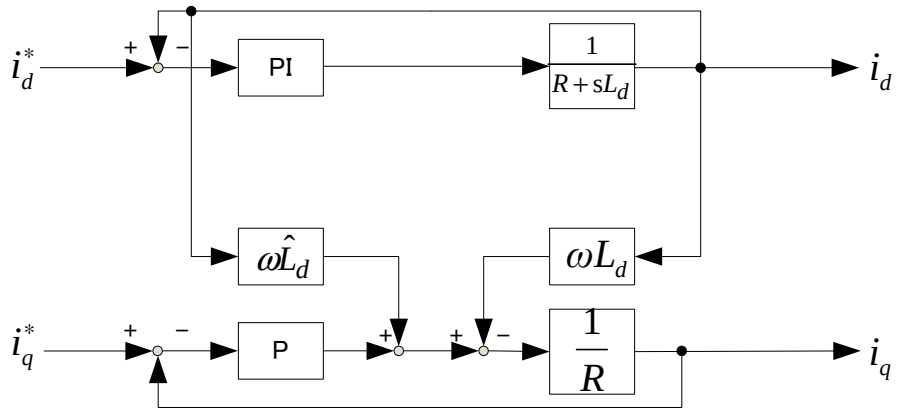

Fig 3.25 Simplified d-axis inductance identification system.

As in Fig. 3.17 the proposed identification system can be using not only for magnetic flux linkage identification but also can be using for d-axis inductance identify.

After identification of L_q and ψ, the identification of L_d is carried out in the similar manner as described in the previous sections.

This identification is still based on the system configuration shown in Fig. 3.25. The only difference from the case of the ψ identification is the operating condition of the system, i.e., $i_q^* = 0$ and $i_d^* \neq 0$ are given to the system. In this case, the current controller is simplified as shown in Fig. 3.8, and its mathematical expressions in terms of the d-axis and q-axis currents can be derived from the block diagram as follows:

$$i_q = \frac{i_d^* K_d \omega_c (\hat{L}_d - L_d)}{(K_q + R)(K_d + R)}, \text{ and} \qquad \text{(m)}$$

$$i_d = i_d^*, \text{ and} \qquad \text{(n)}$$

When $\hat{L}_d = L_d$ is satisfied, the q-axis current expressed by (m) reaches the zero point value, and the current norm reach the minimum point of it. And by searching this current norm minimum point it is possible to identify the L_d. By changing the $\hat{L}_d$ current norm characteristic will show a parabola characteristic.

3.4.2. L_d identification simulation

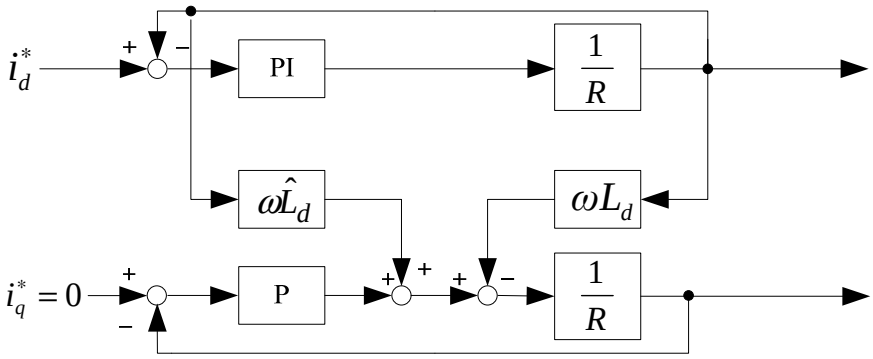

Fig. 3.26 simplified d-axis inductance identification system.

After identification of L_q and ψ, the proposed L_d simplified identification system shows in Fig 3.26. Based on the proposed identification system, the simulation circuit are created as the Fig. 3.26. And the block diagram is shows in Fig 3.27.

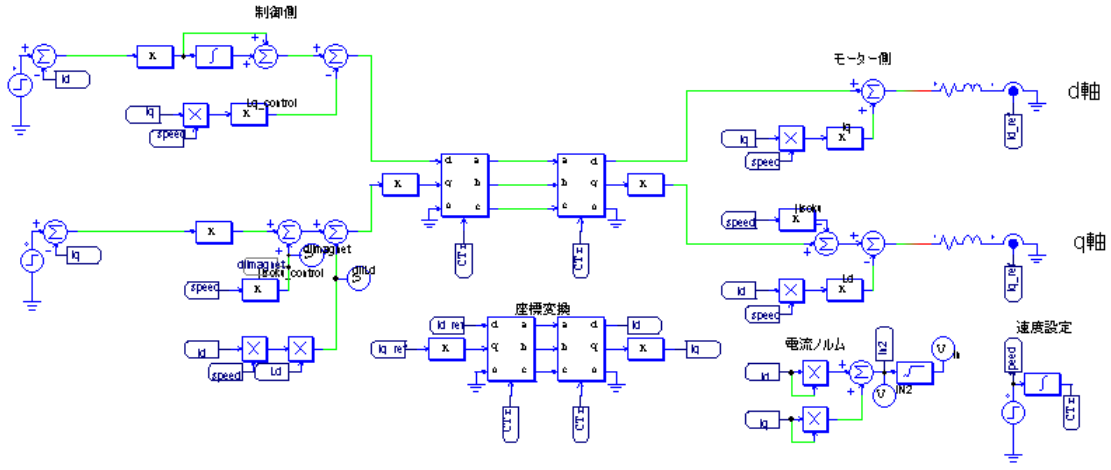

Fig. 3.27 Simulation circuit of proposed d-axis inductance identification system.

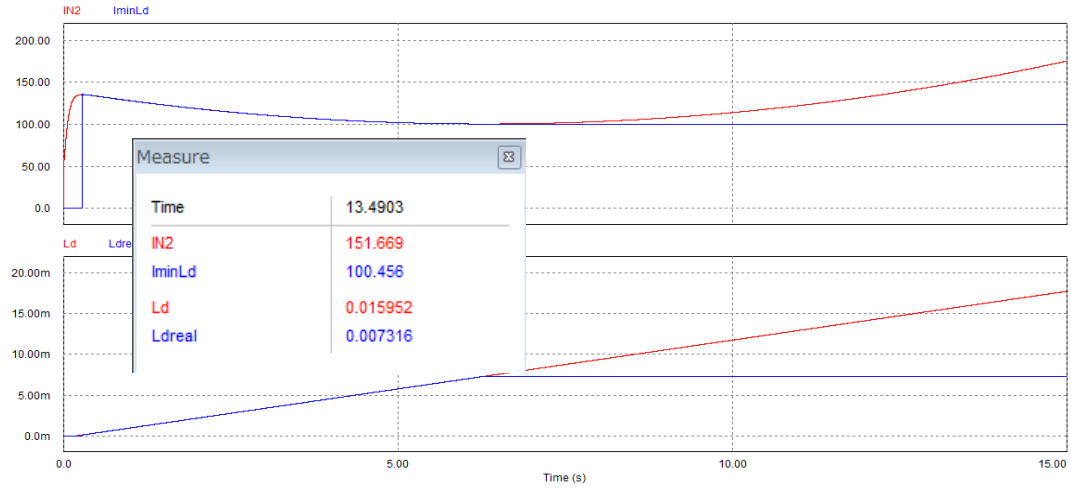

Fig. 3.28 Simulation current characteristic of employing d-axis inductance identification system.

The circuit had been created as shown in Fig. 3.27. The circuit includes two axes and each of the axes is designed as the miasmatic mode shows. By using this simulation circuit the current norm characteristic of the proposed identification method is also shown in Fig. 3.27.

The simulation setup is following as Table. 1. Figure 3.28 shows a simulation result of the current norm i_n with respect to the L_d mismatch. As can be seen in the figure, the current norm curve has a parabolic characteristic as a function of the L_d mismatch. To confirm the simulation results and calculation results the two results are compared with each other, and the comparison results are shows in Fig. 3.29.

It should be noted that i_n becomes minimum only at the point of $\hat{L}_d = L_d$ as the L_d mismatch is varied by changing the set value in the controller; hence, it is possible to identify L_d by adopting the similar hill-climbing algorithm as described previously.

Then the simulation results of employing hill-climbing method had been shown in Fig. 3.30. Figure 3.31 show the detail of the hill-climbing action process of it. By changing the d-axis inductances which setup in the controller the program can find the minimum point of the current norm value. And the identification result is 7.316 mH the identification error is 2.2%.

In addition, the minimum point of i_n can be observed only when $\hat{L}_d = L_d$, no matter how much the winding resistance R varies. This means that the proposed method is basically robust to the temperature variation of the windings and the motor cable length.

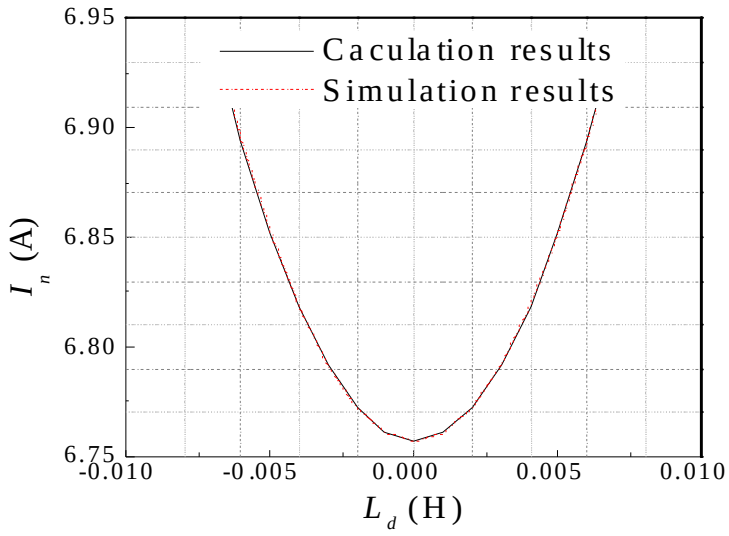

Fig. 3.29 Characteristic comperiation between caculation and simulation results.

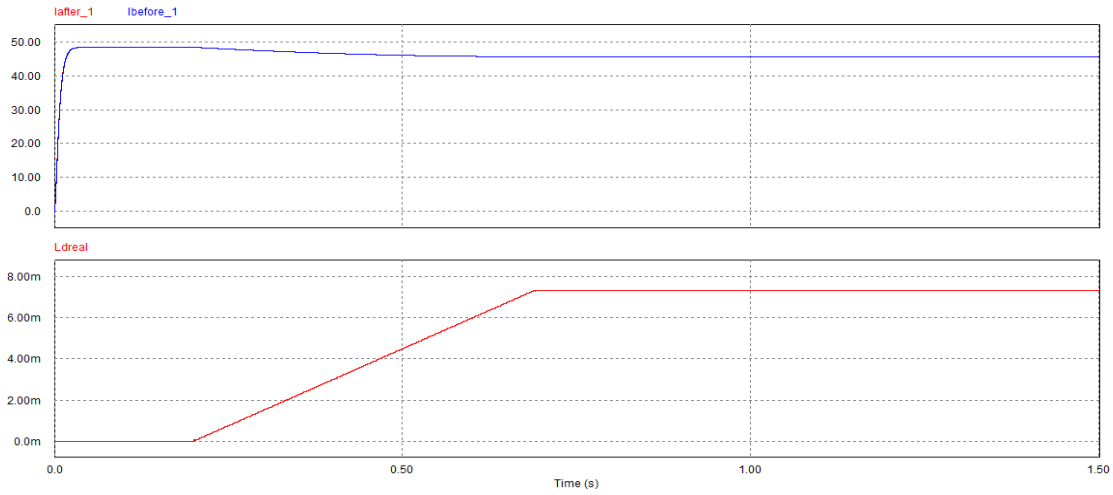

Fig. 3.30 Simulation results of empolying hill-climbing method to identify L_d.

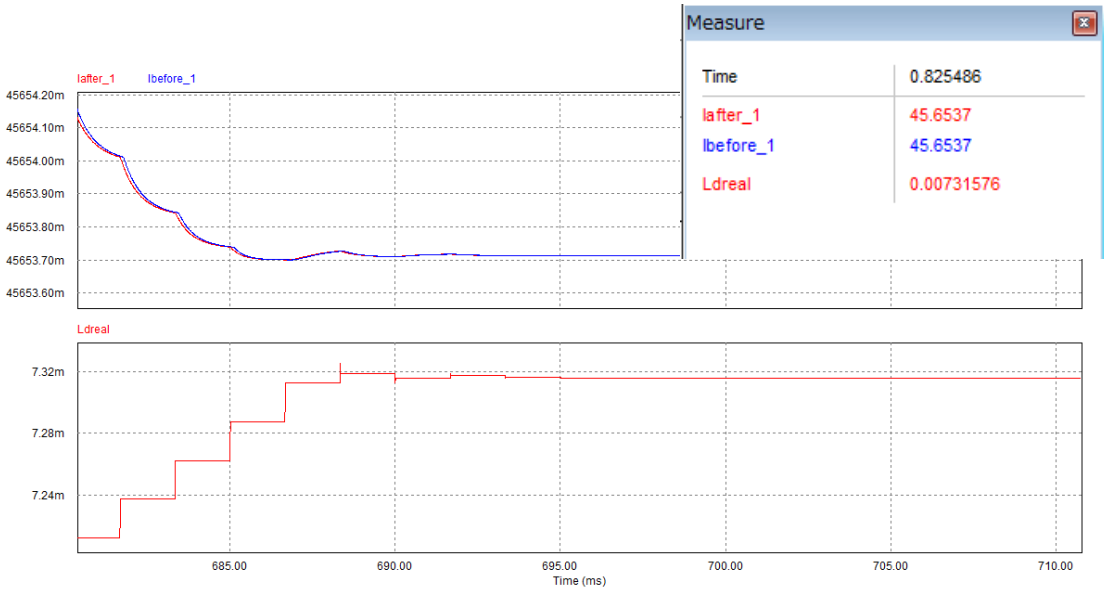

Fig. 3.31 Detail of the hill-climbing method.

3.4.3. L_d identification experiment

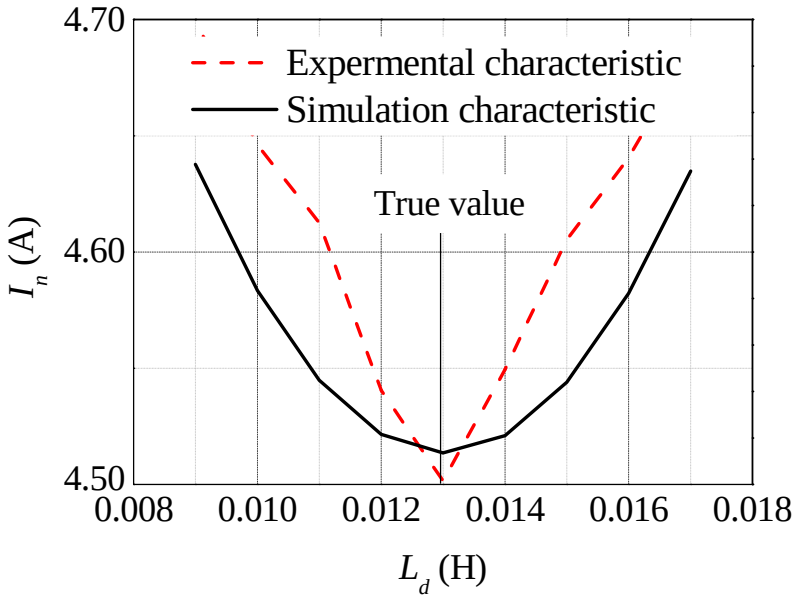

Fig. 3.32. Experiment current characteristic.

First experiment result is configuration of current norm characteristic. Figure 3.32 is the current norm characteristic. Black line is the simulation results and the red line is the experiment results. As the d-axis inductance setup in the controller changing from 9.0 mH to 17.0 mH, the experiment results and simulation results shows similar characteristic between each other. It reaches the minimum point when the setup d-axis inductance in the controller is near the true value of the d-axis inductance.

The experiment result shows in Fig 3.32. The experiment just confirms the simulation results. But two curves are little difference between each other.

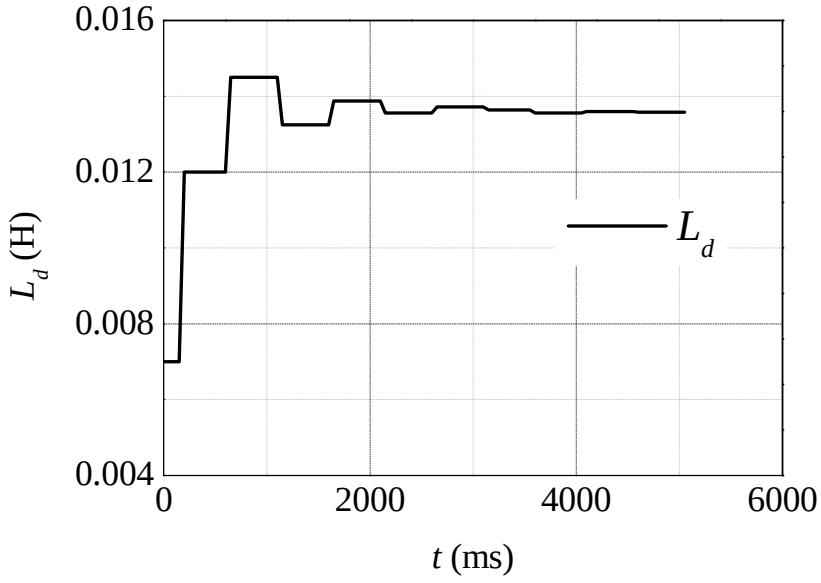

Fig. 3.33. Experiment L_d inductance identification.

After the current norm characteristic had been confirmed. Then the hill-climbing method is employed in here. As the d-axis inductance setup value in the controller changes, the current norm value also changes. As the current norm changes, the hill-climbing method searching direction changes and the changing variation also reduced.

In the end of the identification, the d-axis inductance reaches its current norm minimum. And the identification value is 13.6 mH, the identification error is 4.5 %. This experiment results is proposed in Fig. 3.33.

Then the next experiment is checking the sensitive problem. To simulate the resistance variation due to the temperature change, the external resistance is inserted between the motor and the inverter. The added external resistance is 0.2Ω. Compared with the motor winding resistance, the total resistance is changed by 41.7 %, and this can simulate the winding resistance temperature rise of over 133.2° .

After connect 0.2 Ω into the circuit the identification program is used to confirm the d-axis inductance. As the Fig.3.34 shows even the winding resistant is changed the

d-axis inductance can still identify the unknown parameter, and the identification results is 13.6 mH, and the identification error is also not changed. The identification error is also 4.5%.

Based on the experiment results that the proposed identification technical can help to identify the unknown parameter and even the winding resistance is changed.

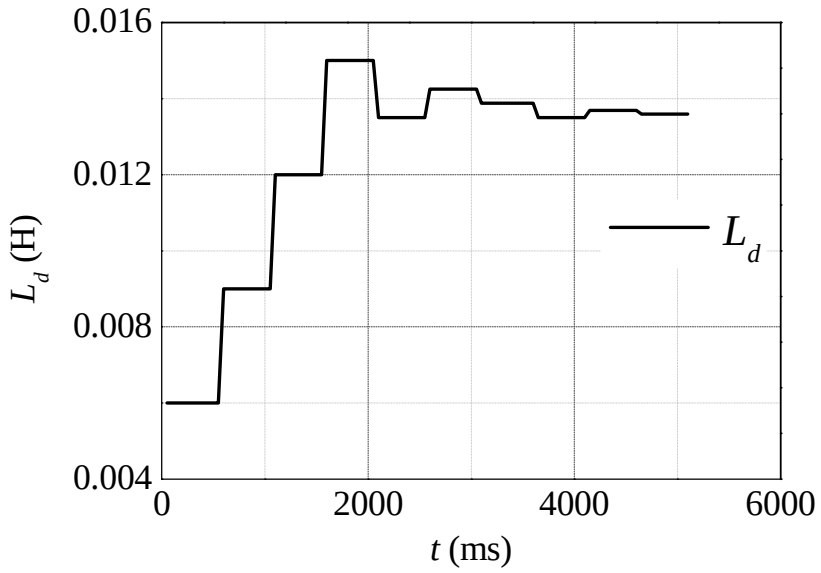

Fig. 3.34. Experiment L_d identification.

3.5. *R* identification

The resistance identification is also one of the missions of the proposed identification method. And feature of the proposed identification method is it forcing on the current signal.

And the proposed identification method can mainly separate into two different situations. One is the motor stopped, and another situation is the motor rotated in a low speed range.

3.5.1. *R* identification theory

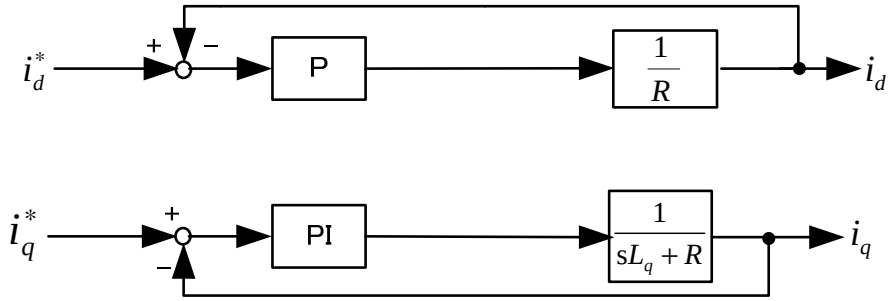

Fig.3.35 Simplified resistance identification system.

As described in the above discussion, the proposed identification technique of the IPM motor parameters does not require any information of the winding resistance *R*, and is basically robust to the variation of *R*; thus, it is not necessary to identify *R* inherently. The *R* identification, however, can be optionally realized by using the identification algorithms described so far. And because of it is the off-line identification, this proved a possibility to changing the identification system easily.

After other parameters had been identified or the motor is stopped, the simplified identification system is same with each other. And the proposed identification also had two different ways. One is changing d-axis PI regulator into P regulator, another is changing q-axis PI regulator into P regulator. These two kinds of changing all shear the same mathematic model. Then the d-axis changing system, is proposed as an example.

From d-axis current control loop proposed in Fig. 3.35, *R* is simply calculated by the following expression:

$$R = \frac{K_d (i_d^* - i_d)}{i_d} . \qquad \text{(o)}$$

By using (o), the winding resistance can be identified.[18][19]

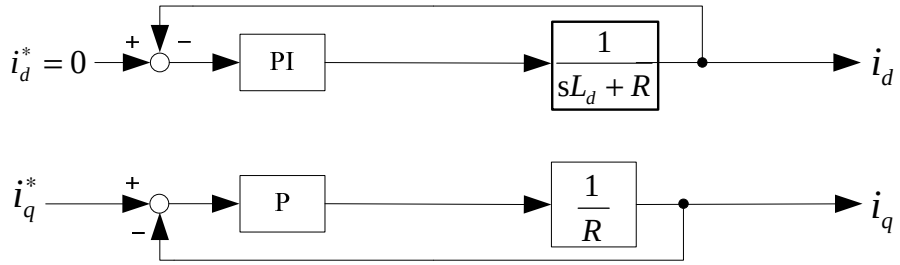

Fig.3.36 Simplified resistance identification system.

And another kind of resistance identification situation shown in Fig 3.10 also can use the similar theoretical. The proposed q-axis resistance identification system is shown in Fig. 3.36.

$$R = \frac{K_q (i_q^* - i_q)}{i_q}. \qquad \text{(p)}$$

3.5.2. *R* identification simulation

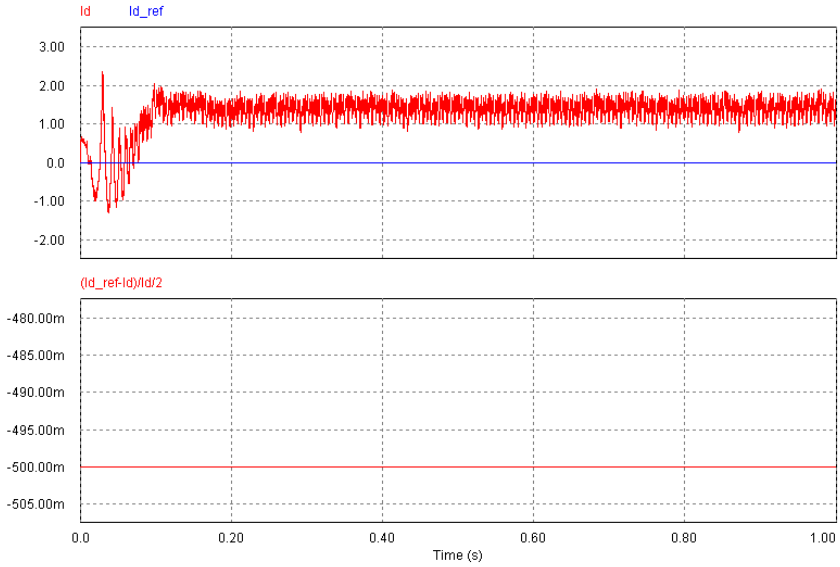

Fig.3.37 Simulation results of calculate resistance based on using d-axis current.

Figure 3.37 is the resistance identification simulation results. As the motor become stable. The proposed identification system can identify the resistance, and the identification results is 0.5 Ω, but the true value of resistance is 0.48 Ω. The identification error is 4.17 %.

3.5.3. *R* identification experiment

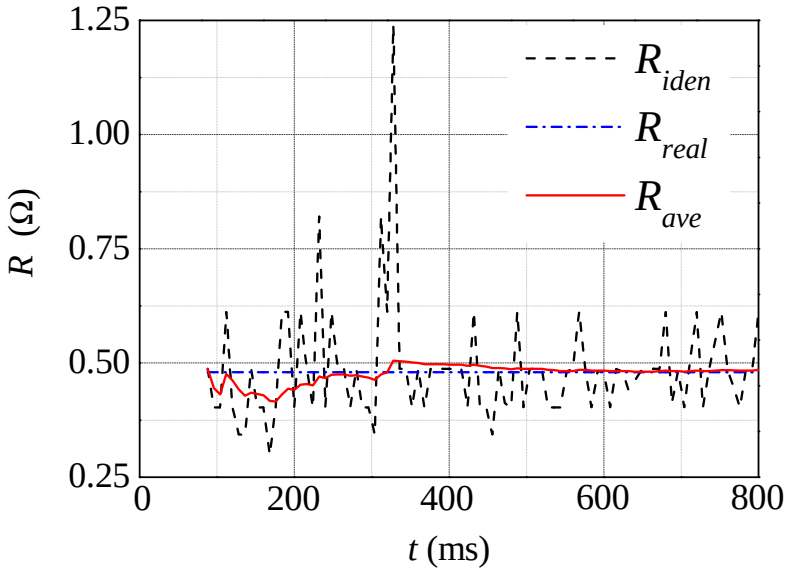

Fig. 3.38. Resistance identification.

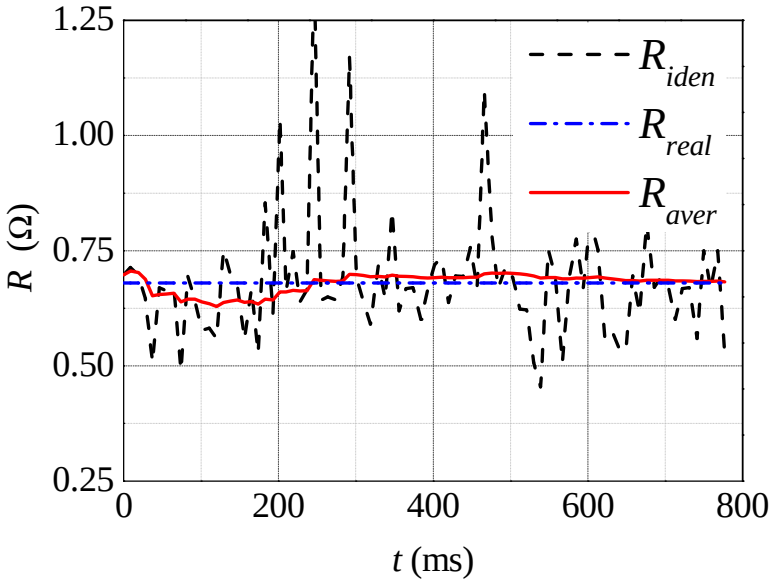

Fig. 3.39. Resistance identification with extra *R*.

The R identification is provided as an optional function of this system. The calculate is based on the current signal, after using average process, the current ripple caused by PWM switching can be reduced but it still effect the identification result. Figure 3.38 shows the experimental test result. The dotted line is the winding resistance value R_{iden} calculated by (12), and the solid line is its average value R_{ave}. As can be seen in the figure, the R_{ave} converges to the true value R_{real} that has been measured by the parameter measurement test. The R_{ave} is 0.485 Ω, while the R_{real} is 0.48 Ω, where the identification error is approximately 1 %.

One of the advantage of the proposed identification technique is insensitiveness to the winding resistance variation. Owing to this feature, the temperature does not affect the identification. Even when the temperature changes, with no sensitivity to the winding resistance the changed parameters can be identified by running the identification again.

And this proposed identification technical had no sensitive problem to resistance. To confirm this, the experiment was conducted. To simulate the resistance variation due to the temperature change, the external resistance is inserted between the motor and the inverter. The added external resistance is 0.2 Ω. Compared with the motor winding resistance, the total resistance is changed by 41.7 %, and this can simulate the winding temperature rise of over 133.2° . Figures 3.39 show each parameter identification result. The resultant identified value of R is 0.683 Ω (error 0.5 %). Every identification error is within approximately 5 %.

4. On-line IPMSM parameters identification

4.1. Introduction

And the on-line identification also chooses to use current signal to identify the parameters. The identification also divided the identification into many steps. And each parameter identification has own identification structures and identification conditions.

Figure 4.1 is the normal IPMSM control system. Based on Fig. 4.1 two different identification systems Fig. 4.2 and Fig. 4.3 are proposed for q-axis inductance, magnetic flux linkage and d-axis inductance identification. And in the identification step, the IPMSM has to control the rotation speed by its own self.

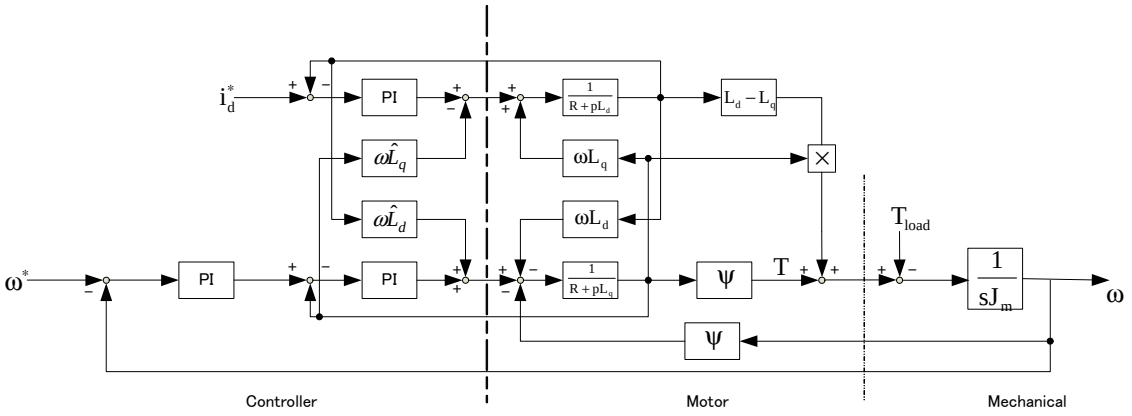

Fig. 4.1 Mathematic model of IPMSM control system

Based on the theoretical and simulation results, linear current characteristic can be confirmed. By searching the current zero cross point it is possible to identify the unknown parameters. And by focusing on this zero cross point, it is possible to found out the true value of it.[13][14]

In the end the experiment also using to confirm these identification theory. The experiment equipment physical constants are following as Table. 2.

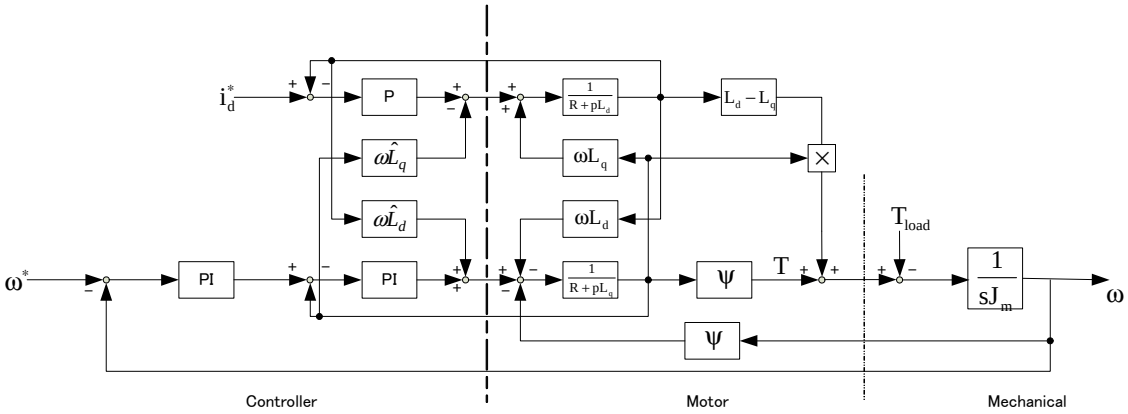

Fig. 4.2 Proposed q-axis inductance identification system.

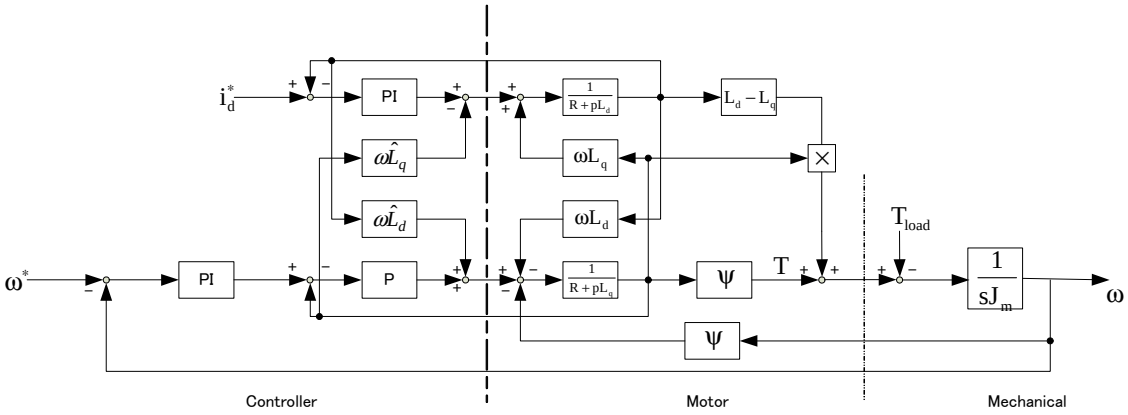

Fig. 4.3 Proposed magnetic flux linkage and d-axis inductance identification system.

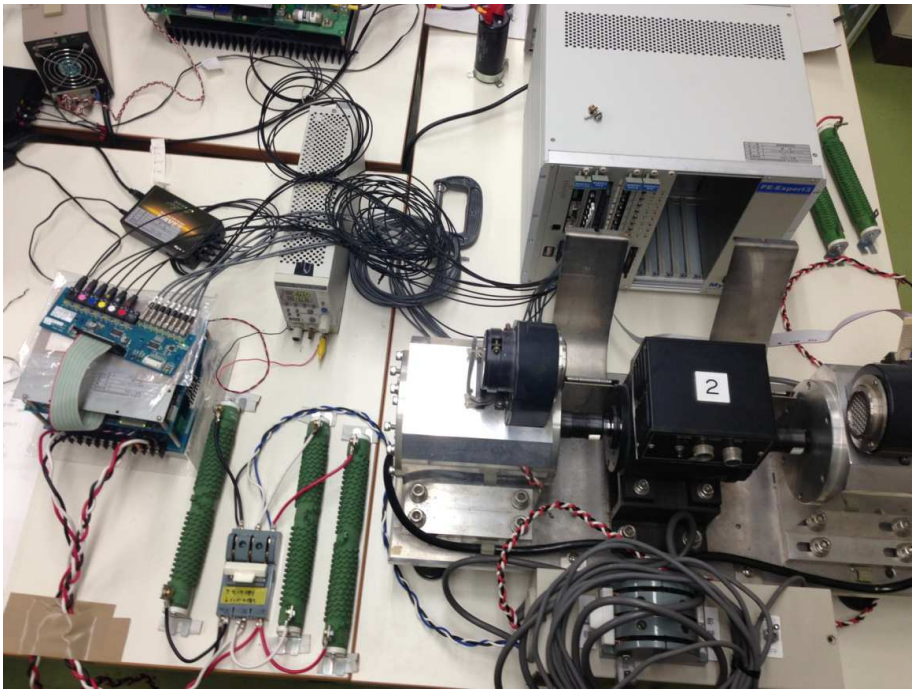

Fig. 4.4. Experiment test equipments.

As showing Fig. 4.4. The on-line identification system compared with off-line identification system, that the on-line identification system had only one IPMSM motor in used and also only one inverter.

And parameters identification experiment results are presented in this part. And each section use experiments to confirm the current characteristic, and by using this current characteristic the two points speculated method is employed to identify the unknown IPMSM parameters. And the identification can finished in few hundred milliseconds. The experiment current characteristic shows similar characteristic with simulation results.

By using this characteristic it is easy to identify the unknown motor parameters. To achieve the high speed identification, the two-point speculate method is used. By employing this method, the identification results had an identification error within 13 %.

To reduced the identification error that by using double times identification it is

possible to reduce the identification error, and the identification error can keep it under 18 %.

4.2. L_q identification

Figure 4.2 is the L_q identification system. In the system, the PI regulator using in d-axis is replace by P regulator. Because of that the influence effect of q-axis inductance can be get.

In the same time the speed control system can keep the rotation speed stable. So the q-axis inductance influence effect also can keep stable.

4.2.1. L_q identification theory

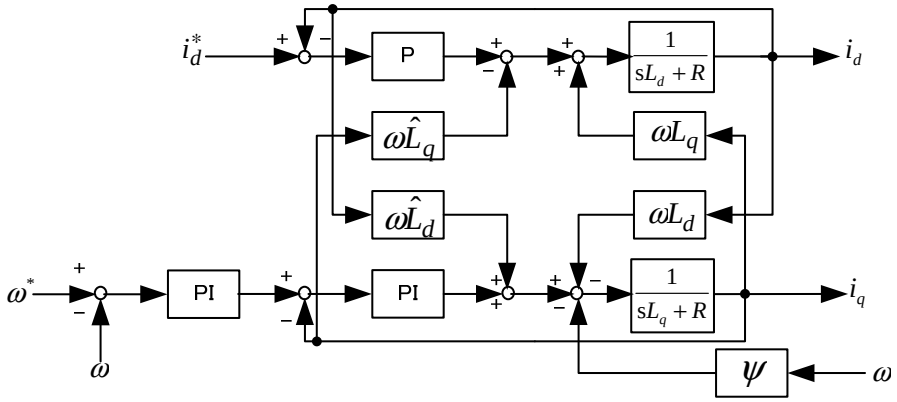

Fig. 4.5 Proposed L_q identification system.

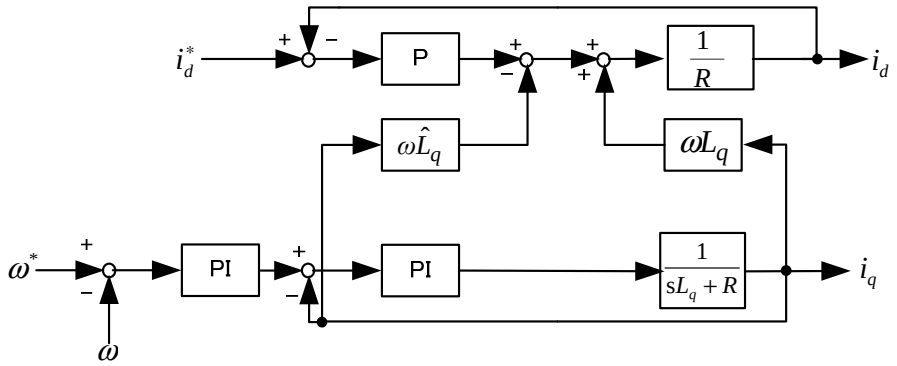

Fig. 4.6 Simplified L_q identification system.

Figure 4.5 shows the proposed current control system and speed control system of L_q identification system. In the system, the PI regulator used in the *d*-axis current control loop is replaced with a P regulator. Because the P regulator is unable to eliminate the steady-state error, the mismatch of L_q affects the *d*-axis feedback current. Figure 4.6 shows the simplified L_q identification system.

From Fig. 4.6, theoretically the rotation speed is equal to its command, and the *q*-axis current is stable when the motor is operated in the steady state because both of the controllers consist of the PI regulators.[21] By setting the *d*-axis current command at zero, the *d*-axis feedback current can be expressed as

$$I_d = \frac{\omega I_q}{K_{pd} + R}(L_q - \hat{L}_q). \qquad \text{(q)}$$

From (q), it is found that the mismatch of L_q has a linear relationship with the d-axis feedback current I_d when the command of the d-axis current is set at zero.[22] Based on this linear characteristic, it is possible to estimate the true value of L_q. As shown in Fig. 3.13. The basic mathematic knowledge tells that if two points on the line is known the whole equation of the line is known.[23][24]

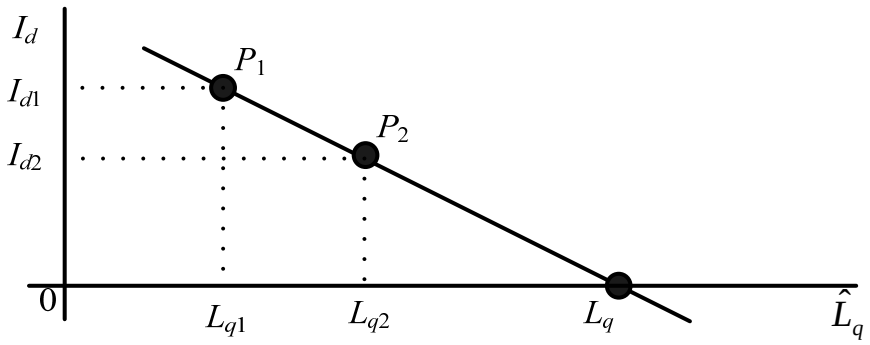

Fig. 4.7. L_q identification description.

By setting two different values of L_q to the system, which may have the parameter mismatch, two corresponding *d*-axis feedback current values are recorded in the memory. Assuming that the following consecutive sampling actions are performed:

$I_d = I_{d1}$ when $\hat{L}_q = L_{q1}$, and

$I_d = I_{d2}$ when $\hat{L}_q = L_{q2}$,

the true value of L_q can be calculated by the following equation:

$$L_q = \frac{I_{d1}L_{q2} - I_{d2}L_{q1}}{I_{d1} - I_{d2}}. \qquad \text{(r)}$$

Equation (n) implies that the true value of L_q can be calculated regardless of any parameters and any variables used in (m). Therefore, the proposed identification technique requires only the *d*-axis feedback current information to estimate L_q.

The q-axis PI regulator which control the *q*-axis current has the following transfer function:

$$G_{PIq}(\mathrm{s}) = K_{Pq}\left(1+\frac{1}{\mathrm{s}\tau_q}\right). \qquad \text{(s)}$$

In the above transfer function, the P gain K_{Pq} and the integral time constant τ_q are designed as follows:

$$K_{Pq} = \omega_c L_q, \text{ and } \tau_q = \frac{L_q}{R}, \qquad \text{(t)}$$

where ω_c is a designed crossover frequency of the *q*-axis current control loop. The PI regulator used in the speed control also employs the simile theory. But the mechanical system's response time was slower than the current control system, in the experimental test integral time constant of speed control had setup to millisecond level.[25]

4.2.2. L_q identification simulation

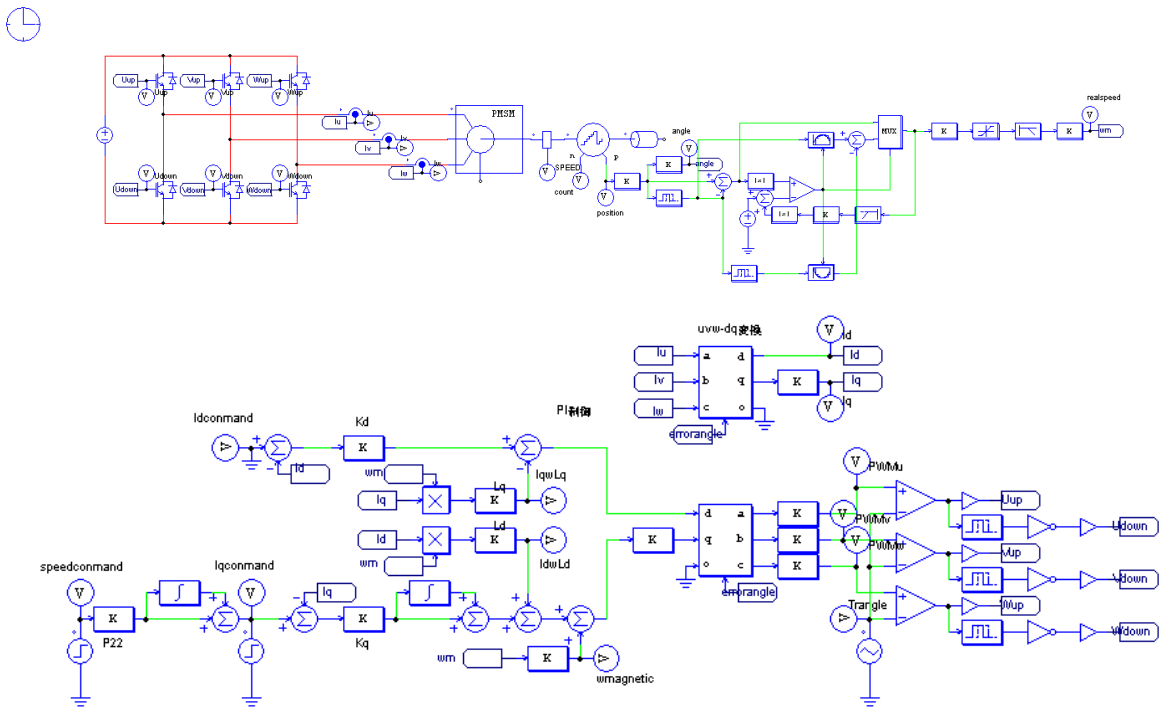

Fig. 4.8 On-line q-axis inductance identification system.

Figure 4.8 is the simulation circuit of q-axis inductance identification system. In above are the power source, inverter and IPMSM. Rest part is the control circuit of this proposed L_q identification system. As Fig 4.5 shows the d-axis employ P regulator to replace the PI regulator.

Then the d-axis current characteristic had been confirmed by using this proposed simulation identification circuit shown in Fig 4.8. Based on the simulation results shown in Fig 4.9, as the q-axis inductance changing in controller, the IPMSM rotation speed and q-axis current can keep stable. At the same time the d-axis current changing following the L_q changing. When the L_q is bigger then the true value of it, the d-axis current is smaller then 0 A, but when it is smaller then the true value, d-axis current is bigger then 0 A. And d-axis current is equal to zero when L_q setup in controller just equal to the true value of it.

From formula (q) and simulation results showing Fig 4.9, it is found that the

mismatch of L_q has a linear relationship with the d-axis feedback current i_d when the command of the d-axis current is set at zero. Based on this linear characteristic, it is possible to estimate the true value of L_q. As shown in Fig. 4.7, the basic mathematic knowledge tells that if two points on the line is known the whole equation of the line is known.

By setting two different values of L_q to the system, which may have the parameter mismatch, two corresponding d-axis feedback current values are recorded in the memory. Assuming that the following consecutive sampling actions are performed:

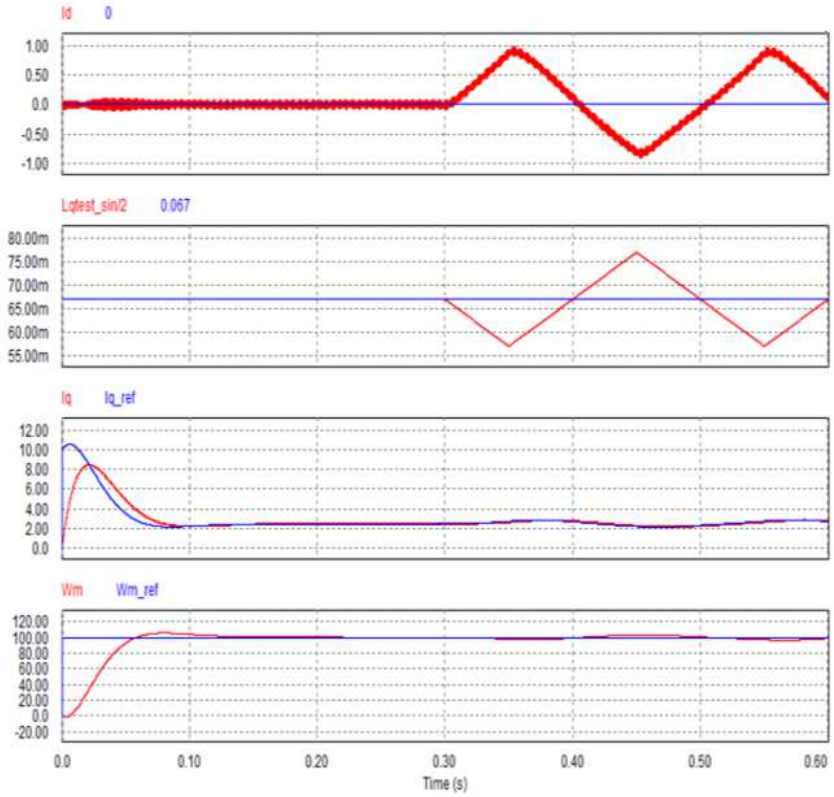

Fig. 4.9 Simulation confirm of current characteristic of q-axis inductance.

Id = Id1 when $\hat{L}_q = L_{q1}$, and

Id = Id2 when $\hat{L}_q = L_{q2}$,

the true value of Lq can be calculated by the following equation:

$$L_q = \frac{I_{d1}L_{q2} - I_{d2}L_{q1}}{I_{d1} - I_{d2}} \quad . \qquad \text{(u)}$$

Equation (u) implies that the true value of L_q can be calculated regardless of any parameters and any variables used in (u). Therefore, the proposed identification technique requires only the d-axis feedback current information to estimate L_q.

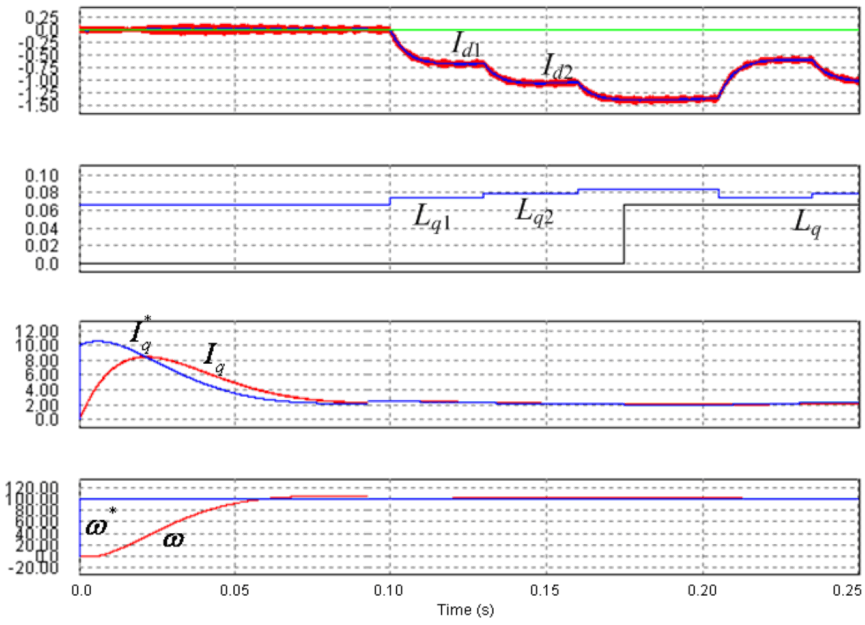

Fig. 4.10 Simulation results of employing two point speculate method of identification q-axis inductance.

The q-axis PI regulator which controls the q-axis current has the following transfer function:

$$G_{PIq}(s) = K_q\left(1 + \frac{1}{s\tau_q}\right).$$

In the above transfer function, the P gain K_q and the integral time constant τ_q are designed as follows:

$K_q = \omega_c L_q$, and $\tau_q = \frac{L_q}{R}$,

where ω_c is a designed crossover frequency of the q-axis current control loop. The PI regulator used in the speed control is also designed on the basis of the similar theory. However, the mechanical response time is much slower than that of the current control system, so in the experimental test the integral time constant of the speed control is setup to the millisecond level.

Some computer simulations have been conducted to verify the identification performance of the proposed technique. Table 3 lists the test motor parameters which are used in the simulations.

And the control circuit is also designed as shown in Fig. 4.3. As shown in Fig.4.5 the PI regulator used in the d-axis current control loop is replaced with a P regulator. Because the P regulator is unable to eliminate the steady-state error, the mismatch of L_q affects the d-axis feedback current. And using this current signal the q-axis inductance could help to identification the unknown parameters.

One of the simulation results shown in Fig. 4.9 illustrates the current characteristic when changing $\hat{L}_q$ in the controller in the steady states. Based on the simulation result, as $\hat{L}_q$ is intentionally changed linearly the d-axis current also follows this change and shows a linear characteristic. According to the simulation result, the identification theory indicated in Fig. 4.7 makes it possible to achieve the on-line estimation of L_q.

Another simulation result is shown in Fig. 4.10 which is based on this identification theory. The rotation speed and the q-axis current are controlled to be equal to their commands. As $\hat{L}_q$ of the controller is changed from L_{q1} to L_{q2} and so on, the d-axis

feedback current also changes accordingly. The final identification result is 66.5 mH, where the true value is 67 mH. The identification error is 0.78 %, and the convergence time needed for the identification is only 0.08 s.

Table 3. Parameters of test IPMSM.

Number of poles	4
Winding resistance	4.3 Ω
Gain of d-axis P regulator	1 V/A
q-axis inductance	67 mH
d-axis inductance	27 mH
Setup d-axis inductance	1.0 mH
Field flux linkage	0.544 Wb
Setup field flux linkage	1.0 Wb
Rotation speed	6000 r/min

4.2.3. L_q identification experiment

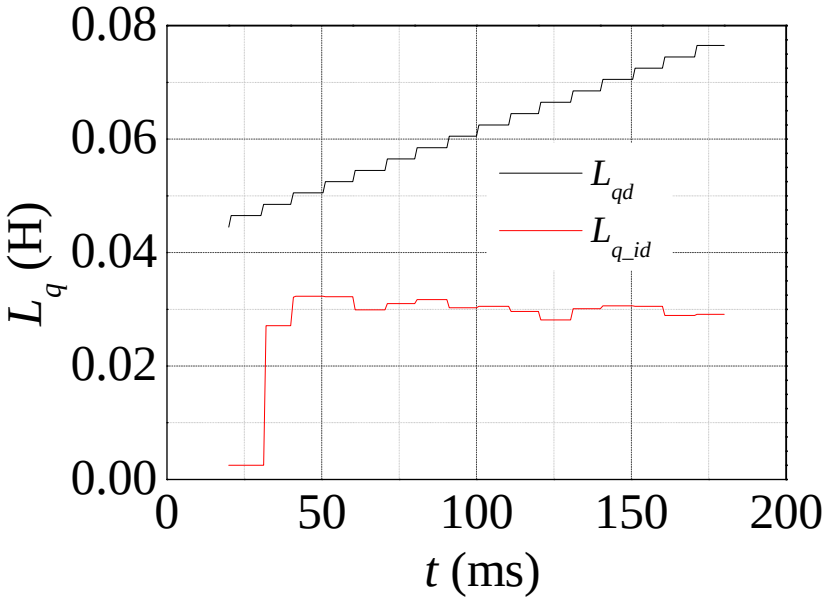

Fig. 4.11. q-axis inductance changing and identify results.

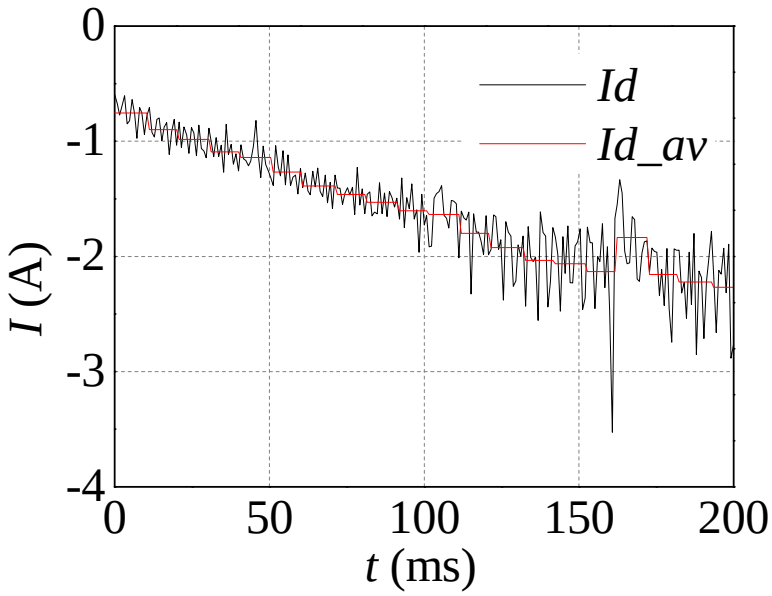

Fig. 4.12. d-axis current changing.

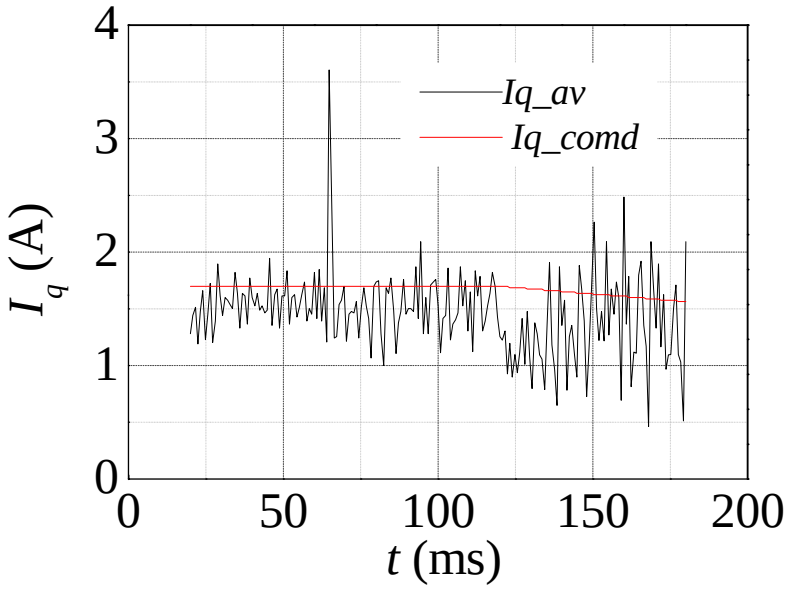

Fig. 4.13. q-axis current changing.

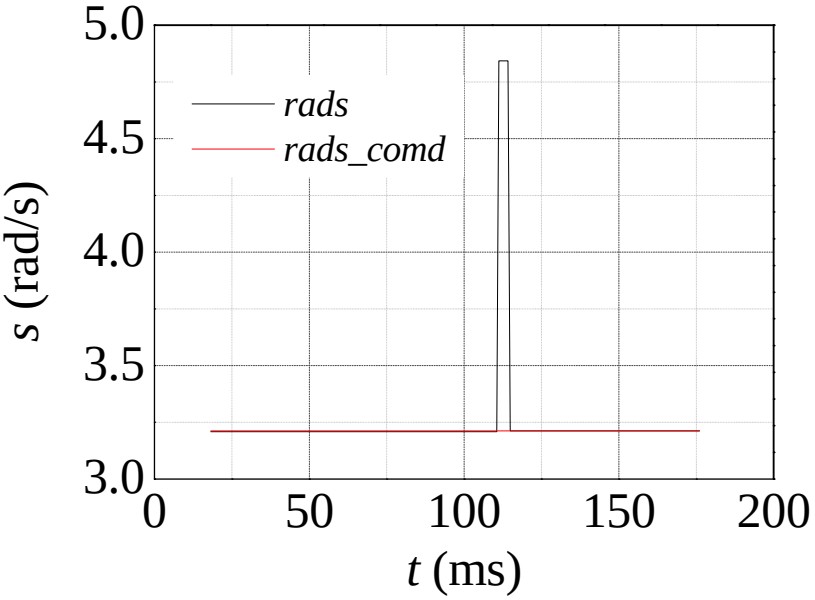

Fig. 4.14. rotation speed changing.

In this section, to proof the identification technical and simulation results. Experiment is used to confirm the current characteristic and L_q identification. The

experiment equipment parameters are listed in Table 4. Figure 4.11 to Figure 4.14 shows the experiment result when $\hat{L}_q$ is changed following the black line in Fig. 4.11. After the $\hat{L}_q$ changed, the Fig. 4.12 and Fig. 4.13 show the changes of *d*-axis current and *q*-axis current. From the results, the *d*-axis current increased along with $\hat{L}_q$. And the *q*-axis current keep stable as the theoretical result. The result of identification is around the true value and the error is within 15 %. As the d-axis increased, the identification result also exhibit decreased tendency because of magnetic saturation. And based on the Fig. 4.14 in the identification the speed keep stable even it go over the command signal the PI regulator can recovery it. But based on Fig. 4.12 when the $\hat{L}_q$ far beyond true value the current fluctuation became larger. And based on Fig. 4.12 and Fig. 4.13 in the experiment test when the $\hat{L}_q$ over 60.0 mH, the current linear characteristic also became inconspicuous.

And based on the performance of Fig. 4.13 and Fig. 4.14, the *q*-axis current ripple also increased and the command signal of *q*-axis became decreased. On the same time the rotation speed shows short-term loss of control. But the PI regulator helps the rotation speed return in stable condition.

Based on these test results, to keep the current characteristic linear the range of $\hat{L}_q$ is setup from -11.0 mH to 60.0 mH. After setup the range of $\hat{L}_q$, it ensure the two point speculate method can be worked.

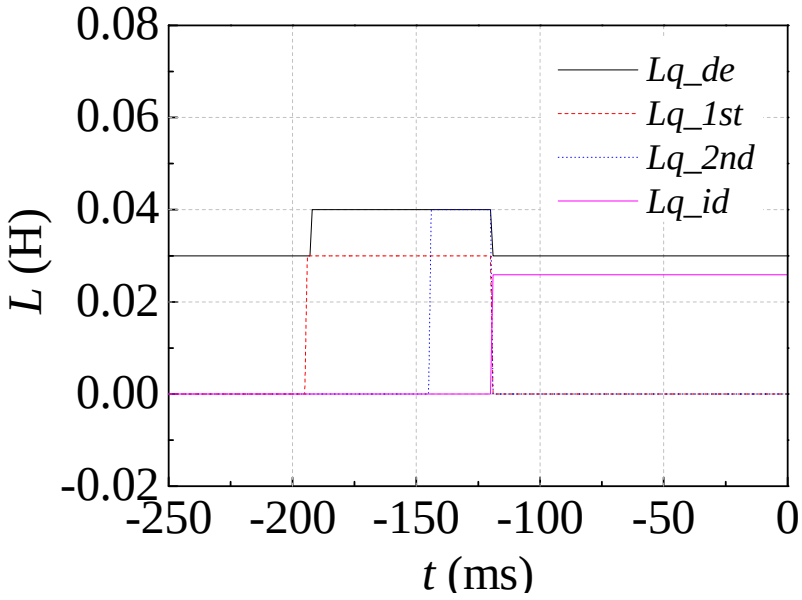

Fig. 4.15. q-axis inductance setup and identification.

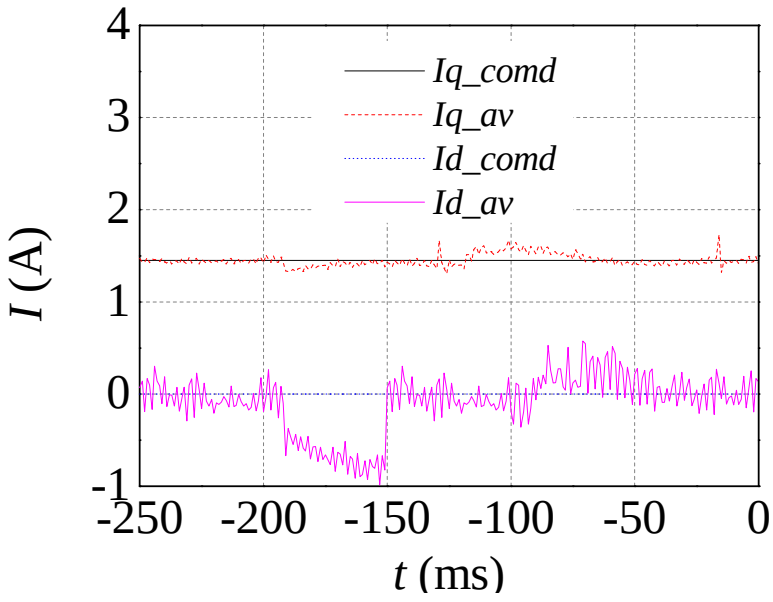

Fig. 4.16. d-axis and q-axis current changing.

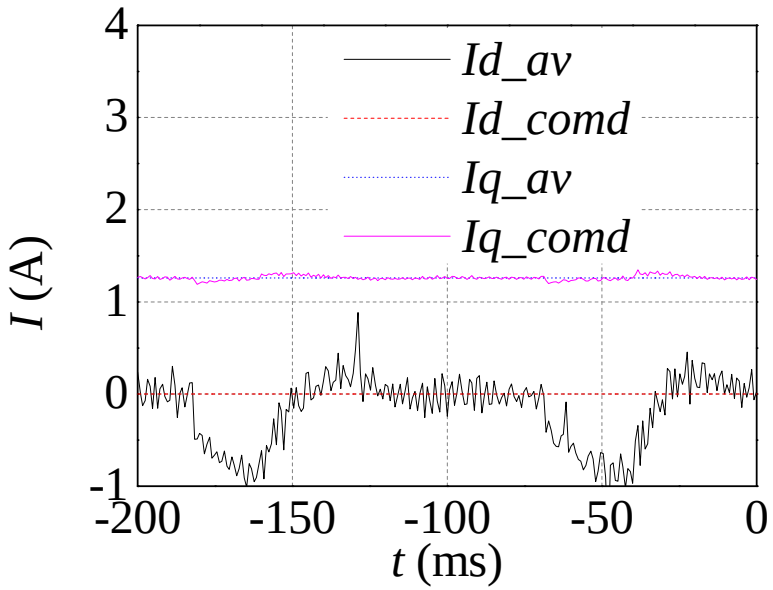

Fig. 4.17. d-axis and q-axis current changing(double times identification).

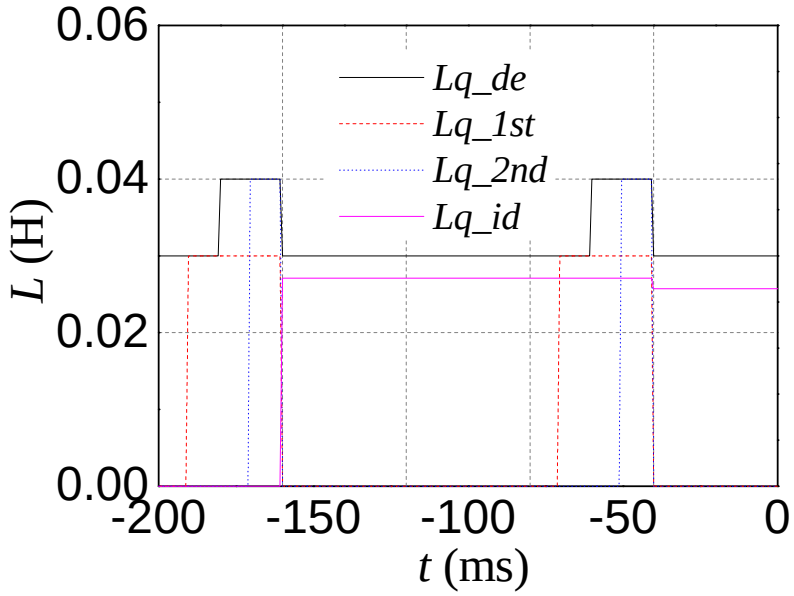

Fig. 4.18. q-axis inductance changing(double times identification).

Figure 4.15 and Figure 4.16 gives an experiment results by employ the two points speculate method. First point is taken at -180.0 ms, and second point is taken at -120.0

ms. By using these two points the speculation result is 25.9 mH. Identification error is 5.7 %.

This result shows two points speculate theoretical can be used to identify L_q. By using several times identification and setup the two points near the true value. It is possible to reduce the identification error.

And one of the most important advantages of this proposed identification method is it has no sensitive to resistance. Then the Fig. 4.17 and Fig. 4.18 shows the identification result when connect the extra resistance to the system to simulate the temperature change effect the resistance changing. By employ two times identification the final result stopped at 25.7 mH and error is 4.9 %. Each identification period only cost within 60.0 ms.

Based on these several times experimental tests it can be shown that the linear current characteristic can be used by employed the two points speculate method to identification the IPM motor's *q*-axis inductance. And the after the IPM motor working in the steady state the resistance changing did effect the identification result.

4.3. ψ identification

The proposed ψ identification system is base on using Fig 4.3. And this proposed identification system also using for $L_{d.}$ The only different between these two parameters identification are the identification conditions are different.

In ψ identification it is necessary to keep the d-axis current equal to zero. In this way the influence from d-axis inductance element can be eliminated. Then by using a special method a modified q-axis current characteristic can be known. By using this current characteristic it is possible to identify the unknown magnetic flux linkage.

4.3.1. ψ identification theory

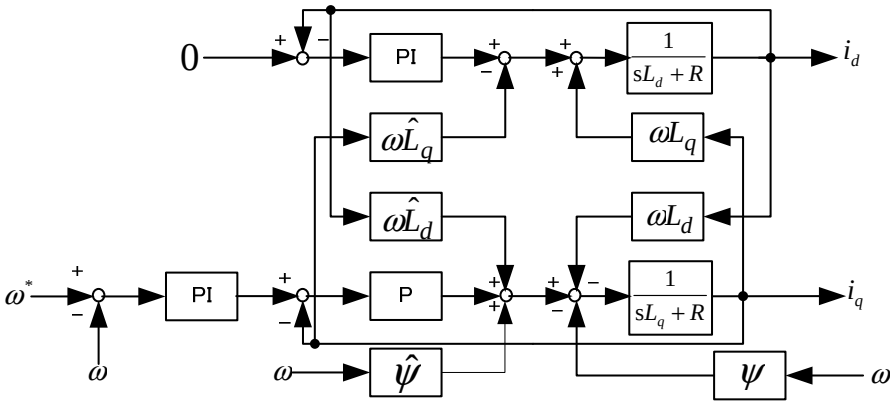

Fig. 4.19 Proposed on-line magnetic flux linkage identification system.

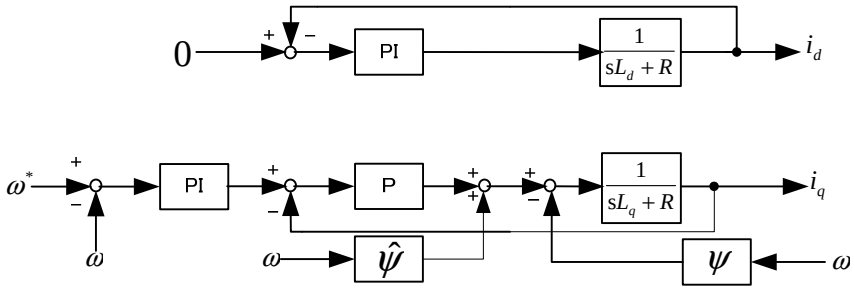

Fig. 4.20 Simplified on-line magnetic flux linkage identification system.

Figure 4.19 shows the proposed identification system used for Ψ and L_d identification. When the motor works in the steady states, Fig.4.19 can be simplified as Fig 4.20. The on-line magnetic flux linkage identification system is similar with the off-line identification method. The only difference between it is the on-line identification method include the speed control part with it.

In order to carry out the separate identification of these two parameters, the identification process is divided into the following two steps.

In the first identification step of ψ, the d-axis current command $i_d^* = 0$ is given to

the controller. Since the d-axis current control loop employs the PI regulator, $i_d = 0$ is achieved with no steady state error. In addition, a cross decoupling term through ωL_d and $\omega \hat{L}_d$ from the d-axis to the q-axis can be ignored because $i_d = 0$ is guaranteed. In this case, only the parameter mismatch of ψ affects the steady state error of the q-axis current. Taking the above discussion into account, the current controller structure can be simplified as shown in Fig. 4.20, where the back e.m.f. compensation block is virtually added to the q-axis current control loop in the controller for the purpose of the ψ identification.

Mathematical expressions of i_d and i_q can be derived from Fig. 4.20 as presented by (q) and (r):

$$i_d = i_d^* = 0 \text{, and} \qquad \text{(q)}$$

$$i_q = \frac{\omega_c(\hat{\psi} - \psi)}{K_q + R} + \frac{i_q^* K_q}{K_q + R}. \qquad \text{(r)}$$

The second term of the right-hand side in (r) affects the identification of ψ, so this part must be eliminated from the calculation without using the winding resistance of the motor. This can be done by using the d-axis current control loop as a simulator of the second term in (r). As mentioned previously, d-axis current control loop no longer has any interference from the q-axis because L_q has been already identified, i.e., $\hat{L}_q = L_q$. Therefore, if the d-axis current regulator is changed to a P regulator whose gain is equal to K_q and the d-axis current command is changed to the value equal to i_q^*, the resultant d-axis current comes to have the same value as the second term of (r). This implies that the second term of (r) can be found with no knowledge of the winding resistance. By memorizing the simulated second term value in the d-axis current control loop from and by subtracting the memorized value (r), the most important part can be extracted from (r) as follows:

$$i_q' = \frac{\omega_c(\hat{\psi} - \psi)}{K_q + R}. \qquad \text{(s)}$$

R is assuming constant in identification period. By using (q) and (s), the motor current norm is expressed as

$$i_n = \sqrt{i_d^2 + i_q'^2} = \frac{\omega_c(\hat{\psi} - \psi)}{K_q + R}. \quad \text{(t)}$$

By tuning the set value $\hat{\psi}$ in the controller, the value of i_n varies accordingly and becomes zero (the minimum value) when $\hat{\psi} = \psi$. And the $\hat{\psi}$ and current norm had a leaner relationship between each other.

4.3.2. ψ identification simulation

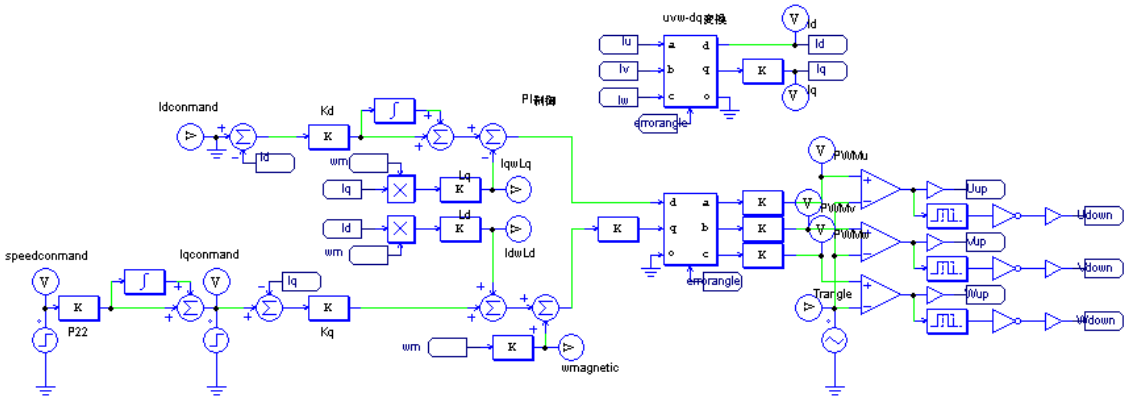

Fig. 4.21 Simplified on-line magnetic flux linkage identification system.

In the first identification step of ψ, the d-axis current command $i_d^* = 0$ is given to the controller. Since the d-axis current control loop employs the PI regulator, $i_d = 0$ is achieved with no steady state error. In addition, a cross decoupling term through ωL_d and $\omega \hat{L}_d$ from the d-axis to the q-axis can be ignored because $i_d = 0$ is guaranteed. In this case, only the parameter mismatch of ψ affects the steady state error of the q-axis current. Taking the above discussion into account, the current controller structure can be simplified as shown in Fig. 4.20, where the back e.m.f. compensation block is virtually added to the q-axis current control loop in the controller for the purpose of the ψ identification.

Mathematical expressions of i_d and i_q can be derived from Fig. 4.21 as presented by (u) and (v):

$$i_d = i_d^* = 0, \text{ and} \qquad \text{(u)}$$

$$i_q = \frac{\omega_c(\hat{\psi} - \psi)}{K_q + R} + \frac{i_q^* K_q}{K_q + R}. \qquad \text{(v)}$$

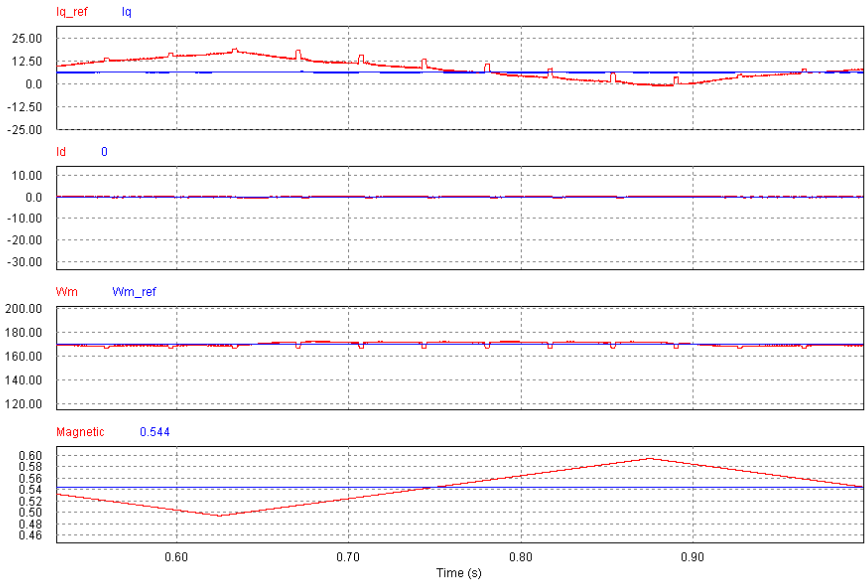

Fig. 4.22 Calculate results of current norm characteristic.

The second term of the right-hand side in (v) affects the identification of ψ, so this part must be eliminated from the calculation without using the winding resistance of the motor. This can be done by using the d-axis current control loop as a simulator of the second term in (v). As mentioned previously, d-axis current control loop no longer has any interference from the q-axis because L_q has been already identified, i.e., $\hat{L}_q = L_q$. Therefore, if the d-axis current regulator is changed to a P regulator whose gain is equal to K_q and the d-axis current command is changed to the value equal to i_q^*, the resultant d-axis current comes to have the same value as the second term of (v). This implies that the second term of (v) can be found with no knowledge of the winding resistance. By memorizing the simulated second term value in the d-axis current control loop from and by subtracting the memorized value (v), the most important part can be extracted from (v) as follows:

$$i_q' = \frac{\omega_c(\hat{\psi} - \psi)}{K_q + R}. \qquad \text{(w)}$$

R is assuming constant in identification period. By using (u) and (w), the motor current norm is expressed as

$$i_n = \sqrt{i_d^2 + i_q'^2} = \frac{\omega_c(\hat{\psi} - \psi)}{K_q + R}. \qquad \text{(x)}$$

By tuning the set value $\hat{\psi}$ in the controller, the value of i_n varies accordingly and becomes zero (the minimum value) when $\hat{\psi} = \psi$. And the simulation results shown in Fig. 4.34 just show the same simulation results. As the simulation results that when the $\hat{\psi} = \psi$ the current norm equal to zero. And also can see the $\hat{\psi}$ and current norm had a leaner relationship between each other.

4.3.3. ψ identification experiment

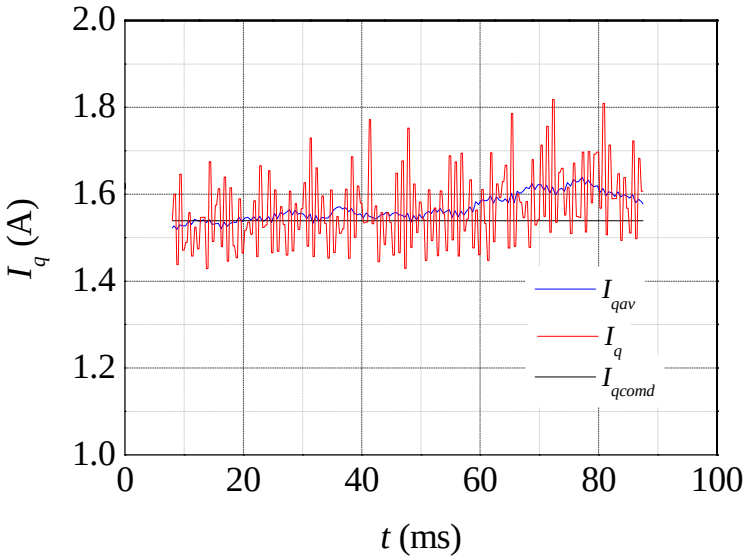

Fig. 4.23. q-axis current changing.

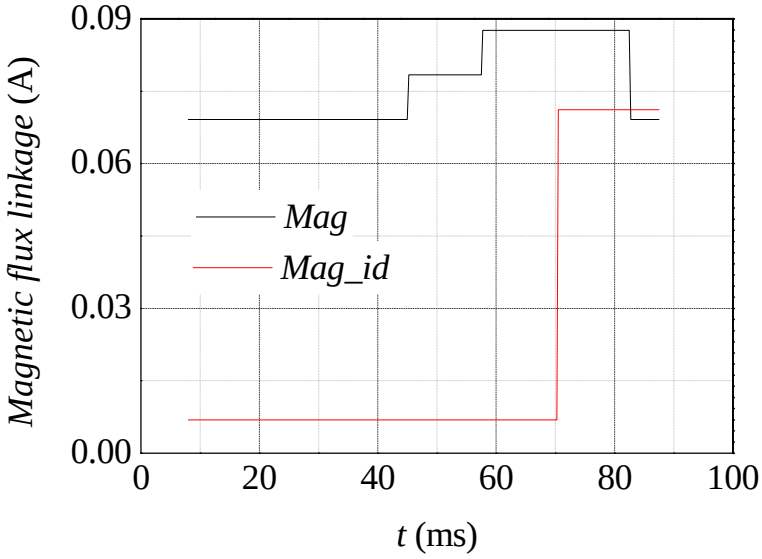

Fig. 4.24. Magnetic flux linkage changing.

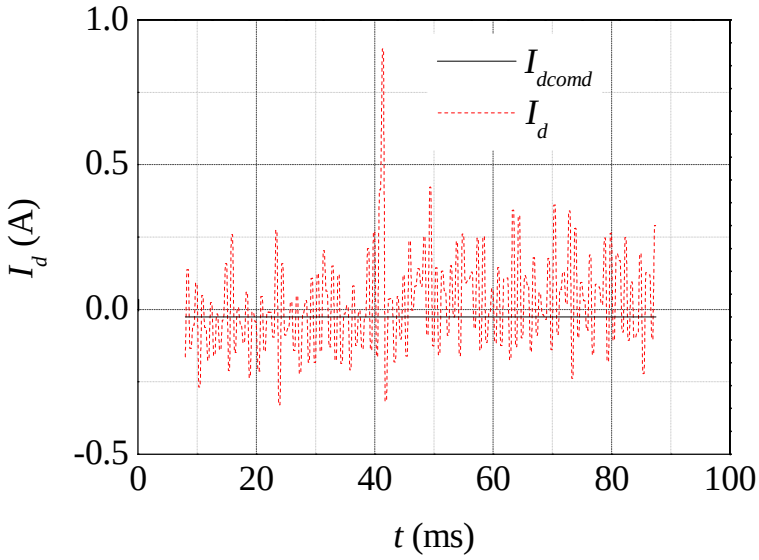

Fig. 4.25.Rotation speed.

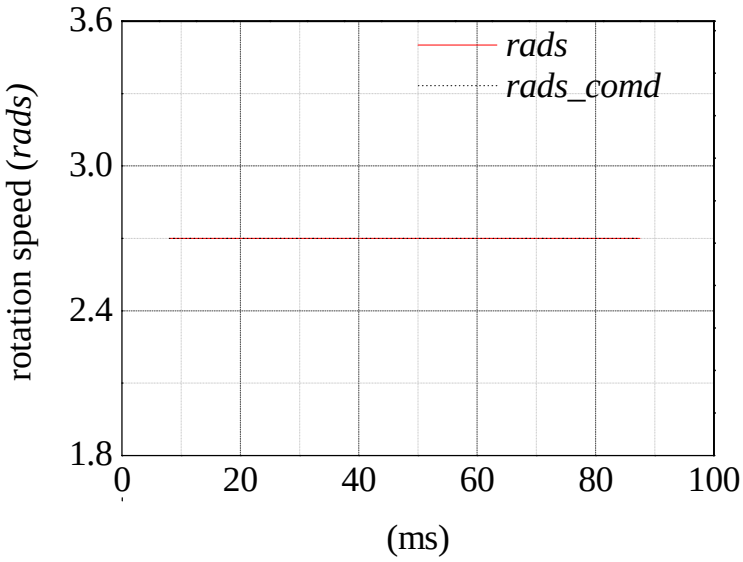

Fig. 4.26.Rotation speed.

To confirm the proposed magnetic flux linkage identification method, the experiment is setup. And there are mainly four figures and based on these four figures, the d-axis current, q-axis current, rotation speed and magnetic flux linkage changing can be confirmed.

Fig. 4.23 is the q-axis current changing in the identification period. And the magnetic flux linkage setup is bigger than the true value. Because of that the q-axis current value also increased as the setup magnetic flux linkage changes. And by using the two point speculate identification method, the speculate Ψ value is 0.0696 Wb, the identification error is 3.26 %.

In the identification system, P regulator gain is set to 0.1. And the identification only cost 100 ms.

4.4. L_d identification

After magnetic flux linkage had been identified, the only influence left in the proposed identification system is the unknown d-axis inductance. To identify the d-axis inductance it is necessary to set up the d-axis current signal be stable and not equal to zero.

Then in this chapter, the identification theory, simulation results and experiment results had been infirmed.

4.4.1. L_d identification theory

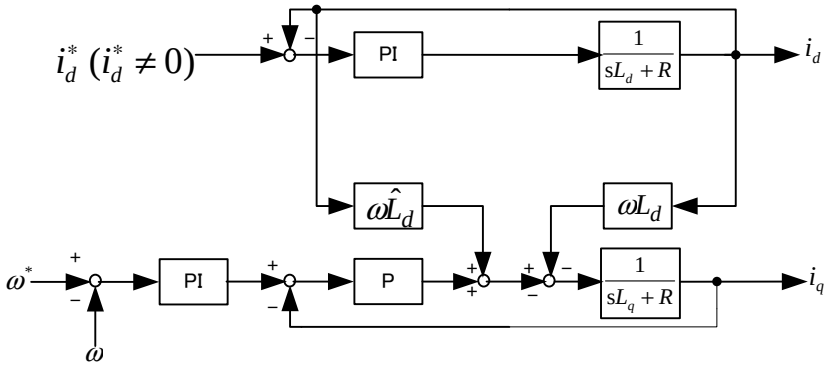

Fig. 4.27 Simplified d-axis inductance identification system.

As the on-line d-axis inductance identification system use the same system with magnetic flux linkage identification system. But the magnetic flux linkage identification condition needs to set the d-axis command signal not equal to zero. When the motor works in the steady state and the rotation speed will became stable. Based on that the q-axis current also will became stable.

As previous chapter referred the similar identification system is used with the same approach. However, some minor modification is required to identify these parameters separately. To keep the d-axis inductance affecting the q-axis current the d-axis command signal cannot be set to zero.

Figure 4.27 is the proposed on-line d-axis inductance identification system. The system includes the speed control system and decoupling control system. And the decoupling control system include two axis. And synchronous rotating reference frame (dq-reference-frame) changed the current signal into PWM control signal.

By focusing on q-axis the q-axis current expressions can be expressed as (y). By using the similar method when identification the magnetic flux linkage used, the second term of (y) can be canceled. After canceled out the second part of (y) formula (z) can be get.

$$i_q = \frac{\omega i_d (\hat{L}_d - L_d)}{K_q + R} + \frac{i_q^* K_q}{K_q + R}. \qquad \text{(y)}$$

$$i_q' = \frac{\omega i_d (\hat{L}_d - L_d)}{K_q + R}. \qquad \text{(z)}$$

Based on the expression (z), when the d-axis inductance setup in the controller is equal to the true value the (z) is equal to zero. And also by using the two point speculate method the unknown d-axis inductance can be identified.

4.4.2. L_d identification simulation

As the on-line identification system had a similar system as the off-line identification method. But the on-line identification include the speed control part with it. When the motor works in the steady state and the rotation speed will became stable. Based on that the q-axis current also will became stable.

As previous chapter referred the similar identification system is used with the same approach. However, some minor modification is required to identify these parameters separately. To keep the d-axis inductance affecting the q-axis current the d-axis command signal can not be set to zero.

Figure 4.27 is the proposed on-line d-axis inductance identification system. The system includes the speed control system and decoupling control system. And the decoupling control system include two axis. And synchronous rotating reference frame (dq-reference-frame) changed the current signal into PWM control signal.

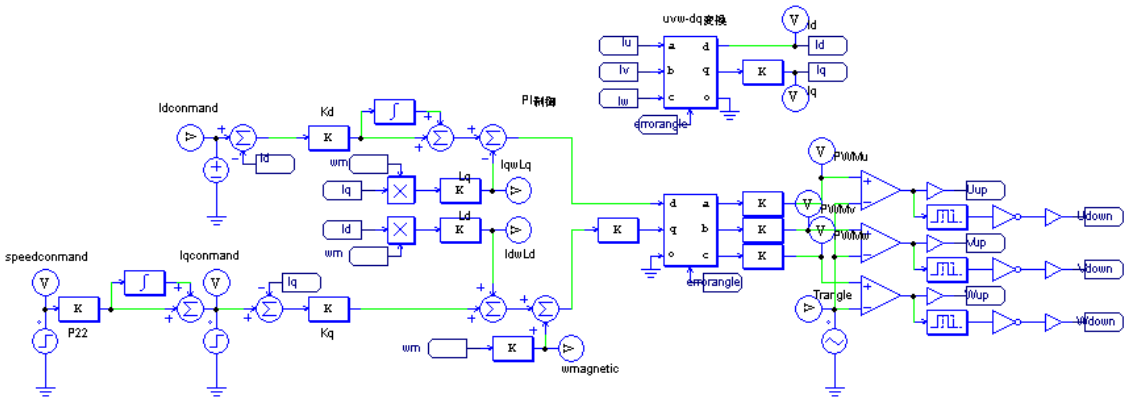

Fig. 4.28. Simplified on-line and d-axis inductance identification system.

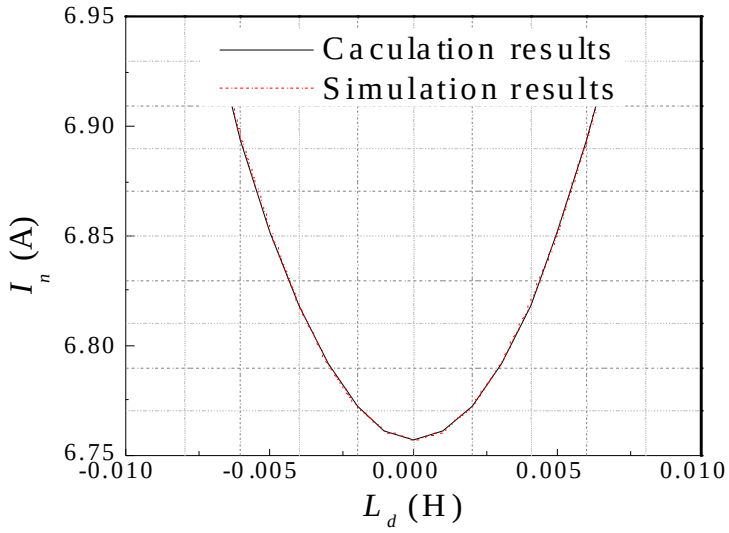

Fig. 4.29 Calculate results of current norm characteristic.

The Fig 4.28 shows the simulation control circuit. And in the circuit the PI regulator used in the q-axis current control parts had been replaced by P regulator. And based on this simulation theory the d-axis current characteristic is shown in Fig. 4.29. The black line is the calculation result and the red line is the simulation current result. And the two current norm characteristic had a same characteristic, and reach the minimum current point when the d-axis inductance setup in the control is just equal to the true value of d-axis inductance.

4.4.3. L_d identification experiment

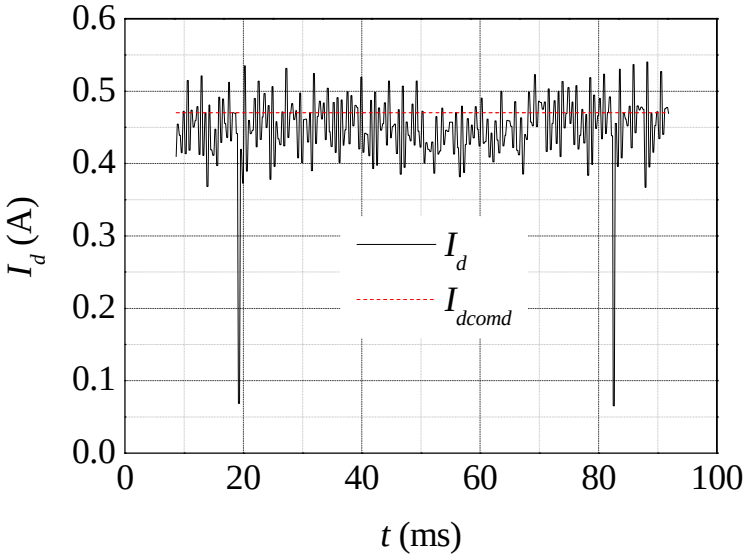

Fig. 4.30. d-axis current changing.

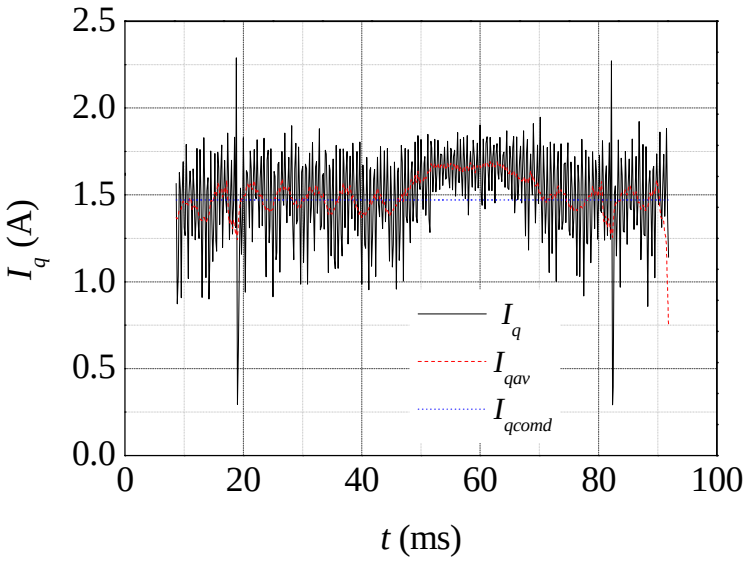

Fig. 4.31. q-axis current changing.

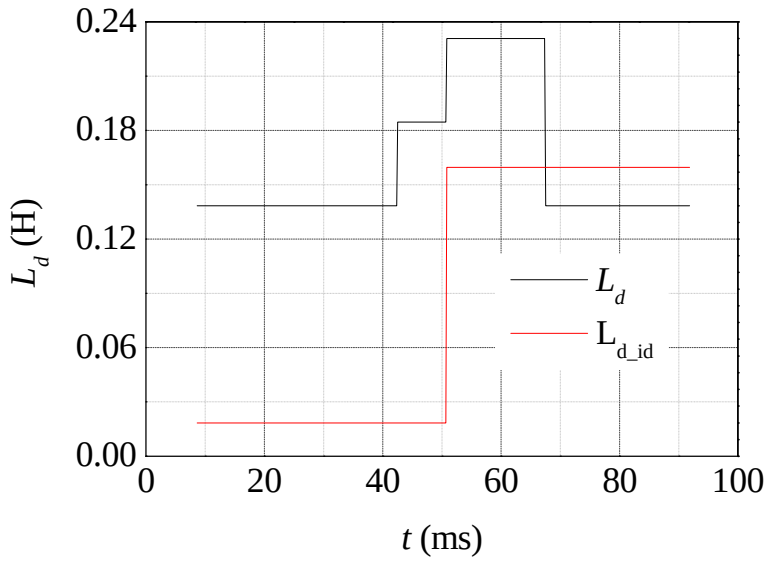

Fig. 4.32. d-axis inductance changing.

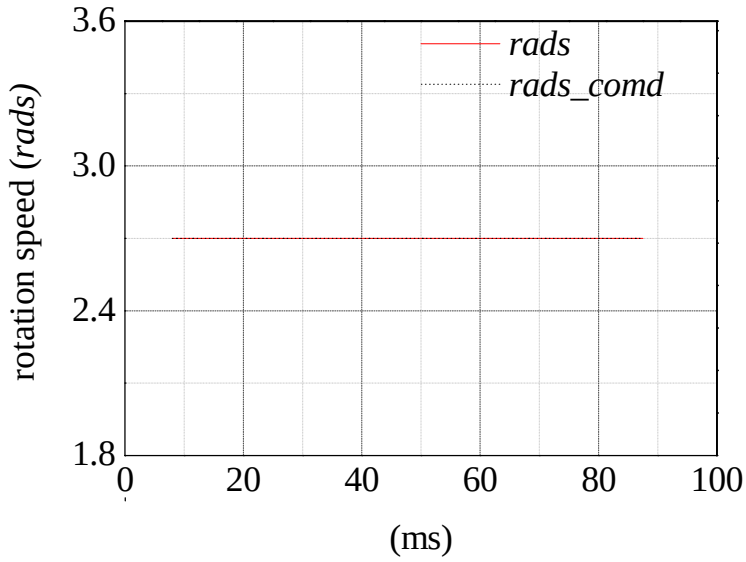

Fig. 4.33. Rotation speed.

The on-line identification system includes the speed control system. After the motor works in the steady state and the rotation speed also became stable. Based on the q-axis current also will become stable. Then the identification starts identify the d-axis inductance.

As previous chapter referred the similar identification system is used with the same approach. However, some minor modification is required to identify these parameters separately. To keep the d-axis inductance affecting the q-axis current the d-axis command signal cannot be set to zero.

Figure 4.30 and Figure 4.31 shows the current changing of the on-line identification in the identification period. And the Fig 4.32 is the d-axis inductance setup changing in the controller. The Fig 4.33 is the rotation speed signal in the identification period.

Based on these experiment results, before the identification period start the current signal and rotation speed is working in a steady state. Then the identification period get involved. As the d-axis inductance setup in the controller changed for two times, the current value also changed for two times. And when the current value became stable the current value is recoded and the by employed the two-point speculate method that the true value of d-axis inductance can be known. The identification result is 15.3 mH, and the identification error is 17.7 %. And in the identification period the rotation speed can keep steady.

4.5. *R* identification

After other parameters had been identified, the only unknown parameters is the resistance in the motor.

The identification theory of identify the resistance is almost like the off-line resistance identification. And the only different is the proposed identification system need to control the speed by itself and the block figure of the control system had speed control system with it.

4.5.1. *R* identification theory

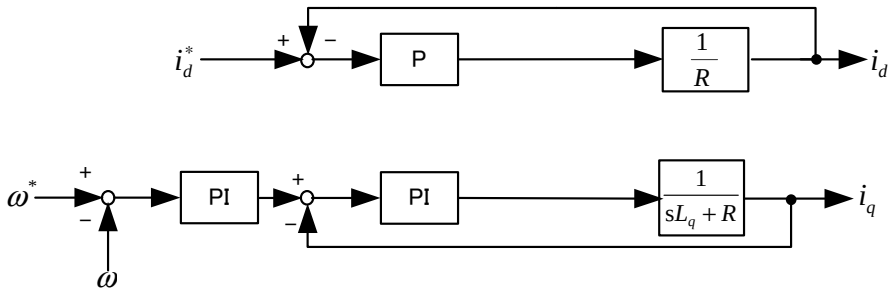

Fig. 3.24. Simplified resistance identification system.

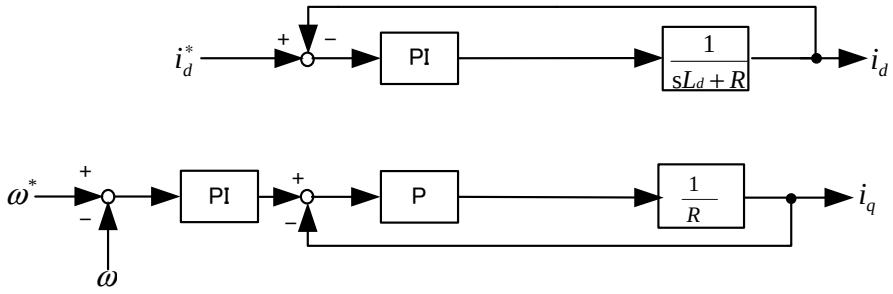

Fig. 3.25. Simplified resistance identification system.

The resistance on-line identification simplified system is shown in Fig 3.24and Fig 3.25. Compare with the off-line resistance identification system, the new identification system include the speed control loop with it.

And the proposed technical also had no sensitive problems. Because of the identification technical also base on using the current signal. Even the resistance is changed; the proposed technical could also be used to identify the unknown and changed parameters.

And the on-line resistance identification also had two kinds of situations. First kind of situation is the motors is stopped. But in this kind of situation only the

Fig.3.24 can be used. The Fig. 3.25 cannot be used in this kind of situation. The second kind of situation is after the other parameters had been identified. And both of the situation used the proposed identification system is shown in Fig. 3.24 and Fig. 3.25.

In the first kind of situation when the motor is stopped the $\omega = 0$, then the proposed identification system is equal to the Fig.3.24 and Fig. 3.25. And in another case, after the other parameters had identified, then identification system also equal to Fig.3.24 and Fig. 3.25. And command signal of q-axis current is can be known.

As described in the above discussion, the proposed identification technique of the IPM motor parameters does not require any information of the winding resistance R, and is basically robust to the variation of R; thus, it is not necessary to identify R inherently. The R identification, however, can be optionally realized by using the identification algorithms described so far.

By focusing on d-axis or q-axis, R is simply calculated by the following expression(aa), (ab)

$$R = \frac{K_{Pd}(i_d^* - i_d)}{i_d} \quad . \qquad \text{(aa)}$$

$$R = \frac{K_{Pq}(i_q^* - i_q)}{i_q} \qquad \text{(ab)}$$

By using formula (aa) or (ab), the winding resistance can be identified by only using the current signal.

4.5.2. *R* identification simulation

The simulation results are totally same with the off-line identification method.

4.5.3. *R* identification experiment

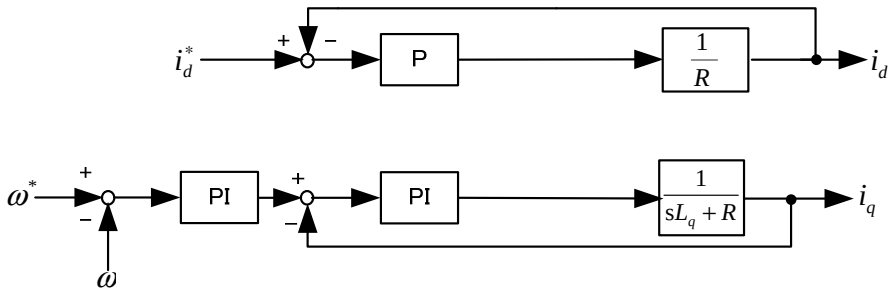

Fig. 4.26. Simplified resistance identification system.

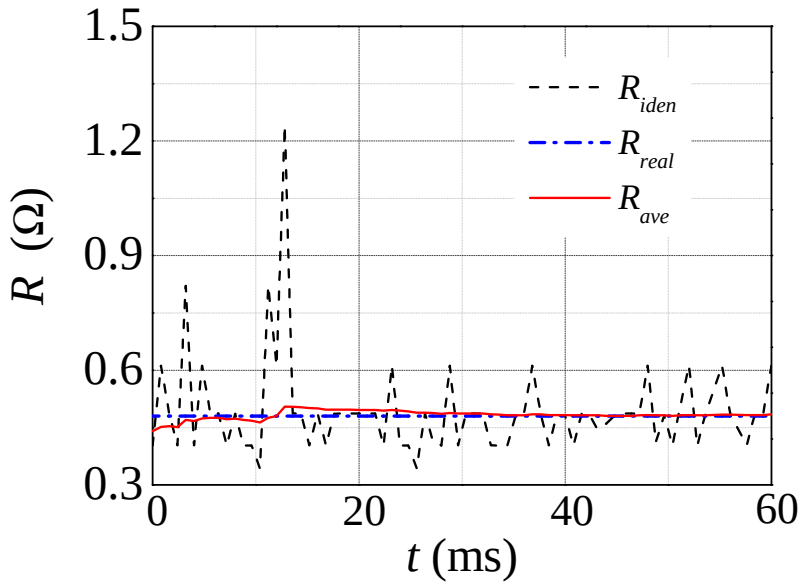

Fig. 4.27. Resistant identification result.

One of the most important feature is the proposed identification method had no sensitive to the winding resistance. And it can identify the unknown resistance. The Fig. 4.26 is the simplified resistance identification system. In which the d-axis use the P regulator to replaced the PI regulator. When the motor works in the steady state, by using the d-axis current signal the resistance can be identified. Based on the Fig. 4.27 the resistance can be identified by using current signal. The black line is the resistance

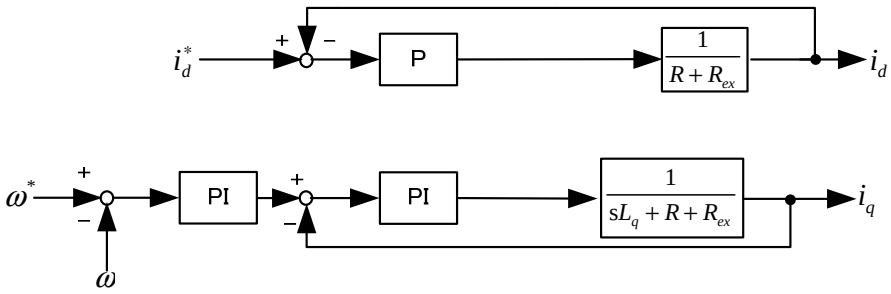

Fig. 4.28. Simplified resistance identification system with extra resistance.

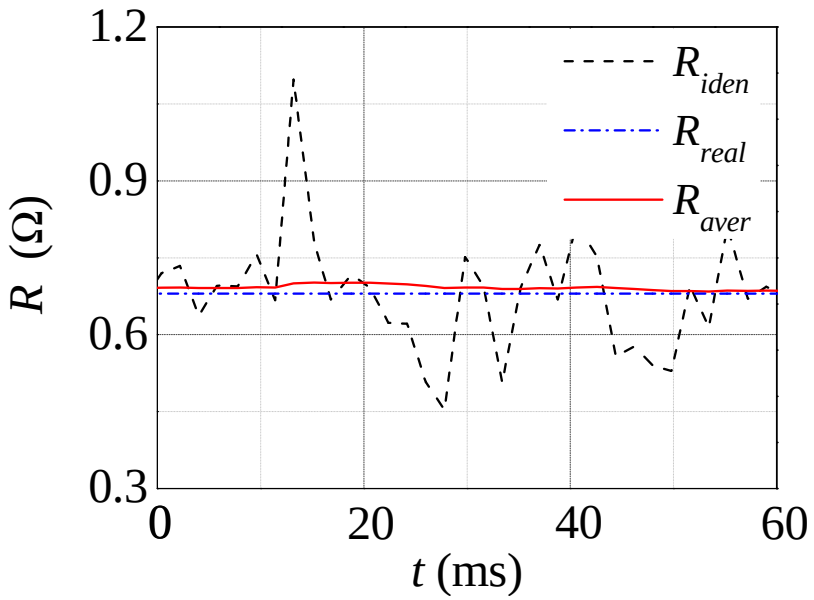

Fig. 4.29. Resistant identification result with extra resistance.

value, the red line is the resistance average value of using the resistance value. In the end the average value of the resistance is almost equal to the true value of resistance. And in the Fig. 4.27, the blue line and the red line is almost coincide with each other. The identification results are 0.493 Ω, and the identification error is 2.7 %.

To confirm the sensitive to winding resistance, the extra resistance is connected into the circuit. In that kind of situation, then simplified resistance identification system is

changed into Fig. 4.28. And the extra resistance is 0.2 Ω. And the real resistance of motor is 0.48 Ω. The total resistance is 0.68 Ω. The experiment results of this kind identification situation are shown in Fig. 4.29.

In the experiment result, the black line is the calculation results, because of the current fluctuate. The red line is the average calculation result. And after 60 ms, the average value is equal to the true value of the resistance. The identification results of the changed resistance are 0.675 Ω with the identification error 0.74 %.

5. Conclusion

In this thesis, two kinds of IPMSM parameters identification method had been proposed. One is off-line IPMSM identification method, and another identification method is on-line identification method.

The off-line identification technique of the IPM motor parameters has been proposed. The most unique features of the technique are capability to identify the parameters by using the motor current norm information, angle signal and robustness to the winding resistance variation.

The identification proceeds step by step with changing the structure of the current controller and with seeking the minimum point of the current norm on the basis of the well-known hill-climbing algorithm. The identification of the motor parameters can be achieved because the minimum point of the current norm is found if and only if the specified parameter mismatch is cancelled out between the controller and the real motor. But it need two motor in the experiment. One is used to control the motor rotation speed. Another motor is used to test the proposed identification theory. The proposed identification technique is also theoretically proven by the mathematical model of the IPM motor drive. Several simulations and experiments were conducted to check the motor current norm characteristics and the identification process of the motor parameters. In addition, the experimental tests to identify L_q, L_d and ψ were conducted to confirm the performance of the proposed technique. The overall identification error was within approximately ±5 %.

The online parameter identification technique of the IPM motor also had been proposed in this paper. The most unique features of the technique are capability to identify L_q and R by using only the motor d-axis feedback current information, and robustness to the winding resistance variation as well as the control variables. And it only uses one IPMSM and inverter in the experiment. According to the simulation results and experiment results, the proposed technique can estimate L_q, R, L_d and ψ within the identification error of 5.7 %, 2.7 % 3.2 % and 17.7 %. The identification

stage only cost within 100 ms.

Several simulations and experiments were conducted to check the motor current norm characteristics and the identification process of the motor parameters. In addition, the experimental tests to identify L_q, L_d and ψ were conducted to confirm the performance of the proposed technique. The overall identification error was within approximately ±18 %.

6. Future task

Until now, the thesis had proposed two kinds of IPMSM parameters identification methods by using the current signal and angle signal. The off-line IPMSM identification methods had better identification accuracy, but the experiment needs more equipment then the on-line identification. And off-line method identification cost more timed. But the on-line identification only cost milliseconds in the identification period. And less experiment equipment is required. But the on-line IPMSM identification accuracy is worse than the off-line identification method.

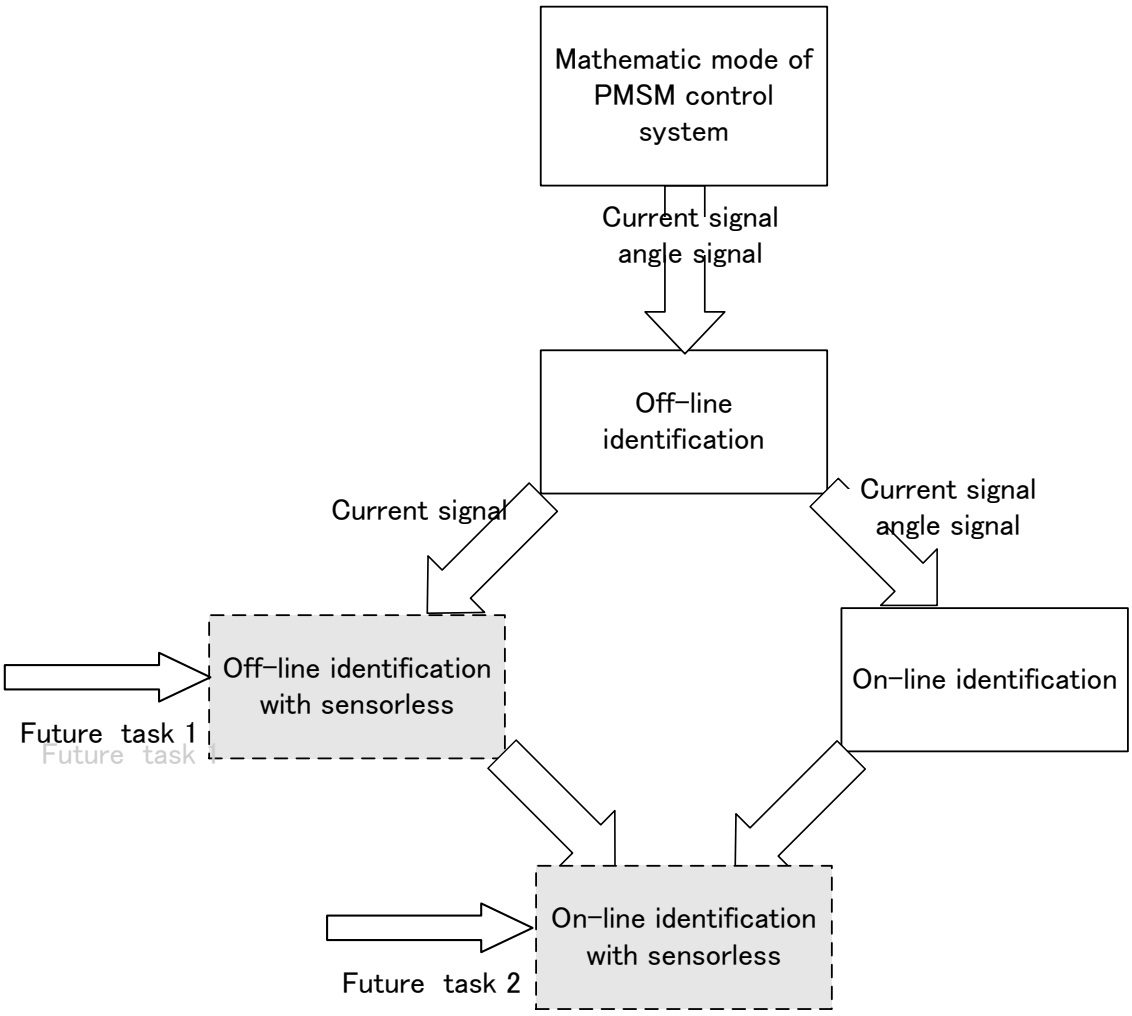

Fig 6.1 Future task.

In the future, the sensor less identification of using the proposed identification theory will be the next purpose of this research. First task is make the off-line identification method works without an angle sensor. Then the second task is integration of online and offline method sensor less method to achieve IPMSM on-line identification method.

Because of the sensor less identification will help to reduce the experiment equipment, and made this proposed identification theory much practical to use. And only the current signal is required.

Base on the calculation results showing in the present stage. The calculation results shows that when the angle signal had an angle mismatch within ±13˚ error can keep the parameters identification error in 3 %. Based on this calculation results this identification theory is possible to achieve the sensor less identification.

7. Reference

1. Fitzgerald, A. E.; Charles Kingsley, Jr.; Alexander Kusko (1971). "Chapter 6, Synchronous machines, steady state".Electric Machinery, 3rd Ed. USA: McGraw-Hill. pp.283–330. Library of Congress Catalog No. 70-137126.

2. Fitzgerald, A. E.; Charles Kingsley, Jr.; Alexander Kusko (1971). "Chapter 11, section 11.2 Starting and Running Performance of Single-phase Induction and Synchronous Motors, Self-starting Reluctance Motors". Electric Machinery, 3rd Ed. USA: McGraw-Hill. pp. 536–538. Library of Congress Catalog No. 70-137126.

3. James G Stallcup, Stallcup's Generator, Transformer, Motor and Compressor, page 15-13, Jones & Bartlett, 2012 ISBN 1-4496-9519-1.

4. R. Islam; I. Husain; A. Fardoun; K. McLaughlin."Permanent-Magnet Synchronous Motor Magnet Designs With Skewing for Torque Ripple and Cogging Torque Reduction". Industry Applications, IEEE Transactions on. 2009. doi: 10.1109/TIA.2008.2009653

5. Ki-Chan Kim; Seung-Bin Lim; Dae-Hyun Koo; Ju Lee. The Shape Design of Permanent Magnet for Permanent Magnet Synchronous Motor Considering Partial Demagnetization". Magnetics, IEEE Transactions on. 2006. doi: 10.1109/TMAG.2006.879077

6. P. Pillay; R. Krishnan. "Application characteristics of permanent magnet synchronous and brushless DC motors for servo drives". Industry Applications, IEEE Transactions on. 1991. doi:10.1109/28.90357 quote: "The permanent magnet synchronous motor (PMSM) and the brushless DC motor (BDCM) have many similarities; they both have permanent magnets on the rotor and require alternating stator currents to produce constant torque."

7. Y. Honda; T. Nakamura; T. Higaki; Y. Takeda. "Motor design considerations and test results of an interior permanent magnet synchronous motor for electric vehicles". Industry Applications Conference, 1997. Thirty-Second IAS Annual Meeting, IAS '97., Conference Record of the 1997 IEEE. 1997. doi: 10.1109/IAS.1997.643011

8. M.A. Rahman; Ping Zhou. "Analysis of brushless permanent magnet synchronous motors". Industrial Electronics, IEEE Transactions on. 1996. doi: 10.1109/41.491349

9. Markus Lindegger. "Economic viability, applications and limits of efficient permanent magnet motors". p. 7, p. 21

10. 野口　敏彦 :「高調波瞬時無効電力に着目したサーボモータのロータ位置センサレス制御に関する研究」, 課題番号 11650281, 平成 11 年度～平成 12 年度　科学研究費補助金(基盤研究(c)(2))研究成果報告書(平成 13 年 3 月)

11. 小原, 野口 :「モデル規範適応システムに基づく永久磁石モータのセンサレス制御法」　平成 22 年電気学会全国大会講演論文集　No.4-107 pp.183-184(2010)

12. 織田, 野口, 川上, 佐野:「磁極位置センサレス PM モータの推定誤差要因とその対策」　平成 20 年電気学会産業応用部門大会講演論文集　No.1-55 pp.273-276(2008)

13. Masaki Ohara and T. Noguchi.: "Sensor less Control of Permanent Motor Based on Model Reference Adaptive System", IEEJ 2010, Conference Proceedings, no. 4,107, pp.183-184.

14. Toshihiko Noguchi, Shigenori Togashi, and Ryo Nakamoto.: "Short-Current Pulse-Based Maximum-Power-Point Tracking Method for Multiple Photovoltaic-and-Converter Module System", IEEE Trans. on Ind. Elec. 2002, 49, 1, pp.217-22.

15. J.K. Seok, K.T. Kim, D.C. Lee.: "Automatic mode switching of P/PI speed control for industry servo drives using online spectrum analysis of torque command", IEEE Transactions on Industrial Electronics, Vol. 54, pp. 2642-2647,2007.

16. P. Pillay andR. Krishnan.: "Modeling analysis and simulationoCa high perfonnance, vector controlled", pennanent magnet synchronous motor drive, presented at the IEEE IAS Annu. Meeting, Atlanta, 1987.

17. M. Lajoie-Mazenc, C. Villanueva, and 1. Hector.: "Study and implementation of a hysteresis controlled inverter on a permanent magnet synchronous machine", IEEE Trans. Industry Applications.vol. 1A-21, no. 2, pp. 408-413, Mar.lApr. 1985.

18. Consoliver, Earl L., and Mitchell, Grover I. (1920). Automotive ignition systems. McGraw-Hill. p.4.

19. [ab]Robert A. Millikan and E. S. Bishop (1917). Elements of Electricity. American Technical Society. p.54.

20. A. Mujanovic, P. Crnosija, Z. Ban.: "Determination of transient error and signal adaptation algorithm coefficients in MRAS", Proceedings of the IEEE International Symposium on Industrial Electronics, ISIE 99, Maribor, p. 631-634, 1999.

21. Yan Liang and Yongdong Li.: Sensorless Control of PM Synchronous Motors Based on MRAS Method and Initial Position Estimation, ICEMS 2003, Vol. 1, 9-11, pp:96 – 99, Nov. 2003.

22. H.W.Kim,N.V Nho and M.J.Youn.: Current Control of PM Synchronous Motor in Overmodulation Range, IECON 2004 , pp. 896-901.

23. Izrail Moiseevich Gelfand (1961), Lectures on Linear Algebra, Interscience Publishers, Inc., New York. Reprinted by Dover, 1989. ISBN 0-486-66082-6

24. Thomas S. Shores (2007), Applied Linear Algebra and Matrix Analysis, Undergraduate Texts in Mathematics, Springer. ISBN 0-387-33195-6

25. J.K. Seok.: "Frequency-spectrum-based antiwindup compensator for PI controlled systems", IEEE Transactions on Industrial Electronics, Vol. 53, pp. 1781-1790, 2006.

26. K. Paponpen and M. Konghirum.: "An Improved sliding mode observer for speed sensor less vector control drive system", Power Electronics and Motion Control Conference, 2006. IPEMC 2006. CES/IEEE 5th international p.no 1–5, vol: 2, isbn:1-4244-0448-7.

27. 工藤, 野口, 川上, 佐野: 「IPM モータ制御システムの数学モデル誤差とその補償法」 電学半導体電力変換研究会, SPC-08-25(平 20)

28. Toshihiko Noguchi, Shigenori Togashi, and Ryo Nakamoto, “Short-Current Pulse-Based Maximum-Power-Point Tracking Method for Multiple Photovoltaic-and-Converter Module System, IEEE Trans. on Ind. Elec. Vol.49, pp.217-223 (2002)

29. B.K. Bose, “A High-Performance Inverter-Fed Drive System of an Interior Permanent Magnet Synchronous Machine,” IEEE Trans. on Ind. Appl., vol. 24, pp. 987-997, Sep./Oct. 1988.

30. Masaki Ohara and T. Noguchi.: “Rotor Position Sensorless Control and Its Parameter Sensitivity of Permanent Magnet Motor Based on Model Reference Adaptive System”, IEEJ Trans. on Industry Applications, Vol.132, No. 3, pp.426-436 (2012)

31. Jun Zheng, Yunkuan Wang, Xiaofei Qin, Xin Zhang: “An offline parameter identification method of induction motor”, Proc. 7th World Congress on Intelligent Control and Automation, China. pp. 8898-8901 (2008)

32. I. H. Altas and A. M. Sharaf, "A novel on-line MPP search algorithm for PV arrays", IEEE Trans. Energy Conversion, Vol. 11, pp.748 -754 (1996)

33. Pahlevaninezhad, Majid; Pritam Das; Gerry Moschopoulos; Praveen Jain (March 17, 2013). "SENSORLESS CONTROL OF A BOOST PFC AC/DC CONVERTER WITH A VERY FAST

TRANSIENT RESPONSE". Twenty-Eighth Annual IEEE Applied Power Electronics Conference and Exposition. Long Beach, CA: IEEE. pp. 356–360.

34. "Frequently Asked Questions". Powersim Inc. Retrieved Nov 26, 2013.

35. WW Cohen, R Greiner, D Schuurmans, "Probabilistic hill-climbing", Workshop on Computational Learning Theory & Natural Learning Systems: Intersections Between Theory & Experiment: Intersections Between Theory & Experiment, pp.171--181(1994)

8. Gratitude

This is my final Doctor’s Thesis in the Doctor’s Program System, Environment and energy system department at Shizuoka University in Japan. First of all, I would like to thank my Professors Mr. Toshihiko Noguchi for all his help, theoretical questions, alternative approaches to problems and encouragement. I would also like to thank my wife for her fully support help me finish the doctor course. I would like to thank all the student members for all their kindness and support, and for making me feel most welcome during my thesis work.